Wnt/β-catenin signaling in hypoxia-induced pulmonary artery smooth muscle cell proliferation - Role of bioactive molecule of *Mucuna pruriens*

Doctor of Philosophy
In
Allied Health Sciences
(Biotechnology)

By

Ms. Supriya Bhosale

PhD Research Scholar
Reg.No:20PHD025

Laboratory of Vascular Physiology and Medicine

Department of Physiology

BLDE
(DEEMED TO BE UNIVERSITY)
Smt. Bangaramma Sajjan Campus, B. M. Patil Road (Sholapur Road), Vijayapura-586103, Karnataka, India

2025

BLDE
(DEEMED TO BE UNIVERSITY)
Smt. Bangaramma Sajjan Campus, B. M. Patil Road (Sholapur Road), Vijayapura-586103. Karnataka, India

Declaration by the Candidate

I hereby declare that this thesis entitled **"Wnt/ β-catenin signaling in hypoxia-induced pulmonary artery smooth muscle cell proliferation -Role of bioactive molecule of *Mucuna pruriens*"** is a genuine research work carried out by me under the supervision of Professor Kusal K. Das, (Guide), Department of Physiology, Shri B. M. Patil Medical College, Hospital and Research Centre, BLDE (Deemed to be University), Vijayapura, Karnataka, India and supervision of Dr. Shrilaxmi Bagali, (Co-Guide) Professor. Department of Physiology, Shri B. M. Patil Medical College, Hospital and Research Centre, BLDE (Deemed to be University), Vijayapura, Karnataka, India.

S. D. Bhosale
Signature of the Candidate

Ms. Supriya Bhosale
Registration No: 20PHD025
Faculty of Allied Health Sciences (Biotechnology)
Shri B. M. Patil Medical College, Hospital and Research Centre,
BLDE (Deemed to be University), Vijayapura, Karnataka, India.

BLDE
(DEEMED TO BE UNIVERSITY)
Smt. Bangaramma Sajjan Campus, B. M. Patil Road (Sholapur Road), Vijayapura-586103. Karnataka, India

Certificate from the Guide

This is to certify that the thesis entitled **"Wnt/ β-catenin signaling in hypoxia-induced pulmonary artery smooth muscle cell proliferation - Role of bioactive molecule of *Mucuna pruriens*"** is a genuine research work carried out by Ms. Supriya Bhosale under my supervision and guidance in the Laboratory of Vascular Physiology and Medicine, Department of Physiology, Shri B. M. Patil Medical College, Hospital and Research Centre, BLDE (Deemed to be University), Vijayapura, Karnataka, India in the fulfillment of the requirements for the degree of Doctor of Philosophy in Allied Health Sciences (Biotechnology).

Signature of the Guide

Prof. Kusal K. Das
Distinguished Chair Professor
Laboratory of Vascular Physiology and Medicine
Shri B. M. Patil Medical College, Hospital and Research Centre,
BLDE (Deemed to be University), Vijayapura, Karnataka, India.

Kusal K. Das, PhD
Distinguished Chair Professor
Laboratory of Vascular Physiology and Medicine
Department of Physiology,
Shri B M Patil Medical College
BLDE (Deemed to be University)
Vijayapur-586103, Karnataka

BLDE
(DEEMED TO BE UNIVERSITY)
Smt. Bangaramma Sajjan Campus, B. M. Patil Road (Sholapur Road), Vijayapura-586103. Karnataka, India

Certificate from the Co-Guide

This is to certify that the thesis entitled **"Wnt**/β-catenin signaling **in hypoxia-induced pulmonary artery smooth muscle cell proliferation - Role of bioactive molecule of *Mucuna pruriens*"** is a genuine research work carried out by Ms. Supriya Bhosale under my co-supervision and guidance in the Department of Physiology, Shri B. M. Patil Medical College, Hospital and Research Centre, BLDE (Deemed to be University), Vijayapura, Karnataka, India in the fulfillment of the requirements for the degree of Doctor of Philosophy in Allied Health Sciences (Biotechnology).

Signature of the Co-Guide

Dr. Shrilaxmi Bagali
Laboratory of Vascular Physiology and Medicine
Shri B. M. Patil Medical College, Hospital and Research Centre,
BLDE (Deemed to be University), Vijayapura, Karnataka, India.

Professor
Physiology
BLDE(DU) Shri B M.Patil Medical
College, Hospital & R.C.
Vijayapur-586103.

BLDE
(DEEMED TO BE UNIVERSITY)
Smt. Bangaramma Sajjan Campus, B. M. Patil Road (Sholapur Road), Vijayapura-586103. Karnataka, India

Certificate from the Head of the Department

This is to certify that the thesis entitled **"Wnt/ β-catenin signaling in hypoxia-induced pulmonary artery smooth muscle cell proliferation - Role of bioactive molecule of *Mucuna pruriens*"** submitted by Ms. Supriya Bhosale (Reg. No.:20PHD025) for the award of the degree of Doctor of Philosophy, Allied Health Sciences (Biotechnology) to BLDE (Deemed to be University), Vijayapura, is a record of genuine research works carried out under supervision of Prof. Kusal. K. Das (Guide), Distinguished Chair Professor, Department of Physiology, Shri B. M. Patil Medical College, Hospital and Research Centre, BLDE (Deemed to be University), Vijayapura, Karnataka, India and co-supervision of Dr. Shrilaxmi Bagali (Co-Guide), Professor Department of Physiology, Shri B. M. Patil Medical College, Hospital and Research Centre, BLDE (Deemed to be University), Vijayapura, Karnataka, India in fulfillment of the requirements for the degree of Doctor of Philosophy in Allied Health Sciences (Biotechnology).

Signature of the HoD

Prof. and Head
Dept. of Physiology
BLDE(DU) Shri B M Patil Medical College, Hospital & R.C.
Vijayapur-586103

Dr. Lata Mullur
Head, Department of Physiology
Shri B. M. Patil Medical College, Hospital and Research Centre,
BLDE (Deemed to be University), Vijayapura, Karnataka, India.

BLDE
(DEEMED TO BE UNIVERSITY)
Smt. Bangaramma Sajjan Campus, B. M. Patil Road (Sholapur Road), Vijayapura-586103. Karnataka, India

Endorsement by the Dean, Faculty of Allied Health Sciences

This is to certify that this thesis entitled **"Wnt**/β-catenin signaling **in hypoxia-induced pulmonary artery smooth muscle cell proliferation - Role of bioactive molecule of *Mucuna pruriens*"** is a genuine research work carried out by submitted by **Ms. Supriya Bhosale (Reg. No.:20PHD025)** under the supervision of Prof Kusal K. Das (Guide), Distinguished Chair Professor, Department of Physiology, Shri B. M. Patil Medical College, Hospital and Research Centre, BLDE (Deemed to be University), Vijayapura, Karnataka, India and co-supervision of Dr. Shrilaxmi Bagali (Co-Guide), Professor, Department of Physiology, Shri B. M. Patil Medical College, Hospital and Research Centre, BLDE (Deemed to be University), Vijayapura, Karnataka, India in fulfillment of the requirements for the degree of Doctor of Philosophy in Allied Health Sciences (Biotechnology)

DEAN
Faculty of Allied Health Sciences
BLDE (Deemed to be University)
VIJAYAPURA-586103. KARNATAKA

Signature of the Dean

Dr. S. V. Patil
Dean, Faculty of Allied Health Sciences
BLDE (Deemed to be University), Vijayapura, Karnataka, India.

Dedicated To My Father

SHREE DASHARATH N BHOSALE

Acknowledgments

First, I thank **God Almighty** for giving me the strength, knowledge, ability, patience, and power to keep going against all hurdles and reach my goal.

I express my gratitude to all those who have contributed immensely to my work; without their support, it would have been impossible to complete the project.

First and foremost, I owe much gratitude to my Research Guide, **Prof Kusal K. Das,** Distinguished Chair Professor, Laboratory of Vascular Physiology and Medicine, BLDE (Deemed to be University), Shri B.M. Patil Medical College, Hospital and Research Centre, Vijayapura. His vast research experience and international exposure added quality and refined my work. He has always been inspiring, and his optimism has kept me going. His motivation and unconditional support gave me the strength to start afresh in the face of challenges. His meticulous approach and punctuality have been lessons for research and a lifetime. You are a great role model; I feel privileged to have worked for you. I look forward to publishing more with you in the future.

Thank you, sir…

I am sincerely thankful to my co-guide, **Dr Shrilaxmi Bagali.** Professor, Department of Physiology, BLDE (Deemed to be University) Shri B.M.Patil Medical College, Hospital & Research Centre, Vijayapura. Her endless enthusiasm has inspired me. I thanked her for her valuable time whenever I approached her. Her invaluable suggestions helped me to improve my research work and my thesis. Without her precious support, completing the thesis would have been impossible.
I am incredibly thankful to **Dr. Lata Mullur**, Professor and Head of the Department of Physiology, for providing all the departmental facilities for my research work. I also thank her for her invaluable support and cooperation in completing the thesis.

I am incredibly thankful to **Dr Sumangala Patil**, Department of Physiology, Vice Principal Pre & Para Clinical, Shri B M Patil Medical College, Hospital and Research Centre Vijayapura. For her timely help whenever there was a need and constant support throughout the project.

My special thanks to **Dr. Prachi P. Parvatikar**, Assistant Professor, Faculty of Allied Health Science (Biotechnology), for providing all the technical support in the form of expert suggestions, advice and technical knowledge during my research work. Without her precious support, completing the thesis would have been impossible.

I sincerely thank Dr**. Manohar S. Kugaji** for his support, valuable guidance, input and suggestions during every step of the research and for his kind help in learning instrumental techniques. His meticulous approach while performing cell culture experiments has been an essential lesson.

I thank **Dr. S, V Patil** Dean, Faculty of Allied Health Sciences, Shri B. M. Patil Medical College, Hospital and Research Centre, BLDE (Deemed to be university), Karnataka, India. Thank you for your constant support and timely administrative help.

I thank **Dr. Y M. Jayaraj**, Pro-Chancellor, BLDE (Deemed to be University), Vijayapura, **Dr R S Mudhol**, Vice-Chancellor, BLDE (Deemed to be University), Vijayapura, **Dr. Arun C Inamdar,** Pro Vice-Chancellor BLDE (Deemed to be University), Vijayapura, **Dr Raghavendra V. Kulkarni,** Registrar, BLDE (Deemed to be University), Vijayapura, **Dr. Arvind V. Patil**, Principal, Shri B. M. Patil Medical College, Hospital and Research Centre, Vijayapura, **Mr. Satish B. Patil**, Deputy Registrar, BLDE (Deemed to be University), Vijayapura for their constant support and timely administrative help.

An expression of endless gratitude to **Dr. Nilima Dongre,** Professor of Biochemistry, for providing all the facilities and expert opinions during the entire PhD curriculum.

I further thank Dr **Jyoti Khodnapur, Dr S. M. Patil**, and **Dr Sujatha Talikoti** for their valuable assistance in all my accomplishments. I thank my senior staff and colleagues for their timely help and assistance.

I express my sincere thanks to **Dr. Nandish Karkadol** (Assistant Professor, Medical Genetics) and **Dr. R. Chandramouli Reddy** (Assistant Biochemistry) and all the staff members of **Centre for Advanced Medical Education and Research**, BLDE (Deemed to be University) Vijayapura, and all the staff member of Centre for Advanced Medical Education and Research, BLDE (Deemed to be University) Vijayapura.

I thank the staff members of the **central library**, Shri B. M. Patil Medical College, Hospital and Research Centre, BLDE (DU), Vijayapura.

I thank all the **PhD committee members** for giving valuable input that helped me improve my work.

I gratefully acknowledge **BLDE (Deemed to be University)** for providing a research grant to carry out the work.

I thank the supporting staff of the Department of Physiology, **Sri G. M. Mathapati**, **Sri Shivu Biradar** and **Smt. Ranjeeta**. Special thanks to **Sri Mallu and Sri Ashok** for all the timely assistance, which eased my work.

I have no words to thank my dearest parents, **Shri Dasharath N Bhosale** and **Smt. Late Renuka Bhosale**. They have been the most wonderful people in my life. Their endless support, love, faith, trust and blessings have held my hands and guided me through some of the most demanding and most challenging moments of my life with ease. They have been an inspiration to me all my life. I thank my brothers **Sampat and Manoj** for their support.

I thank my mother-in-law, **Smt. Shanta Maruti Jadhav**, for my life's most precious and unique gift. I thank my sister **Suman** for her kind support and unconditional love throughout the journey.

I thank **Rajendra M Jadhav**, my soul mate, for his unconditional support, shouldering and sharing my responsibilities, and caring for everything during my long work hours.

I thank my lovely daughter **Suryada** and son **Soham,** who boosted my confidence from time to time during this endeavor and for tolerating all my eccentricities in the name of concentration. Their energy levels and their enthusiasm have always motivated me to do more.

I am immensely thankful to all those who have directly and indirectly contributed to completing my thesis.

Index

Sl. No.	CONTENTS	PAGE No.
1	**Certificate and declaration**	**1-7**
2	List of Figures	13-14
3	List of Tables	15
4	List of Abbreviations	16-17
5	**CHAPTER1: INTRODUCTION**	**20-23**
6	**CHAPTER2: REVIEW OF LITERATURE**	24-40
	2.1: Hypoxia	25
	2.2: Types of Hypoxias	25
	2.3: Pulmonary Hypertension	26
	2.4: Histology of Pulmonary artery smooth muscle cell	28
	2.5: Pathophysiology of Pulmonary Hypertension	29
	2.6: Wnt / β catenin signaling pathway	31
	2.7: Role Wnt / β catenin signaling pathway in pulmonary hypertension	33
	2.8: The Interplay of WNT/β-Catenin Signaling, Pulmonary Hypertension, and Hypoxia	35
	2.9: *Mucuna pruriens*	36
	2.10: Bioactive Compound from *Mucuna pruriens*	37
	2.11: In-silico analysis /Wnt/β-catenin signaling pathway/*Mucuna pruriens*	39
	2.12: Invitro analysis /Wnt/β-catenin signaling pathway /*Mucuna pruriens*	40
7	**CHAPTER3: AIM AND OBJECTIVES OF STUDY**	41-43
	3.1: Research Question	43
	3.2: Aim	43
	3.4: Objectives	43
	3.5: Hypothesis	43
8	**CHAPTER4: MATERIALS AND METHODOLOGY**	44-64
	4.1: Objective 1 *In-silico* analysis	45
	4.1.1: List of databases and tools /software used in silico Analysis	45
	4.2: Target protein Preparation	45
	4.3: Screening of Bioactive molecules	46

	4.4: Analysis of Drug Likeness Properties	47
	4.5: Molecular interaction study	47
	4.6: Molecular dynamics simulations (MD simulations)	48
	4.7: Molecular mechanics generalized Born surface area (MM-GBSA) analysis.	49
	4.8: Objective 2 Phytochemical Extraction	50
	4.9: Phytochemical extraction, identification, and isolation of bioactive molecule of *Mucuna pruriens* flow chart	50
	4.10: Collection of Seeds	51
	4.11: Preparation of Plant Extract	51
	4.12: Identification and isolation of bioactive molecules from *Mucuna pruriens* seeds	52
	4.13: In-vitro Study design	55
	4.14 Description of Pulmonary artery smooth muscle cell line	56
	4.15 Preparation of Complete growth media	56
	4.16 Seeding of cells or culture of cells	57
	4.17 Subculturing procedure	58
	4.18 MTT Assay for cell Cytotoxicity and cell viability	59
	4.19 Culture of Cells for Normoxia	59
	4.20 Culture of cells for Hypoxia condition and treatment of cells with bioactive compounds from Mucuna pruriens.	60
	4.21 Gene Expression Study Design	61
	4.22 Protocol for Isolation of RNA from Cells	62
	4.23 RNA Quantification	62
	4.24 cDNA Synthesis Protocol:	63
	4.25 real-time PCR	63
	4.26 Statistical analysis	64
9	**CHAPTER5: RESULT AND DISCUSSION**	65-
	5.1 Retrieval of the target protein from RCBS-PDB (http://www.rcsb.org/pdb)	66
	5.2 Screening of bioactive molecules	67
	5.3 Analysis of Drug Likeness Properties	69
	5.4 Molecular Interaction Study	70-71

	5.5 M D Simulation.	76
	5.6 Molecular Mechanics Generalized Born surface area (MM-GBSA) analysis.	78
	5.7 In-silico Discussion	79-8
	5.8 Phytochemical Extraction Result	81
	5.8.1 Collection of seeds	81
	5.9 Mucuna pruriens seed extract yield	81
	5.10 Isolation and identification of bioactive molecules	82
	5.10.1 Quantification of Gallic acid by HPLC	82
	5.10.2 Flash Chromatography of Gallic Acid	83
	5.10.3 Quantification of β –sitosterol by HPLC	84
	5.10.4 Flash Chromatography of β –sitosterol	85
	5.11 Phytochemical Extraction Discussion	87-88
	5.12 Result from Seeding of the cells or Culture of cells:	89
	5.13 MTT Assay Result	91-94
	5.14 Microscopic Changes of the Human pulmonary artery cell line are exposed to Hypoxia (5% Oxygen)	95
	5.15 Result of Gene Expression Studies	95
	5.16 Effect of Hypoxia on the expression Wnt/β-catenin signaling pathway molecules (Wnt5a/β-catenin/cyclin D1)	96
	5.17 Result of Wnt5a gene expression in hypoxia-exposed cells treated with bioactive molecules of Mucuna pruriens seed	97
	5.18 Result of β catenin expression in hypoxia-exposed cells treated with bioactive molecules of Mucuna pruriens seed	98
	5.19 Result from Cyclin D1 gene expression in hypoxia-exposed cells treated with bioactive molecules of Mucuna pruriens seed	100
	5.20 Invitro Discussion	102-107
9	**CHAPTER 6 SUMMARY AND CONCLUSION**	108-110
	6.1 Summary	108
	6.2 Conclusion	110
10	**CHAPTER 7 REFERENCES**	111-123
11	**ANNEXURES**	124-150

LIST OF FIGURES

FIGURE No.	FIGURE	PAGE No.
1.1.1	Mucuna pruriens, DC From Garden of BLDE Association of AVS Ayurveda Maha vidyalaya Vijayapura Karnataka	
2.4.1	Three layers of Pulmonary artery smooth muscle cells	27
2.6.1	WntWnt/β-catenin signaling pathway	30
2.9.1	Mucuna pruriens, DC From Garden of BLDE Association of AVS Ayurveda Maha vidyalaya Vijayapura Karnataka	37
2.10.1	A Structure of Biomolecule β-sitosterol	37
	B Structure of Biomolecule Gallic acid	37
4.9.1	M. pruriens seed and powder diagram	50
4.10.1	Soxhlet apparatus for extraction	52
4.11.1	Jasco Autosampler HPLC	53
4.11.2	Combi Flash RF+ Lumen	54
5.1.1	A Protein 3D structure of Wnt5a	66
	B Protein 3D structure of Frizzled1	
	C Protein 3D structure of LRP5/6	
	D Protein3D Structure of β-catenin	
	E Protein3D Structure of Disheveled	
	F Protein3D Structure of Cyclin D1	
5.2.1	A Biomolecule 3D structure of LDOPA	68
	B Biomolecule 3D structure of B-sitosterol	
	C Biomolecule 3D structure of Glutathione	
	D Biomolecule 3D structure of 6-methoxyharman	
	E Biomolecule 3D structure of Gallic acid	
	F Biomolecule 3D structure of Stearic acids	
	G Biomolecule 3D structure of Lecithin	
	H Biomolecule 3D structure of Oleic acid	
5.4.1	1A Docking of Wnt5a with Gallic acid	
	1B Docking of Wn53a with βsitosterol	
	1C Docking of Wnt5a with L-Dopa	

	2A Docking of Frizzled 1with Gallic acid	73
	2B Docking of Frizzled 1 with βsitosterol	
	2C Docking Frizzled 1with L-Dopa	
	3A Docking of LRP 5/6with Gallic acid	74
	3B Docking of LRP 5/6 with βsitosterol	
	3C Docking of LRP 5/6 with L-Dopa	
	4A Docking of β--catenin with Gallic acid	
	4B Docking of β--catenin with βsitosterol	
	4C Docking of β--catenin with L-Dopa	
	5A Docking of Disheveled with Gallic acid	75
	5B Docking of Disheveled with βsitosterol	
	5C Docking of Disheveled with L-Dopa	
	6A Docking of CyclinD1 with Gallic	
	6B Docking of CyclinD1 with βsitosterol	
	6C Docking of CyclinD1 with L-Dopa	
5.5.1A	Protein RMSD Graph of β catenin with gallic	76
5.5.1B	Protein-ligand RMSF plot	77
5.5.1C	Protein-ligand interactions	77
5.5.1D	Protein-ligand interactions	78
5.10.1A	Chromatogram of Standard Gallic acid at different concentrations	81
5.10.1B	Calibration Curve of Gallic acid	82
5.10.1C	Chromatogram of Gallic acid present plant extract	82
5.10.2A	CombiFlash Rf200i flash chromatography	83
5.10.3A	Chromatogram of Standard β –sitosterol at different concentrations	84
5.10.3B	Calibration Curve of β –sitosterol	84
5.10.3C	Chromatogram of β –sitosterol present plant extract	85
5.10.4A	A CombiFlash Rf200i flash chromatography	86
5.12.1	Normoxia cells observed under Microscope	89
5.14.1A	Cell cultured in Normoxia	89
5.14.1B	Cell cultured exposed to hypoxia.	89
5.16.1A	An Expression of Wnt5a in human PASMCs was analyzed under	96

	normoxia and hypoxia by real-time RT-PCR	
5.16.1B	Expression of β-catenin in human PASMCs was analyzed under normoxia and hypoxia by real-time RT-PCR	96
5.16.1C	The expression of CyclinD1 in human PASMCs was analyzed under normoxia and hypoxia in real time.	97
5.17.1	Wn Wnt5a gene expression in hypoxia-exposed cells treated with bioactive molecules of *Mucuna pruriens* seed extract	97
5.18.1	β catenin expression in hypoxia-exposed cells treated with bioactive molecules of *Mucuna pruriens* seed extract	99
5.19.1	Cyclin D1 gene expression in hypoxia-exposed cells treated with bioactive molecules of *Mucuna pruriens* seed extract	100

LIST OF TABLES

TABLE No.	TABLES	TABLE No.
4.5	Biomolecules present in *Mucuna pruriens* seed chosen from a literature review study.	32
4.24.1	Master Mix Composition	52
4.23.1	Primer base pairs used for amplification	53
4.23.2	Master mix composition	54
5.1.1	Protein Details	57
5.2.2	Bioactive compounds from seeds of *Mucuna pruriens*	60
5.3.1	ADME/T of selected bioactive compounds from *Mucuna pruriens seed*	62
5.4.1	Multiple docking score and glide energy score	66
5.6.1	T Binding free energies of beta-catenin gallic acid along with individual energy components contribution	73
5.17.1	Drug treatment	97
5.18.1	Drug treatment	98
5.19.1	Drug treatment	99

ABBREVIATIONS

O2	Oxygen
ATP	Adenosine5'-Triphosphate
PH	Pulmonary hypertension
PASMC	Pulmonary arterial smooth muscle cells
HPASMCs	Human Pulmonary arterial smooth muscle cells
WU	Wood Units
%	Percent
MP	*Mucuna pruriens*
MD	Molecular dynamics
RMSD	Root Mean Square Deviation
RMSF	Root mean square fluctuation
ns	Nanoseconds
MMP7	Matrixmetalloproteinase7
MMP9	Matrixmetalloproteinase7
NCBI	National Centre for Biotechnology Information
NPACT	Naturally Occurring Plant-based anti-cancer compound Activity Target
ADMET	Absorption, distribution, metabolism, elimination, and toxicity
BBB	Blood-brain barrier
MM-GBSA	Molecular mechanics generalized Born surface area.
XP	Extra precision
VCBM	Vascular cell basal media
ATCC	American Type Culture Collection
DPBS	Dulbecco's Phosphate Buffered Saline
DMSO	Dimethyl sulfoxide
MTT	3-(4,5-dimethylthiazol-2-yl)-2,5-diphenyltetrazolium bromide
PBS	Phosphate-buffered saline
IC50	Half-maximal inhibitory concentration
FBS	Fetal bovine serum
DMEM	Dulbecco's Modified Eagle's Medium
RTPCR	Real-Time Polymerase Chain Reaction
µl	Microliter
µM/L	Micro Moles per Litre
AngII	AngiotensinII
ANOVA	Analysis of Variance
nm	Nanometer
dNTP	Deoxy nucleoside triphosphate
PCR	Polymerase chain reaction
Ct	Cycle threshold
ANOVA	Analysis of Variance
µM/L	Micro Moles per Liter

NO	Nitric Oxide
NOS	Nitric oxide synthase
ROS	Reactive oxygen species
SPSS	Statistical Package for the Social Sciences
HBD	H-bond donor
HBA	H-bond acceptor
TNRB	Total number of rotatable bonds
TPSA	Total polar surface area
AMR	Atomic molar refractivity
PAH	Pulmonary artery hypertension
HPLC	High-performance liquid chromatography
RT	Retention Time
BE	β-sitosterol
CE	Crude extract
GA	Gallic acid
RVH	Right ventricular hypertrophy
LVH	Left ventricular hypertrophy
ISR	In-stent restenosis
WHO	World Health Organization
L-NAME	N^G-Nitro L-Arginine methyl Ester

ABSTRACT

Introduction: Pulmonary hypertension (PH) is a progressive, life-threatening disease characterized by vascular remodeling, constriction, and thrombosis, primarily driven by excessive proliferation of pulmonary arterial smooth muscle cells (PASMCs). Hypoxia is a key trigger in PH pathogenesis. The Wnt/β-catenin signaling pathway, critical for cell fate, migration, and organogenesis, plays a pivotal role in PH, with β-catenin mediating transcriptional activation of target genes upon Wnt ligand stimulation.

Targeting Wnt/β-catenin signaling represents a promising therapeutic strategy for PH. This study examines its role in hypoxia-exposed PASMCs and evaluates the therapeutic potential of gallic acid and β-sitosterol through in-silico and in-vitro approaches.

Objective: To study the role of isolated biomolecules from *Mucuna pruriens* gallic acid and β-sitosterol on Wnt/ β-catenin mRNA expression in the human pulmonary artery smooth muscle cells exposed to hypoxia.

Method: The current study used a computational method based on the ligand-protein interaction technique to determine the therapeutic potential of gallic acid and β-sitosterol with the Wnt/ β catenin pathway. The same compounds are used to investigate. The Invitro study explored the role of gallic acid and β-sitosterol in hypoxia-exposed PASMC lines.

Result and Discussion: The current study identified different pharmacological properties of gallic acid and β-sitosterol bioactive molecules to analyze the in silico

ADME/T properties. All were within Lipinski's rule acceptable range, and molecular docking analysis showed that β-sitosterol has more interaction sites with Wnt5a.

The Invitro study revealed that when HPASMC is exposed to hypoxia, there is downregulation of the Wnt5a gene and upregulation of the β-catenin gene. β-sitosterol and gallic acid can be attributed to inhibiting the β-catenin pathway via the downregulation of β-catenin gene expression.

Conclusion: The present study focused on in-silico phytochemical analysis and in vitro investigations to evaluate the potential therapeutic role of isolated biomolecules from Mucuna pruriens seed extract β-sitosterol and gallic acid in hypoxia-exposed pulmonary artery smooth muscle cells (HPASMCs). These findings suggest that Mucuna pruriens, or its bioactive molecule gallic acid and β-sitosterol, may exert protective effects against hypoxia-induced vascular remodeling by targeting the Wnt/β-catenin signaling pathway.

KEYWORDS

Wnt/ β catenin pathway, bioactive molecule, In silico methods, β-sitosterol, Gallic acid, Invitro study

Chapter-I

Introduction

1.1 Introduction

Oxygen (O2) is involved in many living organisms' everyday functioning and survival. It is used in the aerobic respiration process, being the last electron acceptor in the mitochondrial electron transport chain. This process produces ATP, which is the primary energy currency of the cells. Oxygen levels are well controlled but can significantly change with environmental changes, normal physiological processes, or disease. Hypoxia is a state of oxygen deficiency when the available oxygen is insufficient to fulfill cellular requirements. This condition is a significant component of many pathological conditions, such as chronic obstructive pulmonary disease, ischemic heart disease, and solid tumours (Bae, T., Hallis, et., al 2024).

Pulmonary Hypertension (PH) is a life-threatening progressive disease for which hypoxia is one of the triggers. The typical pathological changes underlying the induction of pulmonary hypertension (PH) are pulmonary vascular constriction, pulmonary vascular remodeling, and thrombosis in situ. The abnormal proliferation of pulmonary arterial smooth muscle is also the most prominent characteristic of PH, which contributes to the development and progression of pulmonary hypertension by narrowing or blocking the arteries. The newest advances in molecular medicine are focused on explaining the signaling pathways and molecular mechanisms involved in an organism's development to aid in preventing and treating diseases. The Wnt signaling pathway is one of the most advanced signaling pathways under the research focus in this concern. According to the research of (Jung, Oark et al. 2020), the Wnt/β-catenin signaling pathway is a multipurpose signaling pathway that determines the fate of cells, the migration of the cells and their polarity, and organogenesis during embryonic development. Different substrates and roles are associated with the Wnt-secreted glycoproteins.

There are many ways through which Wnts can initiate cellular responses. The response mechanisms are: 1) the canonical beta-catenin-dependent pathway, 2) the noncanonical planar cell polarity pathway, and 3) the PKC/calmodulin-dependent kinase signaling and nuclear factor of activated T cell signaling pathway. In the classic way Wnt signaling works, Wnt proteins bind to the cell surface receptors, and β-catenin is secured to the cell's nucleus to interact with target genes and activate them (Liu et al., 2022).

The proliferation of the pulmonary artery smooth muscle cell (PASMC), a crucial feature of PH, is influenced by Wnt/β-catenin signaling; the current treatments for pulmonary hypertension mainly target the contractility of the pulmonary artery smooth muscle cell (PASMC). The side effects of most of the currently used modern medicine for cardiovascular disorders are well known; thus, there is a need to look for new therapies with minimal or no side effects at all. Phytochemicals, also natural biomolecules, have recently been recommended for managing different cardiovascular diseases. It has been reported that *Mucuna pruriens* has various pharmacological properties, including analgesic, anti-inflammatory, anti-neoplastic, anti-epileptic, and antimicrobial properties. It is the most widely used plant in Indian medicine.

A medicinal plant indigenous to tropical regions of Africa and Asia, *Mucuna pruriens*, commonly called velvet bean (Lampariello et al., 2012), was the subject of the current investigation. This plant contains flavonoids and alkaloids, which are biomolecules with immune-stimulating, anti-inflammatory, and antioxidant properties (Rane et al.,2019) (Parvatikar et al., 2023). Ayurveda uses it for immune system strength and fertility. The pharmaceutical markets in India and other countries are

very interested in its medicinal applications. Adapting to warm, humid climes, it grows as a weed in waste areas and agricultural fields in Tamil Nadu, Kerala and Karnataka.

Fig 1.1.1 *Mucuna pruriens*, DC From Garden of BLDE Association's of AVS Ayurveda Maha Vidyalaya Vijayapura Karnataka

This study aims to find out how Wnt/β-catenin signaling mediates hypoxia-induced proliferation of human pulmonary artery smooth muscle cells (HPASMCs) and the effect of possible physiologically active compounds of Mucuna pruriens through both in-silico and in-vitro methodologies.

Chapter-II

Review of Literature

2.1 Hypoxia

Oxygen equilibrium is essential for life (Michiels, C. 2004). The respiratory and cardiovascular systems are the two main organs in charge of controlling this equilibrium. A breakdown in either of these systems can lead to hypoxemia and its potentially disastrous consequences. Numerous factors can contribute to hypoxia or the absence of oxygen in the body's tissues. Most often, a mismatch between ventilation and perfusion results in hypoxemia. This happens when the airflow to the lungs' alveoli (ventilation) and the blood flow via the pulmonary capillaries (perfusion) are not in sync. Therefore, oxygenated blood is not supplied to the tissues even with proper breathing, resulting in hypoxia.

2.2 Types of Hypoxias

- Depending on the duration of exposure, hypoxia can be acute (Seconds to minutes) or chronic (days to years) (Pulgar-Sepulveda et al., 2018)
- Depending on the pattern of exposure, hypoxia can be sustained or intermitted (Nanduri & Nanduri, 2007).

Moderate hypoxia is defined as oxygen concentration in the atmosphere being 8-12%, lower than the standard 21%. Sustained hypoxia is seen in high-altitude climbing and walking and also in patients with chronic obstructive pulmonary disease and cystic fibrosis. Hypoxia is the lack of oxygen; intermittent hypoxia is the temporary lack of oxygen for short periods. It is a condition when oxygen levels are low for a short time. Intermittent hypoxia is a type of hypoxia that occurs in patients with obstructive sleep apnea (Ramirez et al., 2012). Many physiological responses have been linked to hypoxia regulation, including cell division, apoptosis, and inflammation. Hypoxia induces abnormal migration and proliferation in vascular smooth muscle cells. The proliferation of VSMCs is a key event in the

pathophysiology of several vascular proliferative diseases, including atherosclerosis and pulmonary hypertension—hypoxia-induced vascular smooth muscle cell (VSMC) proliferation (Lee J. et al.,2019).

2.3 Pulmonary Hypertension (PH)

Pulmonary hypertension is a significant global health issue, especially among the elderly, and its prevalence is increasing rapidly, particularly in nations where the population is aging. Pulmonary hypertension can affect about 1% of the population, according to recent estimates (Mocumbi A. et al., 2024), and it has been estimated that the prevalence rate among those 65 and older can reach 10%. Nowadays, lung and left-sided cardiac disorders are the leading causes of pulmonary hypertension worldwide. In future decades, low-income nations will account for 80% of patients. (Hoeper, M. M., et al.2016).

Pulmonary Hypertension (PH) is characterized by the accumulation of pressure in the lungs due to the limitation of blood outflow, which can lead to heart failure (Galiè, N. et al., 2009). It affects about 7.6 cases per million, with a prevalence of 26 cases per million. Despite the recent developments, PH is still one of the deadliest diseases with a poor prognosis. About 7.6 cases per million have been reported, and the frequency is 26 cases per million. PH remains one of the fatal conditions with a terrible prognosis, even with the recent advancements. (Peacock, A. J. et al., 2007)

A mean pulmonary arterial pressure of more than 20mm HG at rest, as determined by right heart catheterization, is hemodynamically referred to as pulmonary hypertension. A minimum of 3 Wood Units (WU) of pulmonary vascular resistance further characterizes precapillary pulmonary hypertension associated with

pulmonary vascular disease. In contrast, isolated postcapillary pulmonary hypertension is defined by a pulmonary vascular resistance of less than 3 WU. The increase in mean pulmonary arterial pressure is mainly due to the rise in the left side of the heart filling pressures. (Naranjo, M, Hassoun, P et al., 2021).

Pulmonary hypertension can be classified based on the part of the involved pulmonary vasculature. The pre-capillary form is defined by increased resistance in the pulmonary arterioles, while the post-capillary form is defined by elevated pressures in the pulmonary venous system (Saini, A. S, Meredith et al., 2022). At times, both the pre-and post-capillary elements of the pulmonary circuit can be involved. Pulmonary hypertension is also associated with pathological features of vascular remodeling, inflammation, and altered vasomotor control, leading to a progressive increase in pulmonary vascular resistance (Wu, K., Zhang, Q., et al. 2017).

The onset of hypoxia causes thrombosis, pulmonary vascular remodeling, and pulmonary hypertension (PH). Initially, the most common symptom is vasoconstriction, followed by structural alterations such as artery thickening and aberrant cell proliferation. The precise processes behind these alterations in the pathophysiology of PH remain unclear (Karnati S. et al., 2021).

Pulmonary hypertension is a common morbidity seen in various interstitial lung diseases, including idiopathic pulmonary fibrosis, connective tissue disorders and sarcoidosis (Saetta et al., 2001). However, in these patients, acute respiratory failure can worsen the condition and contribute to high mortality rates. The mechanisms of the development of pulmonary hypertension in this patient population are poorly understood. However, factors such as chronic hypoxia, vascular

inflammation, and structural changes within the lung parenchyma may play a role in its development (Saetta et al., 2001).

Pulmonary hypertension-targeted therapeutic interventions are being developed with novel pharmacological agents that target specific pathways in the disease pathogenesis. However, a multidisciplinary approach is needed to optimize patient outcomes in managing pulmonary hypertension in the presence of underlying lung diseases. Thus, a significant clinical challenge remains.

2.4 Histology of pulmonary artery smooth muscle cells (PASMCs)

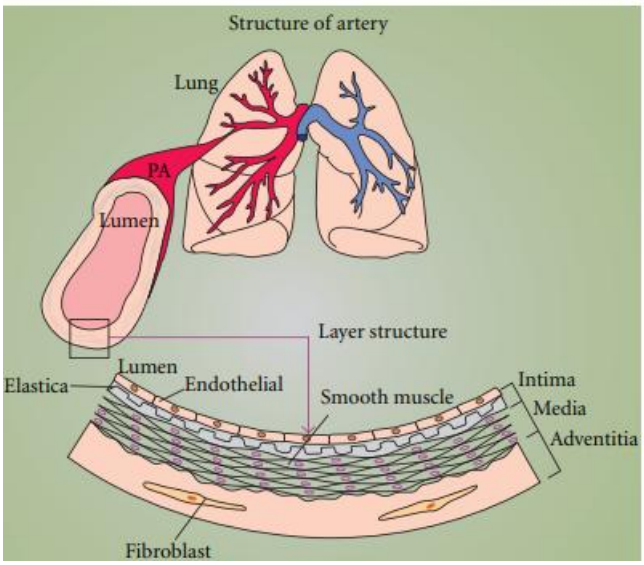

Fig 2.4.1 Three layers of Pulmonary artery smooth muscle cells

Source: Fernandez, R. A., Sundivakkam, P., Smith, K. A., Zeifman, A. S., Drennan, A. R., & Yuan, J. X. J. (2012). Pathogenic Role of Store-Operated and Receptor-Operated Ca2+ Channels in Pulmonary Arterial Hypertension. Journal of signal transduction, 2012(1).

The pulmonary artery, a key part of the cardiovascular system, delivers a lack of oxygenated blood from the heart's right ventricle to the lungs, where gas exchange occurs. The smooth muscle cells of the pulmonary artery are crucial for controlling

vascular tone and blood flow. Like other arteries, the pulmonary artery has three layers, each with its structure and function. The tunica intima is the innermost layer of the artery, and it has a single layer of endothelial cells that assist in exchanging graded nutrients and other materials. The middle layer is the tunica media, which controls the muscle tone and the diameter of the blood vessel (Fernandez, R. A., et al., 2012). Because of the ability of these smooth muscle cells to contract and relax, the pulmonary artery can change its diameter and control blood flow. The outer layer, called tunica adventitia, comprises connective tissue and provides the blood artery with structural and nutritive support. The smooth muscle cells of the tunica media are arranged perpendicularly to the vessel's longitudinal axis, which enables blood flow.

Normal and pathological stimuli may enable the smooth muscle cells of a pulmonary artery to experience different types of morphological and functional transformations. Moreover, smooth muscle cells can relax during exercise or require more oxygen. This phenomenon results in the widening of the pulmonary artery, allowing pathological changes involving vascular remodeling and resistance to blood flow (Vickery, B, Klein et al., 2017), (Zhang R et al., 2011).

Understanding the morphology and histology of the pulmonary arteries, especially their smooth muscle cells, is essential to understanding blood flow regulation and the possible etiology of several cardiovascular diseases.

2.5 Pathophysiology of Pulmonary Hypertension

Pulmonary hypertension is a complex condition with a wide range of possible underlying causes, including heart and lung disorders, blocked blood arteries and mysterious or complex processes (Christou, H. et al., 2022). This illness affects more than 1% of people worldwide. A strong argument exists for focused research

addressing this significant public health issue since it disproportionately impacts individuals in low and middle-income nations (Meredith et al., 2022).

The pulmonary hypertension mechanism is poorly understood (Sun, Y., et al., 2023). A combination of defects in vasomotor control and inflammation in vascular remodeling is believed to be the cause. Chronic obstructive pulmonary disease influences the development of pulmonary hypertension.

Pulmonary arterial hypertension is an intricate and multi-faceted illness characterized by sustained high pressure in the pulmonary arteries; if not managed, it can cause right-sided heart failure and death. Many research efforts have attempted to reveal its possible root causes and mechanisms, but no clear concept has emerged. These pathways are the mechanisms of endothelial dysfunction, alterations in signaling pathways, inflammation, and vascular remodeling.

One characteristic of pulmonary artery hypertension is remodeling of the pulmonary vasculature, which comprises thinking of the arterial walls, proliferation of smooth muscle cells, and luminal narrowing of the width (Dwivedi et al.,2021). Vascular remodeling is usually triggered by enhanced production and accumulation of various growth factors, including crucial fibroblast growth factors, platelet-derived growth factors, vascular endothelial growth factor and epidermal growth factor (Johnson, S. et al., 2023). These growth factors can cause smooth muscle cells to proliferate and migrate, giving the pulmonary arteries their characteristic morphological alteration.

The etiology of pulmonary artery hypertension is dependent on inflammation. The pulmonary arteries can constrict in excess when cytokines and chemokines are

elevated, which plays a role in underlying vascular remodeling. Macrophage accumulation has been reported to perpetuate the inflammatory process, T cell mast cells, B cells neutrophils and dendritic cells in the pulmonary capillaries of patients with pulmonary arterial hypertension (Johnson, S. et al., 2023).

Dysfunction of vasodilatory to vasoconstrictive imbalance is a characteristic feature of endothelial dysfunction associated with pulmonary artery hypertension. Pulmonary artery hypertension patients have increased endothelial 1(ET-1), a potent vasoconstrictor causing vascular remodeling and resistance (Yuan, S. M 2017).

2.6 Wnt/β-catenin signaling pathway

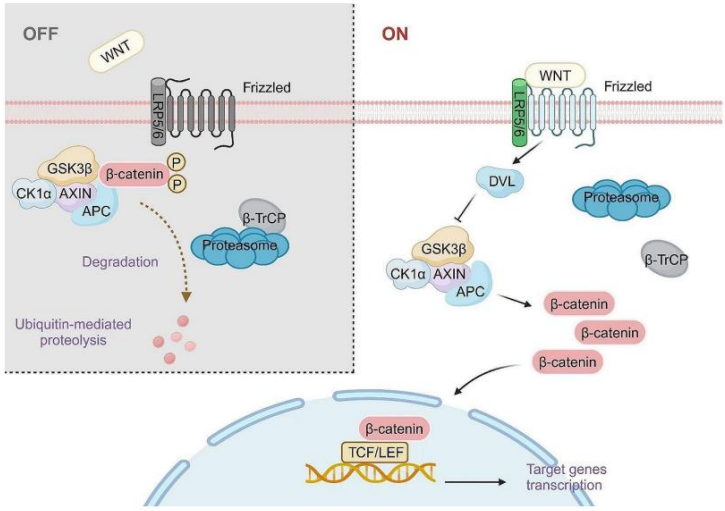

Fig 2.6.1 Wnt Wnt/β-catenin signaling pathway

Source: Song, P., Gao, Z., Bao, Y., Chen, L., Huang, Y., Liu, Y., ... & Wei, X. (2024). Wnt/β-catenin signaling pathway in carcinogenesis and cancer therapy. Journal of Hematology & Oncology, 17(1), 46.

Wnts are a group of secreted glycoproteins with different expressions and functions. The Wnt signaling pathway is one of the oldest and the most conserved among living organisms (Jung, Y. S.et al., 2020). It comprises a total of 19 ligands,

including Wnt 1, 2 2b, 3, 3a, 4, 5a, 5b, 6, 7a, 7b, 8a, 8b, 9a, 9b, 10a, 10b, 11 and Wnt 16 these are cysteine-rich proteins of approximately 350-400 amino acids that have an N- terminal signal peptide for secretion polarity migration and proliferation (Yu, X. M., et al.,2013). One Wnt ligand can have different effects on various cell types. Wnts signal intracellularly through several signal transduction pathways referred to as 1) the canonical pathway through beta-catenin, 2) the noncanonical planar cell polarity pathway, and 3) the PKC/calmodulin kinase/nuclear factor of activated T cell-dependent pathway (Sheikh et al., 2014).

The dynamic control of the transcriptional coactivator β-catenin is a key effector protein at the center of this system (MacDonald et al., 2009). When Wnt signals are not present, a destruction complex consisting of GSK3β, CK1α, AXIN and APC phosphorylates β-catenin, which is then broken down by the proteasome (Yang et al., 2012) (MacDonald et al., 2009). However, the Wnt ligands binding to its receptor stops this degradation complex, allowing β-catenin to stabilize and build up in the cytoplasm (MacDonald et al.,2009)

β-catenin travels to the nucleus after stabilization and binds to TCF/LEF transcriptional factors. This creates a transcriptional cascade that sends to a series of target genes that regulate cell survival, differentiation, and proliferation (Yu, F. Yu C. et al., 2021). This signaling cascade is crucial for embryo development because it maintains adult cell populations and guides the production of various tissues and organs (Hiremath S. et al., 2022). Additionally, it plays a crucial role in canonical Wnt signaling.

The Wnt/ β-catenin canonical pathway has been linked to multiple human diseases. Several malformations, osteoporosis, and cancer have been related to this

failure in the pathway (Yang et al.,2015). For example, oncogenesis in colorectal cancer, breast cancer leukemia, and malignant cell growth have been attributed to genetic disorders that activate the Wnt / β-catenin pathway wrongly (Liu, J., Xiao et al., 2022). However, Wnt / β-catenin signaling deficits have been implicated in developmental and degenerative issues.

The intricate relationship between the canonical Wnt/β-catenin pathway and another signaling cascade and their roles in modulating the immune response has long been well known. Targeting the Wnt/β-catenin pathway could be a promising approach for treating many human diseases, and they have developed new therapeutic intervention options. In order to establish an individualized treatment plan, one should understand the intricate mechanism of the canonical Wnt/β-catenin pathway and its multiple biological activities. In addition, more studies are being conducted to understand how the canonical Wnt/β-catenin pathway intersects with other signaling pathways and how its malfunctions result in disease.

2.7 Role of Wnt/β-catenin signaling pathway in Pulmonary hypertension.

The development and progression of pulmonary artery disease, a possibly fatal disorder, have been associated with disruption of the Wnt/β-catenin signaling pathway, based on scientific evidence (MacDonald et al., 2009) disruption of the Wnt/β-catenin signaling pathway—the pathologic alteration of this disease involving vasoconstriction and pulmonary endothelium. Abnormal Wnt/β-catenin signaling has indeed been found in the pulmonary vasculature of animal models and humans with pulmonary artery hypertension. This indicates that the biological pathway this represents could be a viable therapeutic candidate for controlling this paralyzing

disease. Even though the precise way Wnt signaling plays a role in developing pulmonary artery hypertension is unknown, ongoing research suggests that it can do so by different pathways(Dejana,2010).These are by stimulating fibroblast differentiat ion into myofibroblasts, increasing pulmonary vascular cell migration and proliferation, and controlling the expression of genes that manage vascular remodeling and tone.

Further studies have been conducted on the function that Wnt/β-catenin signaling has in pulmonary artery hypertension development. The noncanonical Wnt ligand Wnt 11 been revealed to induce cardiomyocyte growth by inhibiting the canonical Wnt/β-catenin pathway via a caspase-dependent process (Abdul-Ghani et al., 2010) By regulating key vasomotor proteins such as serotonin endothelin 1 and hypoxia-induced factor 11α, the Wnt signaling pathway also plays a role in the pathogenesis of pulmonary artery hypertension.

Even though many of the functions of Wnt/β-catenin signaling in emerging pulmonary arterial hypertension are becoming more well-defined, more research is necessary to fully comprehend the mechanism at play and identify potential targets within these pathways. More research is necessary because much remains known about the function of Wnt/β-catenin signaling within this condition. The pathophysiology of pulmonary artery hypertension and Wnt signaling system can be studied further to discover novel methods of developing a targeted treatment that could improve patient outcomes.

2.8 The Interplay of Wnt/β-catenin Signaling, Pulmonary Hypertension, and Hypoxia

The deficiency of oxygen, Hypoxia is a recognized etiology of pulmonary hypertension. Nevertheless, recent research indicates that the pathogenesis of hypoxic pulmonary hypertension includes the Wnt/β-catenin pathway (Dejana, 2010).

Earlier research has shown that the Wnt/β-catenin signaling pathway is elevated in different subtypes of pulmonary hypertension, including idiopathic, heritable and those associated with primary lung or congenital heart disease (Shang et al., 2017). Hypoxia has been shown to stabilize and induce nuclear accumulation of β-catenin, an essential element of the canonical Wnt signaling pathway. In pulmonary hypertension, nuclear accumulation of β-catenin leads to increased activity of the cell nucleus, promoting gene transcription to produce proteins that support cell migration, proliferation, and survival.

Hypoxia, pulmonary hypertension, and Wnt/β-catenin signaling are intricately connected to imply a highly complex linkage. According to (Yuan, 2017), β-catenin has been observed to interact with and stabilize hypoxia-inducing factor 1α, one critical regulator of the cellular response to low oxygen levels, thereby enhancing Wnt/β-catenin signaling. According to (Dejana, 2010), the Wnt/β-catenin pathway also regulates the vascular tone and remodeling, both critical events in the development of pulmonary hypertension.

The development of pulmonary hypertension, especially in hypoxia, is highly influenced by the Wnt/β-catenin signaling system (Shang et al., 2017) (MacDonald et al., 2009). The operation of this signaling system in the interaction of hypoxia and pulmonary hypertension may lead to the identification of new treatment strategies

against this crippling disease. Hence, understanding how hypoxia and Wnt/β-catenin signaling converge in generating pulmonary hypertension may provide yet another avenue for developing targeted therapy and better patient care.

2.9 *Mucuna Pruriens* (MP)

Traditional medicinal systems used *Mucuna pruriens*, the Velvet bean, but it thrives more in Africa and India (Moghadamtousi et al., 2015). According to (Senthilkumar et al., 2018), various ailments have been treated with herbs, in particular, diabetes, Parkinson's disease, male infertility, and other neurological disorders. Recent scientific investigations have confirmed many traditional claims regarding the mechanisms and active phytochemicals behind the mentioned therapeutic effects. Thanks to the abundance of phytochemicals, which include secondary metabolites such as L-Dopa, alkaloids, flavonoids, and phenolic substances, this plant has excellent promise as a therapeutic one. Numerous scientific investigations have concentrated on these biomolecules, which have strong and beneficial impacts on several physiological systems.

About 150 species of annual and perennial legumes in the genus *Mucuna pruriens* belong to the Fabaceae family, the Papilionaceous sub-family. An annual climbing legume native to Southern China and Eastern India was once used as a green vegetable crop. Traditionally, *Mucuna pruriens* has been used in ancient Indian medicine, Ayurveda, to assist in managing Parkinson's disease. *Mucuna pruriens* is said to be effective against Parkinsonism and have neuroprotective properties, which may result from antioxidant activity. Additionally, it is used as an aphrodisiac and to cure neurological disorders and male infertility.

For our study, we collected *Mucuna pruriens* plant seeds from APMC Vijayapura Karnataka and the Garden of BLDE Association's AVS Ayurveda Maha Vidyalaya Vijayapura, Karnataka.

Fig 2.9.1 *Mucuna pruriens*, DC From Garden of BLDE Association's AVS Ayurveda Maha Vidyalaya Vijayapura Karnataka

2.10 Biomolecules from Mucuna pruriens (β-sitosterol, Gallic acid)

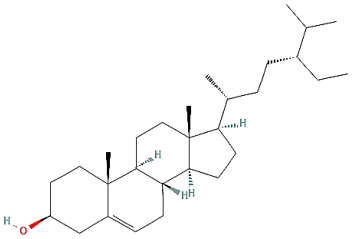

Fig 2.10.1 A β-sitosterol

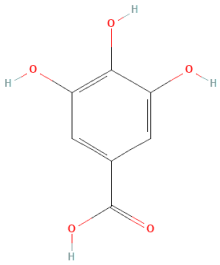

2.10.1 B. Gallic acid

Source: Moreno-Calvo, E., Temelli, F., Cordoba, A., Masciocchi, N., Veciana, J., & Ventosa, N. (2014). A new microcrystalline phytosterol polymorph was generated using CO2-expanded solvents. Crystal Growth & Design, 14(1), 58-68.

The plant-derived phytosterol compound β-sitosterol therapeutic potential has been the subject of intense scientific investigation due to its potential to aid in managing several medical problems. Although it has structural similarities with cholesterol, β-sitosterol and other phytosterol have been studied for their potential to regulate physiological processes. (Hannan et al., 2020)

According to research, a primary mechanism in the development and spread of cancer, tumour angiogenesis can be inhibited by phytosterols such as β-sitosterol and other plant sterol components. It has shown that β-sitosterol directly affects the signaling pathway that controls the growth of blood vessels. It prevents the development of new arteries that supply oxygen and nutrition to tumours, depriving cancer cells of the food they need to survive.

There have been investigations on using the beneficial chemical β-sitosterol to include low-fat and reduced-fat foods. These new formulations of foods would utilize the established cholesterol-lowering properties of β-sitosterol. They would offer a feasible approach to improving cardiovascular health without significant changes in dietary behavior.

Gallic acid is a constituent of naturally occurring substances; however, the genuine interest that this phenolic compound has aroused has everything to do with its extraordinary bioactive characteristics and promising medicinal applications (Cabral E. et al.,2017). This study attempts to acquire an overview of such wondrous phytochemicals and their multiple products.

The hydroxyl phenolic group in the chemical structure of gallic acid is thought to contribute significantly to its potent antioxidant action, which has already been

shown in several studies (Choubey et al., 2018). Furthermore, due to its anti-oxidation qualities, gallic acid is promising as a chemical for various medical purposes to protect the body from the negative impacts of reactive oxygen species and free radicals. The other discovered qualities of gallic acid are its antibacterial, anti-diabetic, and anti-tyrosinase effects (Choubey et al., 2018).

Even outside its medicinal function, gallic acid was known to have some industrial use, as already mentioned. In research, Schiff-base derivatives of this compound have been synthesized and studied for their analgesic, anti-inflammatory, and anticonvulsant properties. Gallic acid indanone derivatives have also been reported to exhibit anticancer activity, which speaks for the wide-ranging medicinal uses of this phytochemical.

2.11 In-silico analysis/Wnt/β-catenin signaling pathway/*Mucuna pruriens*

Many biological sciences have used bioinformatics, and the subject has been essential in improving important fields like forensic DNA analysis and knowledge-based medication design to agriculture biotechnology (Cheba et al., 2019). The Wnt/β-catenin signaling system can be altered to aid in developing novel therapies for PAH. Considering the curative implications of *Mucuna pruriens* in numerous diseases, the present work was undertaken to examine the interactions of different components of *Mucuna pruriens* plant seeds with Wnt/β-catenin pathway at its components such as Wnt 3a, Frizzled 1, LRP 5/6, β-catenin, Disheveled, cyclin D1 by in silico analysis. The proposed work is based on computational analysis by a Swiss ADME server on the putative drugs to be administered and their ADME/T properties.

To identify the molecular interaction pattern, Schrodinger, a standalone software, was used to predict the interaction of bioactive molecules of *Mucuna Pruriens* with the target proteins involved in the Wnt/ β catenin pathway. The top docked complex simulation pattern was subjected to Molecular dynamic (MD) simulation in Desmond for 100 ns. Biomolecules from *Mucuna Pruriens* are drug-like and essentially non-toxic. Three compounds (L-dopa, β-sitosterol, and gallic acid) among the nine compounds screened in the docking study interact well with target proteins. The docked complex was subjected to MD simulation since gallic acid interacted well with all the target proteins. It was stable throughout the simulation time in terms of RMSD and RMSF. The present study's results indicate that the *Mucuna pruriens* biomolecule can potentially improve pulmonary vascular disease. Their effectiveness and pharmacological activity need to be thoroughly established by additional in vivo and in vitro research. (Bhosle S et al.., 2024).

2.12 Invitro analysis/Wnt/β-catenin signaling pathway/*Mucuna pruriens*

According to He and Gan (2023), the Wnt/β-catenin signaling axis is the major regulator of, among other things, motility and growth differentiation. Changes in the pathway are thought to play a role in the initiation and progression of various tumors, among them colorectal cancer. Moreover, it was shown in the study that various phytochemicals, including *Mucuna Pruriens*, can be used therapeutically in targeting and regulating this signaling cascade (Huang et al.,2019).

Mucuna pruriens, a tropical legume with several pharmacological properties, has long been utilized in the medical system (Li et al., 2019). Recent research suggests that *Mucuna pruriens* and its components influence the migration and invasion of cancer cells through the Wnt/β-catenin signaling pathway. The extract of

Mucuna pruriens inhibited cell migration and invasion of colorectal cancer cells through modulating/altering the expression of Wnt/β-catenin target genes MMP7, MMP9, and ZEB1-another property responsible for the inhibition of this invasion (Li et al., 2019).

Chapter-III

Aim & Objectives

3.1 Research Question

If hypoxia exposure alters the Wnt/β-catenin signaling pathway in human pulmonary artery smooth muscle cells, and can the bioactive molecules of Mucuna pruriens seeds modulate this signaling pathway?

3.2 Aim

To study the role of Wnt/ β-catenin signaling in the hypoxia-exposed human pulmonary artery smooth muscle cells and the effect of isolated bioactive molecules of *Mucuna pruriens* seeds.

3.3 Objectives

1. Assessment of interaction between bioactive molecules of *Mucuna Pruriens* seeds with Wnt/β-catenin signaling by in-silico studies.

2. Phytochemical extraction, identification, and isolation of bioactive compound(s) from *Mucuna pruriens* seeds.

3. To study the Wnt/β-catenin mRNA expression in the human pulmonary artery smooth muscle cells exposed to hypoxia and to investigate the effect of isolated bioactive molecule(s) of *Mucuna pruriens* on Wnt/ β-catenin mRNA expression in them.

3.4 Hypothesis

Wnt/β-catenin mRNA expression may be altered in human pulmonary artery smooth muscle cells exposed to hypoxia, which may be modulated by bioactive molecules of *Mucuna pruriens*

Chapter-IV

Materials & Methods

STUDY DESIGN

1. *In-silico* Analysis
2. Phytochemical extraction, identification, and isolation of bioactive molecule of *Mucuna prurines*.
3. Invitro Studies.
4. Gene Expression studies

4.1 Objective 1 *In-silico* Analysis

4.1.1 List of data Bases tools/software used *in silico* analysis

The present investigation was performed in an Intel® Core™ i5-11th gen HP processor laptop. The software and databases used for the current study:

1. Pubmed (Harjacek M, et al 2000)
2. Pubchem (Kim S, et al., 2019)
3. NCBI (Sayers E.W, et al., 2020)
4. Swiss model (Waterhouse A, et al 2018)
5. Uniport (UniProt Consortium. 2019)
6. PDB sum (Laskowski R.A, et al., 2018)
7. NPACT (Shapovalov M.V, et al 2011)
8. Auto dock 4.2 (Morris G.M et al., 2009)
9. Discovery studio visualizer (BIOVIA, Dassault Systèmes. 2017)
10. Protein data bank (Burley S. K et al., 2017)

4.2 Target protein Preparation:

Retrieval of the target protein from RCBS-PDB (http://www.rcsb.org/pdb)

The Wnt/ β-catenin signaling pathway components (Wnt 5a, Frizzaled1, LRP5/6, β-catenin, Dishevelled, CyclinD1) are chosen as a target protein for this study. The 3-D crystal structure of the target proteins Wnt 5a (PDB ID 7DRT), Frizzaled1 (PDB ID

4IU6), LRP 5/6 (PDB ID 3S8V), β-catenin (PDB ID 1LUJ), Dishevelled (PDB ID 6ZC7), CyclinD1(PDB ID 5VZU) were obtained from the Protein Data Bank (Kirubhanand, C.et al., 2020). The protein structures were then imported into Accelrys Discovery Studio for further analysis. Non-receptor atoms, including water molecules, ions, and various compounds, were removed from the systems. The resulting protein structures were then prepared for docking studies.

4.3 Screening of biomolecules:

Retrieval of the chemical structure of bioactive molecules from PubChem and NPACT

Biomolecules from *Mucuna pruriens* plant seeds were chosen based on the literature review; there are a total of nine molecules from the plant were selected, and the corresponding compound structures were obtained from the database of PubChem and Naturally Occurring Plant-based Anti-cancer Compound-Activity-Target database NPACT (Madagi et al., 2018). In order to examine the compound's drug-likeness quality, its canonical smile is taken, including hydrogen atoms that neutralize charged groups and refine their geometrical properties; all ligands were prepared for molecular docking. Table 4.3.1 lists the nine biomolecules selected for investigation based on the literature research.

S.No	BioMolecules	PubChem ID
1	L-Dopa	6047
2	Glutathione	124886
3	Lecithin	823
4	Galic Acid	370
5	B-sitosterol	222284
6	6methoxyharma	135053166
7	Stearic acid	18962935
8	Oleic acid	23665730
9	Linolic Acid	5282798

Table 4.3.1: Biomolecule present in *Mucuna pruriens*

4.4 Analysis of Drug Likeness Properties

The SWISS ADMET tool analyzed the ADMET properties of biomolecules from *Mucuna pruriens* plant seeds (Parvatikar et al .2022). These properties are vital to determine the drug's ability to cross blood-brain barrier (BBB) permeability and oral bioavailability in humans. This tool employs computational methods to estimate the physicochemical properties of a molecule and its structure; how easily this molecule can cross the blood-brain barrier is tremendously important in dictating whether or not it reaches its target in the brain itself. Oral availability in humans will measure how fast and effectively a drug is absorbed and reaches its target in the body after it passes through the gastrointestinal tract. The SWISS ADMET tool predicts properties through machine-learning algorithms based on the molecule (Parvatikar et al., 2013).

4.5 Molecular interaction study:

The molecular interaction study was designed using Schrodinger software, where the interactions of all proteins (Wnt5a, Frizzled, LRP 5/6, β-catenin, Dishevelled, Cyclin D1) with ligands *Mucuna pruriens* (biomolecule) were calculated by a genetic algorithm. A grid box at the centroid of the binding sites was generated and docked in three stages using GLIDE v6.7 (Huey et al., 2012). For the top ten leads, a selected substrate, and the exiting inhibitors, each energy of binding available to each target was calculated using the Prime/MM-GBSA (Parvatikar et al., 2022).

Grid generation around the active site of a target protein is essential for docking studies. A 10 x 10 x 10 Å cubic grid box was established around the β-catenin protein active sites using Glide v5.9 (Schrödinger, 2014), (Hema et al., 2020) (Sandeep et al., 2017). The van der Waals radii scaling factor was assumed to be 1.0

to recognize nonpolar receptor regions, with a partial atomic charge of 0.25 in GH during receptor grid generation.

The glide XP docking method was used to improve the correlation between scoring and binding poses and diminish false positives (Friesner et al., 2006). The different centers of the ligand were placed at 1 Å grid intervals with flexibility for rotation around three Euler angles. False binding modes were then assessed for preliminary score values based on their likelihood of occurrence. Docking solutions were refined under the OPLS-2005 force field with Monte Carlo simulated post-docking minimization for ligand torsion and rigid body movements. The Glide Scoring function computed the optimal docking poses (Hema.et al., 2015) (Sandeep. et al., 2017).

4.6 Molecular Dynamics Simulations (MD Simulations)

MD simulation has been carried out to study the changes in the conformation of the docked complex during the interaction. In this study, energy and force calculations were performed on the docked complex using the Desmond software throughout the simulation. This software can be integrated into a molecular modeling environment and analysis and viewing tools (Chow et al., 2008). A minimized solvated system was used to run the MD for 100 ns at normal pressure (1.01 bar) and temperature (300 K). After simulation, a simulation interaction diagram was constructed to analyze MD results, such as the plots for protein-ligand RMSD and protein-ligand interactions throughout the simulation (Kumar et al., 202).

4.7 (MM-GBSA) analysis: Molecular mechanics generalized Born surface area.

The changes in the position and orientation of the ligand during the simulation study led to modifications in the binding affinity and free energy. Predicting these energies will lead to a better understanding of the movement of the ligand. Molecular Mechanics Generalized Born Surface Area (MM-GBSA) Analysis is the most efficient and compatible technique for calculating binding energies. The MM-GBSA calculations of the composite ligand-protein complexes were done using the Prime module of the Schrodinger software. (Khaparkhuntikar et al., 2024)

4.8 Objective 2 Phytochemical Extraction:

4.9 Phytochemical extraction, identification, and isolation of bioactive molecule of Mucuna pruriens flow chart

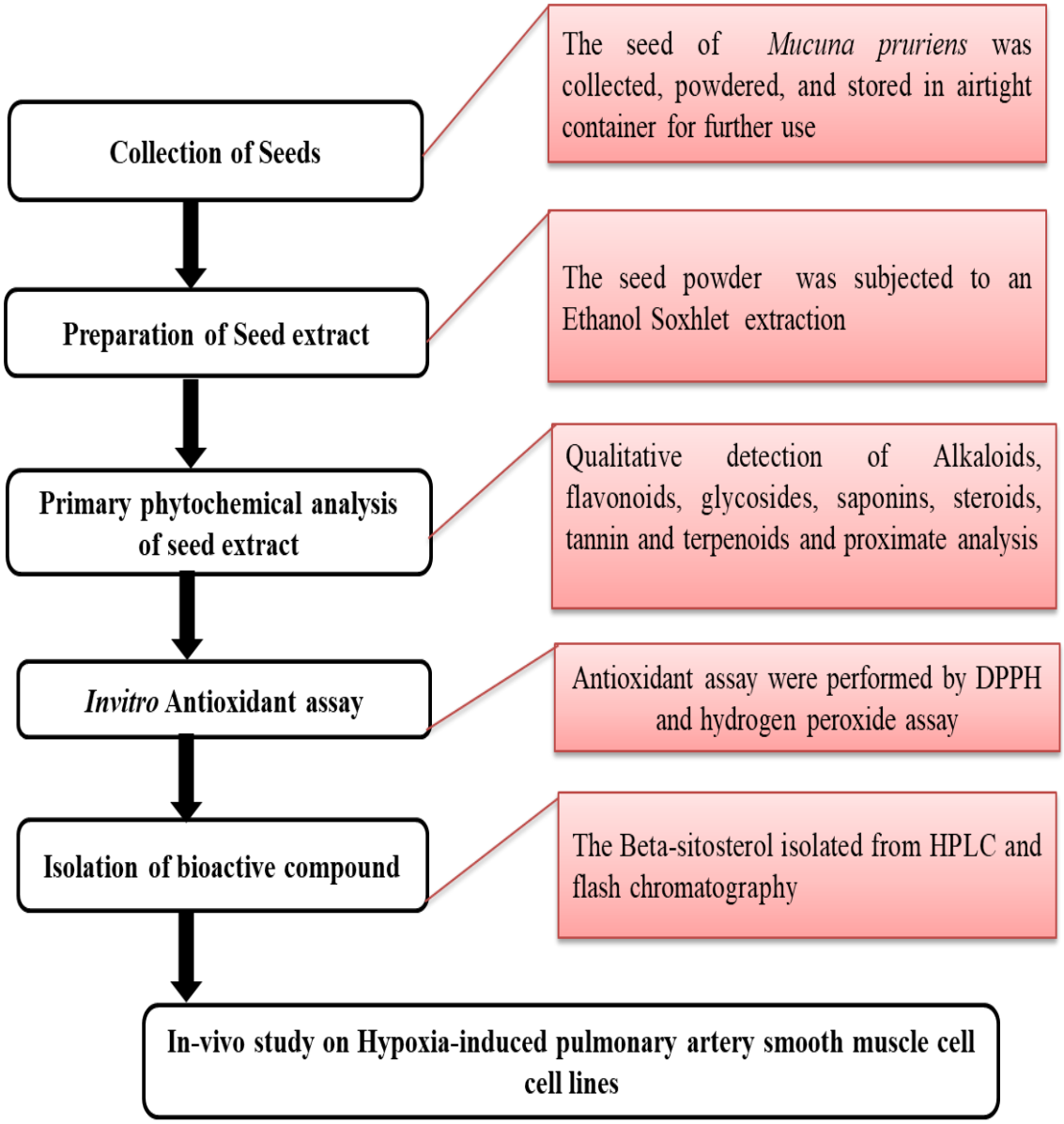

4.10 Collection of Seeds

Mucuna pruriens seeds were collected from the local market and Garden of BLDE Association's AVS Ayurveda Maha Vidyalaya Vijayapura Karnataka, India. The plant seeds were given for authentication to the Department of Dravyaguna BLDE Association of AVS Ayurveda Maha Vidyalaya Vijayapura Karnataka. The seeds were dried under shade and made into a powder. Fig 4.9.1 shows the Mucuna pruriens seed and powder diagram.

Fig 4.10.1 *Mucuna pruriens* seed and powder diagram.

4.11 Preparation of Plant Extract

The *Mucuna pruriens* seeds were cleaned in 99.9% ethanol to remove any surface contaminants (Cowley et al.,2020) and then shade-dried to remove moisture. A laboratory-grade grinder was used to grind them to get the course powdered.

Soxhlet was used for extraction.99.9% pure ethanol was used as a solvent for extraction because of its strong polarity and ability to extract a wide range of phytochemicals. The temperature was controlled between 50°C and 60°C, and cycles during extraction were counted. After extraction, the rotary evaporator removed the solvent from the extract. In order to minimize the extract thermal breakdown and guarantee effective solvent recovery, this procedure was carried out at low pressure. The yield of extract was noted. Figure 4.10.1 shows the Soxhlet.

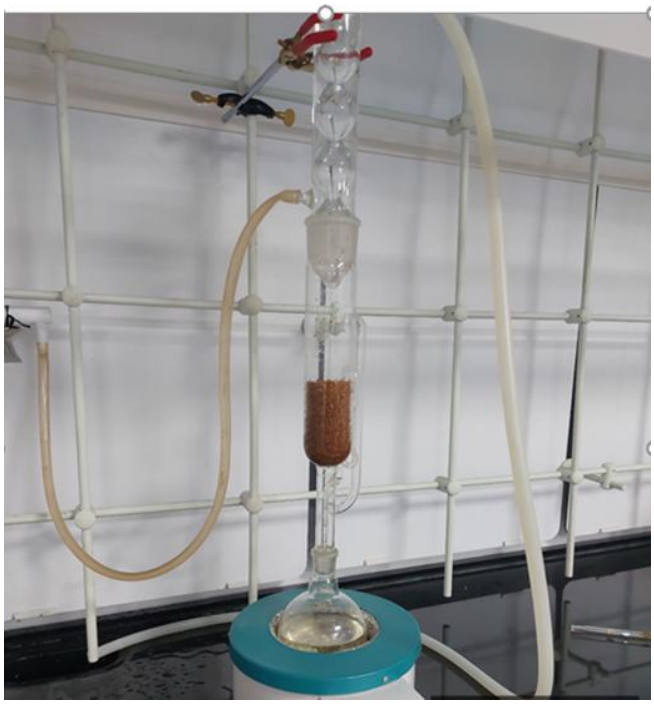

Figure 4.11.1 Soxhlet apparatus for extraction

4.12 Identification and isolation of bioactive molecules from *Mucuna pruriens* seeds

Research on natural products depends on separating and purifying biomolecules (Compounds) from plant sources. Various analytical techniques may isolate and characterize the compounds, including HPLC and flash chromatography. HPLC tested the plant extract for specific compounds, while flash chromatography isolated the compounds from the plant extract.

Instrument Details

HPLC is a powerful analytical technique identifying and quantifying various bioactive compounds from active plant extracts. Figure 4.11.1 JASCO AUTOSAMPLER

- HPLC System Name: JASCO Autosampler
- Stationary phase: Eurosphare, C18, 3.9× 150 mm
- Column oven temperature: 30ºC
- Mobile phase: A mobile phase consisting of A (water) and B (acetonitrile)
- Detection wavelength: 280 nm
- Flow rate: 1.0 ml/min
- Injection volume: 20 µl
- Detector; Diode array detector

Figure 4.12.1 JASCO AUTOSAMPLER

Flash Chromatography

Flash chromatography is a relatively fast purification technique that uses air pressure to separate compounds based on their solubility and polarity. Flash chromatography has proved helpful in pharmaceutical and natural product research applications in various fields. This research employed flash chromatography to isolate compounds from plant extract—details on chromatographic conditions for isolating gallic acid and beta-sitosterol.

- Column and Conditions:
- Column: Silica 4g column, Flow Rate: 18 ml/min.
- Solvents: Methanol (Solvent A) and water (Solvent B).
- Equilibration Volume: 33.6 ml, Air Purge: 0.5 minutes, Loading Type: Solid.

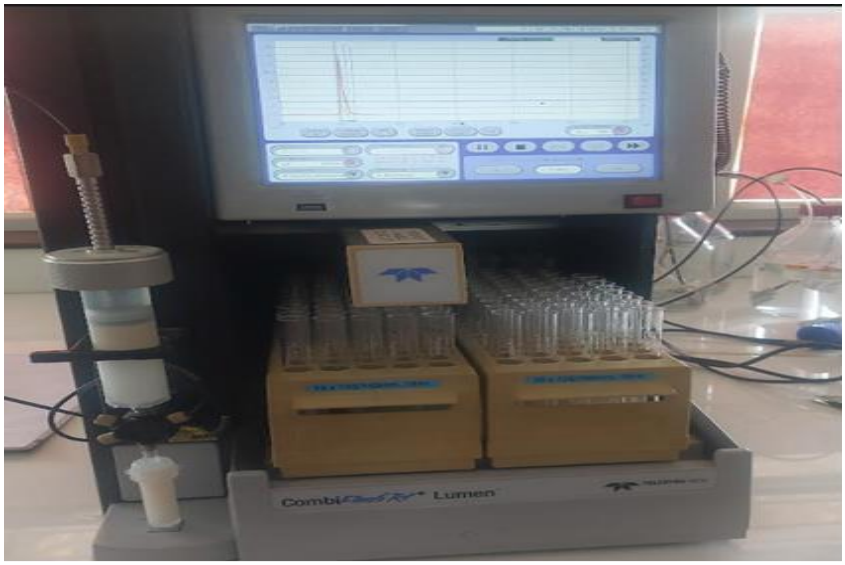

Figure: 4.12.2 Combi Flash RF^{+} Lumen

4.13 Objective 3 In-vitro Study Design

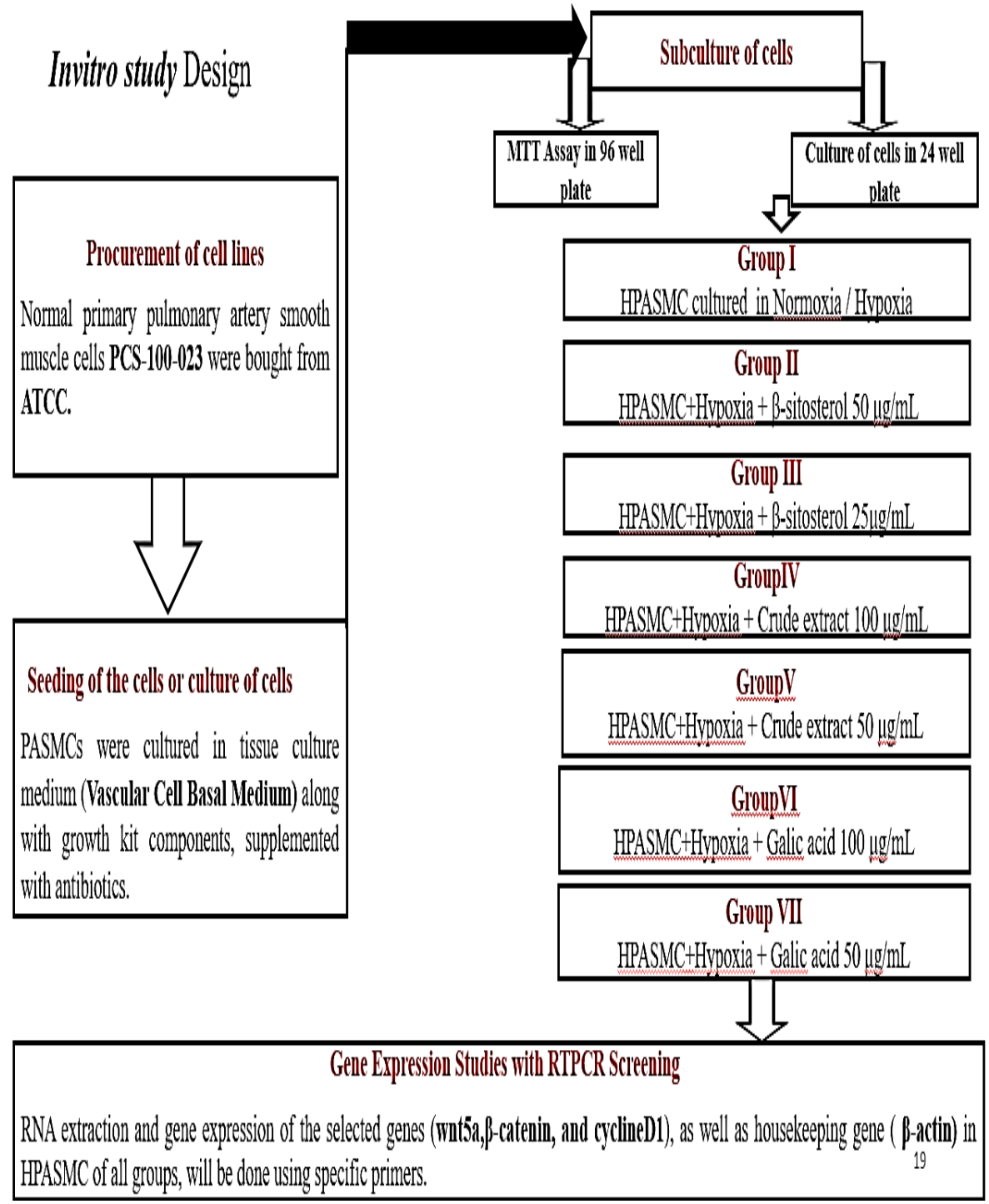

4.14 Description of Pulmonary Artery Smooth Muscle Cell Line

Normal primary pulmonary artery smooth muscle cells PCS-100-023 were brought from ATCC (American Type Culture Collection). Details of cell lines are given below.

- Cell Type: Pulmonary artery
- Organism: Human
- Volume: 1.0 mL
- Product format: Frozen
- Storage conditions: Vapor phase of liquid nitrogen

4.15 Preparation of Complete Growth Media

A growth kit was removed from the freezer, and the cover on each part was tightly closed. They were thawed before adding the growth kit contents to the basal medium. The L-glutamine content was added to the basal medium following warming in a water bath at 37°C and shaken to remove any precipitates. We removed 475 mL of Vascular cell basal medium (VCBM) from the freezer and sanitized the bottle with 70% ethanol. The volume of every growth kit component was added to the basal medium bottle, and a different sterile pipette was used each time in an aseptic manner and within a laminar air flow hood. Growth kit components are listed below.

- rh FGF-basic, 0.5 mL,
- 5 ng/mL rh
- Insulin, 0.5 mL, 5 µg/mL
- Ascorbic acid, 0.5 mL, 50 µg/mL
- L-glutamine, 25.0 mL,
- 10 mM rh EGF, 0.5 mL, 5 ng/mL
- Fetal Bovine Serum, 25.0 mL, 5%

4.16 Seeding of Cells or Culture of Cells

To begin with, the complete growth media was prepared, followed by the initiation of the culture. Subsequently, each flask was plated with 5 mL of complete growth media per 25 cm^2 surface area, and then they were placed in a 37°C, 5% CO_2 humidified incubator for 30 minutes such that they were equilibrated. Meanwhile, a single vial of ATCC PCS-100-023 was quickly thawed with a 37°C water bath for 1-2 minutes to minimize contamination risk. The vial was then cleaned with 70% ethanol. In an aseptic way, the desired volume of growth media was loaded into a sterile conical tube [(1 mL x number of flasks) - 1 mL]. Cells from the cryovial were carefully moved to the conical tube and stirred happily. A 1.0 mL of the cell suspension was aliquoted into each equilibrated flask. Subsequently, the filled flasks were hermetically sealed, slightly wobbled so the cells could be ubiquitously distributed, and then incubated at 37°C with 5% CO_2 for at least 24 hours before the subsequent treatment. (ATCC PCS-100-023 guideline).

4.17 Subculturing Procedure

1. When cells reached approximately 80% confluence, the passage of normal vascular smooth muscle cells was performed.
2. The trypsin-neutralizing solution and the Trypsin- EDTA were brought to room temperature before dissociation. Before using the cells, the entire growth medium was heated to 37°C.
3. Without causing any disruption to the monolayer, the spent media was aspirated from each flask.
4. 1 to 2 mL of Preheated trypsin-EDTA solution was added to each flask.
5. The Trypsin EDTA solution was thoroughly covered over the cells by gently tilting

6. The flask was lightly tapped on multiple sides to encourage the detachment of cells from the surface of the flask, and cells were checked using the microscope to ensure cell detachment.
7. Once it seemed that most cells had detached, an equal amount of trypsin-neutralizing solution was rapidly added to every flask.
8. Dissociated cells were placed into a sterile centrifuge tube and put aside as any remaining cells within the flask were processed.
9. Pour 3 to 5 mL of D-PBS into the flask to get any remaining cells that may have been left on it.
10. Removed the cell/D-PBS mixture into the centrifuge tube of the trypsin-EDTA-dissociated cells.
11. Repeated steps 10 and 11 as many times as needed in order to collect all of the cells out of the flask
12. Centrifuged the cells at 150 x g for 3 to 5 minutes.
13. Aspirated the neutralized dissociation solution from the cell pellet and resuspended the cells in 2 to 8 mL of fresh, pre-warmed, complete growth medium.
14. Counted the cells and seeded new flasks at a density between 2,500 and 5,000 cells per cm^2.
15. Incubate the newly seeded flasks at 37°C, 5% CO_2, for a minimum of 24 to 48 hours before further processing the cells.

(PASMC ATCC PCS-100-023 Guideline).

4.18 MTT Assay for cell cytotoxicity and cell viability.

We bought the Human pulmonary artery smooth muscle cell line from ATCC. Two biomolecules, β-sitosterol and gallic acid, were isolated by flash chromatography and identified by HPLC from *Mucuna Pruriens*. Cytotoxicity of the biomolecules and crude extract of the plant was assessed by the MTT method on the HPAMC cell line. HPASMC cells were cultured with a density of 10,000 cells/well (200 µl) using vascular smooth muscle cell basal media and placed in the incubator for 24 hours at 37°C and 5% CO_2.

Stock solution of β-sitosterol 10 mg/mL was stored in DNA grade ethanol, plant crude extract, and gallic acid at 10 mg/mL in 99.9% ethanol. HPASMC cells were treated after 24 hours with increasing concentrations of each compound from 200 to 6.25 µg/mL in duplicate using vascular smooth muscle cell basal media and incubated for another 24 hours at 37°C and 5% CO_2.

Cells were washed twice with Phosphate-buffered saline (PBS) and treated with 20 µL of 0.5% MTT solution in PBS for 4 hours. Formazan crystals developed after 4 hours were dissolved in 150 µL Dimethyl sulfoxide (DMSO), and the absorbance was read at 570 nm. IC_{50} values of the three compounds against the HPASMC cell line were calculated from the percentage cytotoxicity.

4.19 Culture of Cells for Normoxia

Human pulmonary smooth muscle cells (HPSMC) were cultured in a 24-well plate in a vascular smooth muscle cell basal media containing 20% FB under normoxic conditions. The cells were initially incubated at 37°C for 24 hours in an atmosphere containing 21% oxygen, 72% nitrogen, and 5% carbon dioxide (Yu, X. M., et al.,2013).

4.20 Culture of cells for Hypoxia condition and treatment of cells with bioactive compounds from *Mucuna pruriens.*

Human pulmonary smooth muscle cells (HPSMC) were cultured in a 24-well plate in vascular smooth muscle cell basal media containing 20% fetal bovine serum (FBS) under normoxic conditions (21% oxygen, 5% carbon dioxide,74% nitrogen) (Yu, X. M., et al.,2013). Following this incubation, the cells were removed from the incubator, and the previous media was aspirated. Fresh serum-free media, specifically vascular smooth muscle cell basal media supplemented with 2% FBS, was added to each well. The cells were then exposed to hypoxic conditions (2 to 5% oxygen, 92% nitrogen, and 5% carbon dioxide) for 24 to 48 hours to induce hypoxia.

After the hypoxic incubation period, the cells were treated with serial dilutions of the test compounds at concentrations ranging from 100 µg/mL to 12.5 µg/mL, including β-sitosterol, plant crude extract, and gallic acid, without disturbing the hypoxic conditions, in duplicate.

Our study grouped hypoxia-exposed cells into seven groups and treated them with *Mucuna pruriens* seed extract biomolecules. Group I cells were cultured in normoxia and exposed to hypoxia. In Group II, hypoxia-exposed cells are treated with 50 µg/mLβ-sitosterol. In Group III, hypoxia-exposed cells are treated with 100 µg/mL β-sitosterol. In Group IV, hypoxia-exposed cells are treated with 50 µg/mL of crude extract. In Group V, hypoxia-exposed cells are treated with 100 µg/mL of crude extract. In Group VI, hypoxia-exposed cells are treated with 50 µg/mL of gallic acid. In Group VII, hypoxia-exposed cells are treated with 100 µg/mL of gallic acid.

After the treatment, the 24-well plate was removed from the incubator, and the media was carefully aspirated from each well. The cells were washed twice with 200

µL of PBS to remove residual and non-adherent media. Following the washes, 200 µL of trypsin-EDTA was added to each well to facilitate cell detachment. The plate was incubated at 37°C for 3-5 minutes to allow the trypsin to act.

Once the cells were detached, Dulbecco's Modified Eagle's Medium (DMEM) serum media was added to each well to neutralize the trypsin. The contents of each well were then transferred to separate 5 mL tubes. The tubes were capped and gently inverted to thoroughly mix the cells and media

4.21 Gene Expression Study Design

- RNA Isolation
- RNA Quantification
- cDNA Synthesis
- RT -PCR
- Data analysis

4.22 Protocol for Isolation of RNA from Cells

RNA isolation for both normoxia and Hypoxia cells was done using the TRizol method. Collection of cells Normoxia and Hypoxia cells were collected in different tubes and centrifuged at 5,000RMP for 5 minutes. The supernatant was removed, and a pellet of 1ml Trizol was added and stored at -80 for further use.

Isolation of RNA by Trizol Reagent

Isolate the cells by centrifugation at 5,000 RPM for 5 minutes. Remove the culture media and add 500 µL of Trizol reagent to the pelleted cells. After homogenization or lysis in trizol, the sample can be stored at -70 for up to 1 month.

- To ensure complete dissociation of nuleco-protein complexes, allow samples to stand for 5 minutes at RT.
- Add 250 µL of Trizol reagent (Total volume 750 µL).

- Vortex the samples vigorously for 2-5 min
- Add 150 µL of Chloroform
- Shake Vigorously for 15 seconds; allow to stand for 10 minutes
- Centrifuge at 10000 RPM for 15 minutes at 4 c. 3 Phases are obtained

Red Phase: Organic Contains Protein

An interphase: Contain DNA

Upper colourless Phase: Contain RNA

- Transfer the upper colourless phase to a fresh tube and add 750 µL of 2-Propanol. Allow to stand for 5-10 minutes at room temperature.
- Centrifuge at 10,000 RMP for 10 minutes at 4c
- Remove supernatant. Wash the RNA pellet by adding 750 µL of 75% ethanol.
- Shake gently centrifuge at 8,000 RPM for 5 minutes at 4c. Remove the supernatant.
- Dry the RNA pellet for 5-10 minutes.
- Add an appropriate volume (30 µL) of nuclease-free water.
- Tap the tube gently to dissolve the pellet. Keep at RT for 30 minutes
- Store the RNA at -20/-80

4.23 RNA Quantification:

For RNA quantification, the Biorad Nano Drop spectrophotometer was used. It is a rapid and efficient method for determining RNA concentration and assessing sample purity. This method measures absorbance at specific wavelengths (570nm), allowing for quick analysis with minimal sample volumes.

4.24 cDNA Synthesis Protocol:

High-Capacity Reverse Transcription kit (200RXN) Cat No 4368814 was used for c DNA synthesis. The master mix was prepared using the following composition for 1 reaction and 10 reactions given in Table 4.24.1

Table 4.24.1 Master Mix Composition

S. No	Composition	1 Reaction	10 Reaction
1	10X RT Buffer	2.0 µL	20 µL
2	25X dNTP Mix	0.8 µL	8.0 µL
3	10X RT Random primer	2.0 µL	20 µL
4	Reverse transcription Enzyme	1.0 µL	10 µL
5	Nuclear-free water	4.2 µL	42 µL

After the preparation of the master mix, 10 µL of master mix and 10 µL of isolated RNA sample were taken in Polymerase chain reaction (PCR) Tubes and kept in PCR at given settings.

PCR thermal Cycle Settings

Settings	Step 1	Step 2	Step 3	Step 4
Temperature	25	37	85	4
Time	10 Minutes	120 Minutes	5 Minutes	Hold

4.25 real-time PCR

For this research, we used three primes those were Wnt5a, β catenin and cyclin D1, and β actin was used as a housekeeping gene. Primers were diluted with water according to the chart given in the primer box. After dilution, 10 picomolar primers were prepared. Primer base pairs are given in the following table: 4.25.1

Primer Name	Primer Sequence 5' --> 3'	Length
Wnt5a F	TGAGCACGACGAAGC	**15**
Wnt5a R	GTGAACAGAAATGGAGGT	**18**
B-catenin F	CAAGTGGGTGGTATAGAGG	**19**
B-catenin R	GGGATGGTGGGTGTAAG	**17**
Cyclin D1 F	ACACGGCTCACGCTTAC	**17**
Cyclin D1 R	CCAGACCCTCAGACTTGC	**18**
B actin F	GAGCTACGAGCTGCCTGACG	**20**
B actin R	GTAGTTTCGTGGATGCCACAG	**21**

Table 4.25.1: Primer base pairs used for amplification

PCR Settings

Step	Temperature	Time	Cycle
Denaturation	**95^0c**	**10 min**	**42 Cycle**
Annealing	**95^0c**	**15 second**	
Extension	**60^0c**	**45 second**	

The master mix was prepared by using the following composition for one reaction given in Table 4.25.2

S.No	Composition	1 Reaction
1	Syber green	10 µL
2	Forward Primer	1.0 µL
3	Reverse Primer	1.0 µL
4	Nuclear-free water	6.0 µL

Table 4.25.2 Master mix composition

After preparing the Master mix, 10 µL of the master mix and 2 µL of c DNA sample were taken in PCR Tubes in triplicates and kept in RT-PCR at the given settings. Each gene's cycle threshold (Ct) values were taken, and 2 log fold values were calculated using the 2^- ΔΔCt method formula.

4.26 Statistical Analysis

SPSS software (version 20.0) was used for statistical analysis. Data are presented as Mean ± SD. One-way ANOVA was used to analyze statistical significant differences across multiple groups, followed by the Kruskal-Walli's test to ascertain significant intergroup differences. A $p < 0.05$ was considered statistically significant.

Chapter-V

Result & Discussion

In-silico Result

5.1 Retrieval of the target protein from RCBS-PDB (http://www.rcsb.org/pdb)

Table 5.1.1 Protein Details

Sl. No	Protein Name	PDB ID	Resolution	Molecular weight kDa
1	Wnt 5a	7DRT	2.20 A	104.89
2	Frizzled 1(FZD)	4IU6	1.90 A	43.81
3	LRP 5/6	3S8V	3.10 A	151.43
4	β-catenin	1LUJ	2.5 A	64.50
5	Disheveled	6ZC7	1.48 A	21.51
6	CyclinD1	5VZU	2.71 A	150.14

Table 5.1.1 depicts the crystal structure of Wnt 5a (PDB ID 7DRT), which consists of 893 amino acid residues with a molecular weight of 104.89kDa at 2.20A resolution, Frizzaled1 (PDB ID 4IU6) composed of 384 amino acid residues with a molecular weight of 43.81kDa, at 1.90 A. LRP 5/6 (PDB ID 3S8V) consists of 1334 amino acid residues with a molecular weight of 151.43kDa, at 3.10 A resolution, β-catenin (PDB ID 1LUJ) consists of 589 amino acid residues with a molecular weight of 64.50kDa, at 2.5 A resolution, Disheveled (PDB ID 6ZC7) consists of 190 amino acid residues with a molecular weight of 64.50kDa, at 1.48 A resolution. Cyclin D1(PDB ID 5VZU) consists of 1308 amino acid residues with a molecular weight of 150.14kDa at 2.70A resolution, which were retrieved from the protein data bank. Using Discovery Studio, non-receptor molecules, including water, were removed from these protein structures, and the data was saved in PDB format and the crystallographic structure. It was given in Figure 5.1.1 A, B, C, D, E, F.

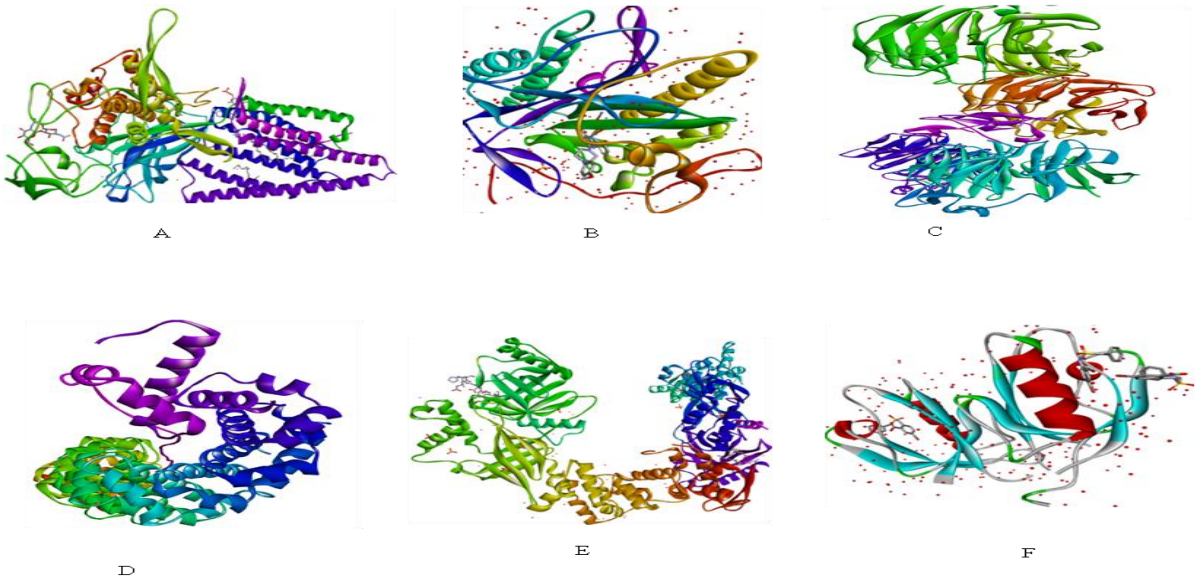

Figure 5.1.1 (A) Wnt 5a, (B) Frizzled1, (C) LRP5/6, (D) β-catenin, (E) Disheveled (F) Cyclin D1 3-D structure of selected target proteins from Wnt/β-catenin signaling pathway

5.2 Screening of Bioactive Molecules:

Retrieval of the chemical structure of bioactive molecules from PubChem and NPACT

Our study is based on a literature review; the structures of bioactive compounds from *Mucuna pruriens* plant seeds were obtained in SDF format from the PubChem database and converted to PDB format. Table 5.2.2 and Figure 5.2 .2 A, B,C, D, E,F, G,H show the bioactive compound and its 3D structures.

Table 5.2.2 Biomolecule from seeds of Mucuna pruriens

Sl. No	Compound name	Family	PubChem ID	Molecular weight
1	L-Dopa	Amino acid	6047	197.19g/mol
2	Glutathione	Amino acid	124886	307.33
3	Lecithin	Fat	823	258.23
4	Gallic acid	Phenolic acid	370	170.12
5	B-sitosterol	Plant sterol	222284	414.7
6	6-methoxyharman	Carbolines	135053166	263.29
7	Stearic acids	Saturated fatty acid	18962935	540.9
8	Oleic acids	Fatty acid	23665730	304.4
9	Linoleic acids	Organic compound	5282798	280.4

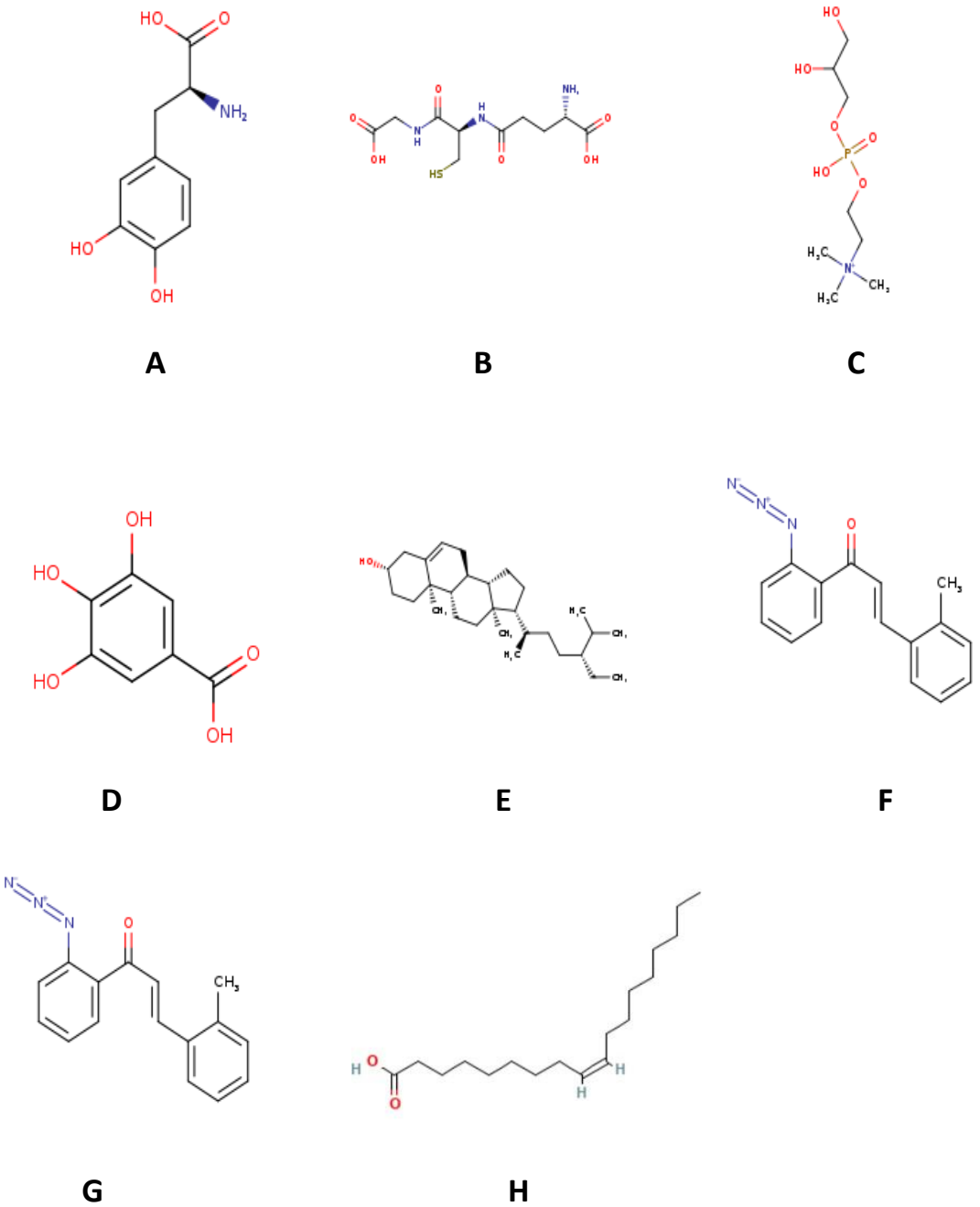

Figure 5.2.2 A) L-Dopa, B) B-sitosterol, C) Glutathione, D) 6-methoxyharman E) Gallic acid F) Stearic acids G) Lecithin, H) Oleic acid 3-D structure of selected biomolecule from *Mucuna pruriens*

5.3 Analysis of Drug Likeness Properties

Table 5.3.1 ADME/T of selected bioactive compounds from *Mucuna pruriens*

S. No	compound Name	Molecular weight (g/mol)	Rotatable bonds	Hydrogen bond acceptor	Hydrogen bond donor	Lipinski Rule	Violation
1	L-Dopa	197.19	3	5	4	yes	0
2	Glutathione	307.33	11	7	5	yes	0
3	Lecithin	258.23	8	6	3	Yes	0
4	Gallic acid	170.12	1	5	4	Yes	0
5	B-sitosterol	414.7	6	1	1	yes	1
6	6-methoxy harman	263.29	4	4	0	yes	0
7	Stearic acids	540.9	30	4	2	No	2
8	Oleic acids	304.4	15	2	0	yes	1
9	Linoleic acids	280.4	14	2	1	yes	1

Table 5.3.1 shows the calculated ADMET properties of bioactive compounds of *Mucuna pruriens* and standard drugs used in pulmonary hypertension treatment. It was predicted that eight bioactive molecules obey Lipinski's rule. The selected active physicochemical properties included a molecular weight of <500, an H-bond donor (HBD), an H-bond acceptor (HBA), a total number of rotatable bonds <10 (TNRB), a total polar surface area of <140 (TPSA), and an atomic molar refractivity of 42–130 (AMR). These properties are significant because they influence the drug's ability to interact with biological targets, its solubility, and its ability to cross cell membranes. The SWISS ADMET tool was used to evaluate these properties. These molecules demonstrated no violation of the rules.

5.4 Molecular Interaction Study:

Molecular docking predicts low binding energy confirmation. The inbuilt glide criteria for docking analysis were used. (Table 5.4.1 &Figure 5.4.1). Gallic acid, β-sitosterol, and L-dopa showed low binding energy with an efficient docking complex

compared to other bioactive molecules. Gallic acid interaction energy of -16.557 kcal/mol inhibition energy of -4.131 kcal/mol. The residues Thr89, Asn87, Arg295, Phe290, and Gly291 formed van der Wals interactions with Wnt5a. β--Sitosterol has an interaction energy of -35.076 kcal/mol and an inhibition energy of -5.246 kcal/mol. The residue Asp294, Arg295, Thr292, Pro283, Gly291, Phe290, Asn87 formed van der Wals interactions with Wnt3a.

With Frizzeled1, Gallic acid has an interaction energy of -29.214 kcal/mol and an inhibition energy of -7.041 kcal/mol. The residues Met309, Leu308, Tyr310, Phe311, Arg562, Asp471, Leu473, Phe603 formed van der Wals. β-sitosterol has an interaction energy of -28.091 kcal/mol and an inhibition energy of -4.728 kcal/mol. The residue Asp471, Arg562, Tyr607, Phe603, Pro538, Leu473, Phe311, Gly470, Val472, Arg562, formed van der Wals interactions with Frizzeled1.

With LRP5/6, Gallic acid has an interaction energy of -20.746 kcal/mol, inhibition energy of -5.101 kcal/mol, and β-sitosterol has an interaction energy of -31.582 kcal/mol inhibition energy of -2.339 kcal/mol. The residueThr393, Asn426, Cys466, Ser425, His470, Asp390, Ser389, Asn387, Arg386, interacted.

With β catenin, Gallic acid has an interaction energy of -20.746 kcal/mol and an inhibition energy of -5.101 kcal/mol. Lys354, Asp390, Asn426, Arg386, and Asn387 formed van der Wals interactions with β-sitosterol. β --sitosterol has an interaction energy of -31.582 kcal/mol and an inhibition energy of -2.339 kcal/mol. Thr393, Asn426, Cys466, Ser425, His470, Asp390, Ser389, Asn387, and Arg 386 formed van der Wals interactions with β--catenin. With disheveled, Gallic acid has an interaction energy of -34.18 kcal/mol and an inhibition energy of -8.559 kcal/mol. Gly1070, Asp1068, His1065, Lys1121, Pro1086, and Asp1063 formed van der Wals

interactions with Disheveled. β--Sitosterol has an interaction energy of -50.81 kcal/mol and an inhibition energy of -6.111 kcal/mol. The residue Thr248, Gly253, Leu284, Tyr159, His236, Lys199, and Arg87 formed van der Wals interactions with Disheveled.

With Cyclin D1, Gallic acid has an interaction energy of -46.299 kcal/mol and an inhibition energy of -7.387 kcal/mol. Gly1079, Asp1068, His1065, Pro1086, and Lys1121 formed van der Wals interactions with CylinD1. β--Sitosterol has an interaction energy of -69.119 kcal/mol and an inhibition energy of -8.711 kcal/mol. The residue Glu253, Thr248, Leu284, Tyr159, His236, Lys199, Arg87 formed van der Wals interactions with CyclinD1 these tables and figures are given in Table 5.4 and Figure 5.4.1 1A, 1B, 1C, 2A, 2B, 2C, 3A, 3B, 3C, 4A, 4B, 4C, 5A, 5B, 5C, 6A, 6B,6C

S. No	Compound Name	Docking Score Kcal/mol unit						Glide energy Kcal/mol unit					
		Wnt5a	Frizzled 1 Receptor	LRP 5/6Receptor	β--catenin	Dishe veled	Cyclin D1	Wnt5a	Frizzled 1 Receptor	LRP 5/6Receptor	β--catenin	Dishe veled	Cyclin D1
1	Gallic acid	-5.101	-5.291	-7.041	-4.131	-8.559	-7.387	-20.746	-22.691	-29.214	-16.557	-34.18	-46.299
2	β sitosterol	-2.339	-3.183	-4.782	-5.246	-6.111	-8.711	-31.582	-29.969	-31.606	-35.076	-50.81	-69.119
3	L-Dopa	-4.015	-5.679	-6.056	-4.361	-6458	-6.860	-22.437	-26.231	-28.091	-22.97	-30.60	-53.964
4	Glutathione	-2.339	-3.183	NR	NR	-2.821	-4.674	-23.907	-29.536	NR	NR	-28.14	-44.202
5	Lecithin	0.72	-2.869	-0.72	-3.649	-6.823	-6.858	-30.625	-37.063	-26.136	-23.887	-42.12	-48.068
6	Linolic acid	-1.604	0.874	-1.22	-0.622	-3.585	-5.848	-26.401	-23.747	-30.087	-26.875	-33.73	-37.796
7	Steoric acid	0.72	-0.74	-0.148	-2.257	-3.460	-6.007	-23.642	-32.085	-29.187	-22.096	-38.93	-37.491
8	Oleic acid	0.927	1.06	0.141	-1.266	-2.962	-7.494	-25.804	-26.877	-27.735	-26.69	-32.72	-47.294

Table 5.4.1 Multiple docking interaction of selected target proteins from Wnt signaling pathway with bioactive molecules from M. purines.

DOCKING RESULTS:

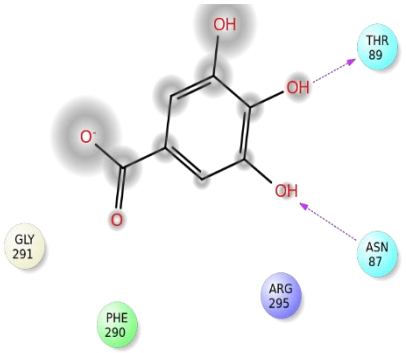

1 A

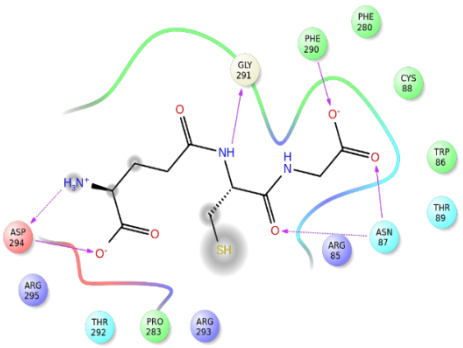

1B

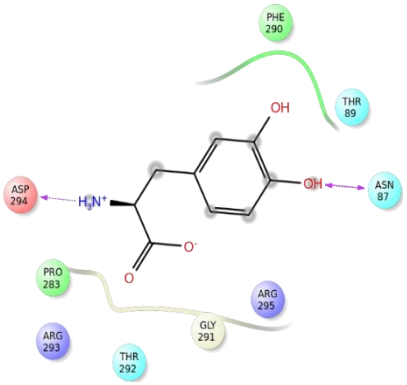

1 C

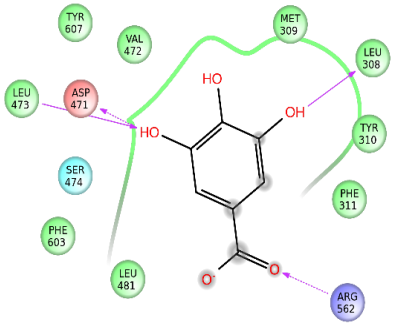

2A

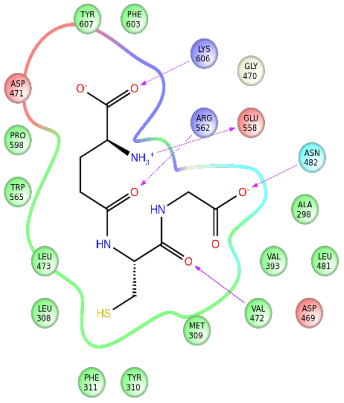

2B

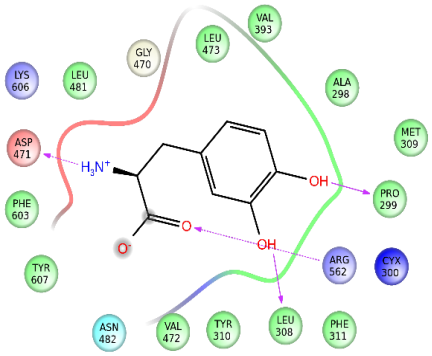

2C

DOCKING RESULTS:

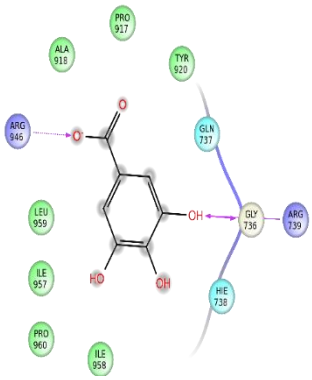

3A

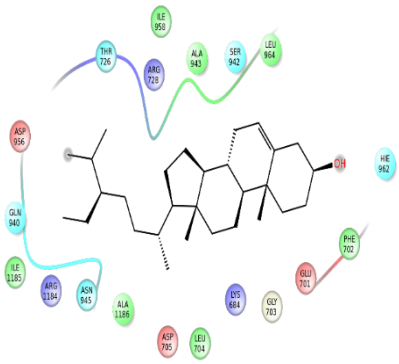

3B

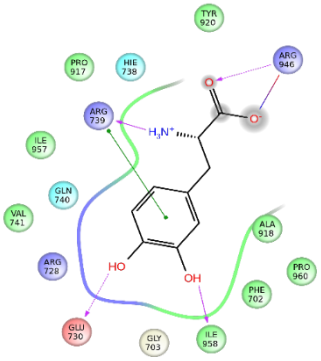

3C

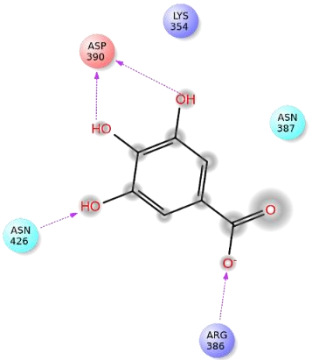

4A

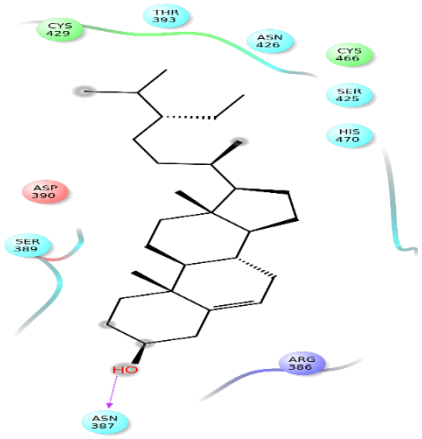

4B

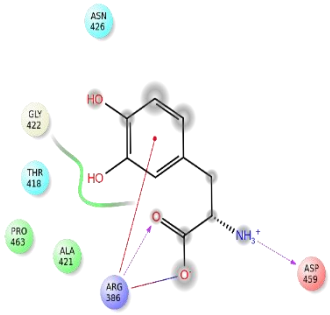

4C

DOCKING RESULTS:

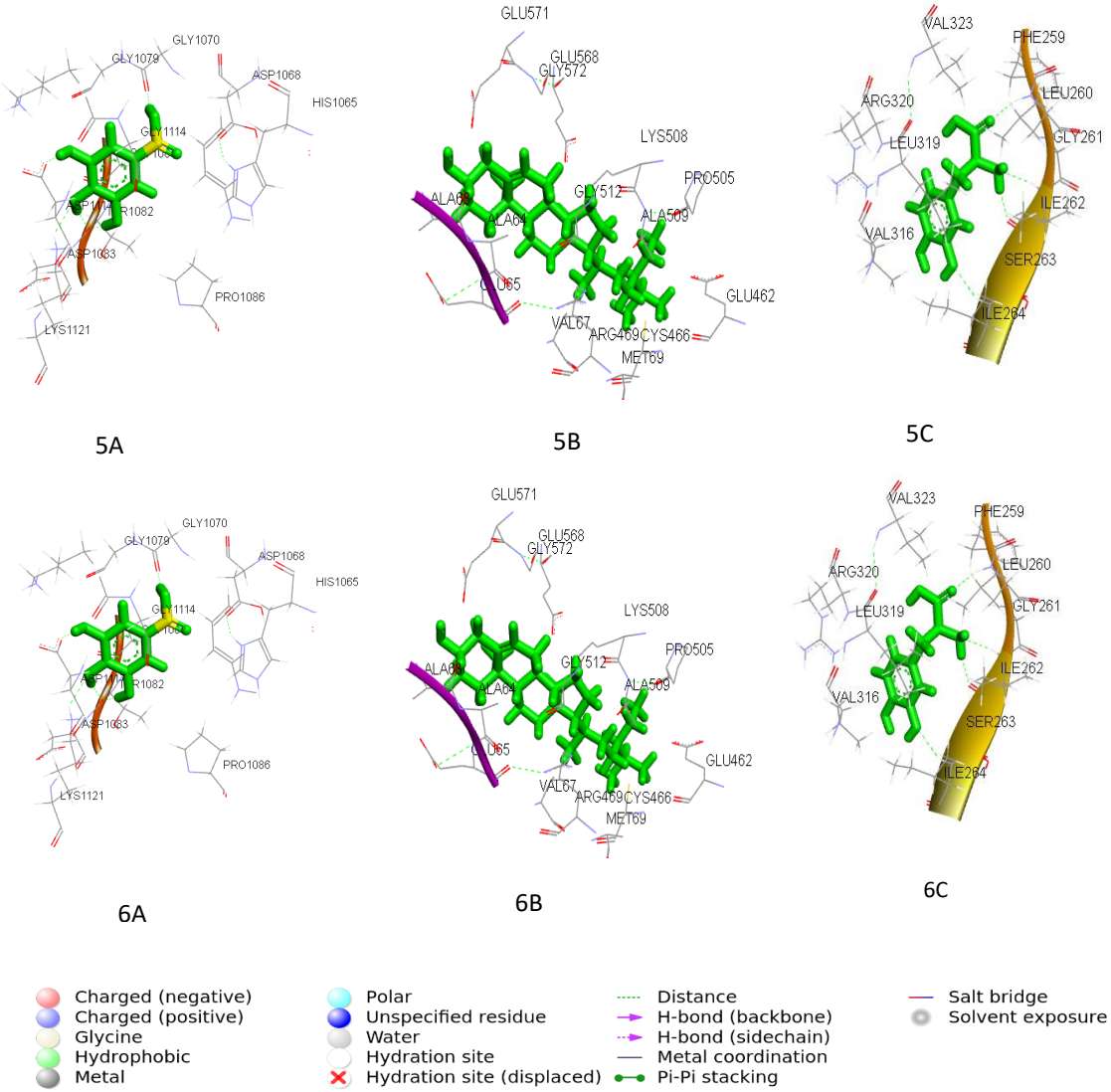

Figure 5.4.1 Multiple docking interaction of selected target proteins from Wnt signaling pathway with bioactive molecules from M. purines.1A) Docking of Wnt5a with Gallic acid 1B) Docking of Wnt5a with β-sitosterol 1C) Docking of Wnt5a with L-Dopa. 2A) Docking of Frizzled 1 with Gallic acid 2B) Docking of Frizzled 1 with β-sitosterol 2C) Docking Frizzled 1 with L-Dopa. 3A) Docking of LRP 5/6with Gallic acid 3B) Docking of LRP 5/6with β-sitosterol 3C) Docking of LRP 5/6 with L-Dopa.4A) Docking of β-catenin with Gallic acid 4B) Docking of β-catenin with β-sitosterol 4C) Docking of β-catenin with L-Dopa. 5A) Docking of Disheveled with Gallic acid 5B) Docking of Disheveled with β-sitosterol 5C) Docking of Disheveled with L-Dopa.6A) Docking of CyclinD1 with Gallic acid 6B) Docking of CyclinD1 with β-sitosterol 6C) Docking of CyclinD1with L-Dopa.

5.5 MD Simulation

Desmond package of Schrodinger was used for MD simulations of the best-docked target proteins. This study used a docked β-catenin complex with gallic acid for MD simulation after molecular docking. Out of the top three biomolecules (Gallic acid, L-dopa, and beta-sitosterol), gallic acid was used, and β-catenin is a key regulator for the pathway. Evaluation of the positional and structural changes of the inhibitor molecule near the protein binding site, which provides insight into the stability of the ligand-protein complex, was the primary goal of the MD simulation study. The Root Mean Square Deviation (RMSD) calculates the average displacement change of a set of atoms for a given frame concerning a reference frame. This process is applied to each simulation trajectory frame.

Figure 5.5.1A shows that The RMSD evolution of a protein is depicted in the simulation of the β-catenin protein; the initiation of individual proteins in the trajectory was found to be from 3.5 Å RMSD.

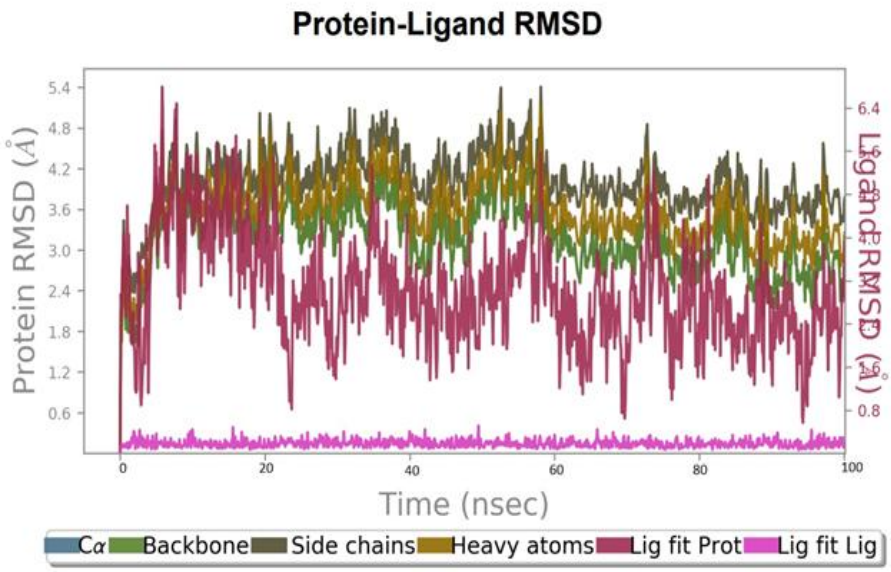

Figure 5.5.1A Protein RMSD Graph of β catenin with gallic

Figure 5.5.1B indicates that the protein-ligand complex was determined to be between 3 Å RMSF in simulation analysis. The protein complex at 50 ns had 3.5 Å RMSF, but by 100 ns, it stabilized to an RMSD value of approximately 4.5 Å.

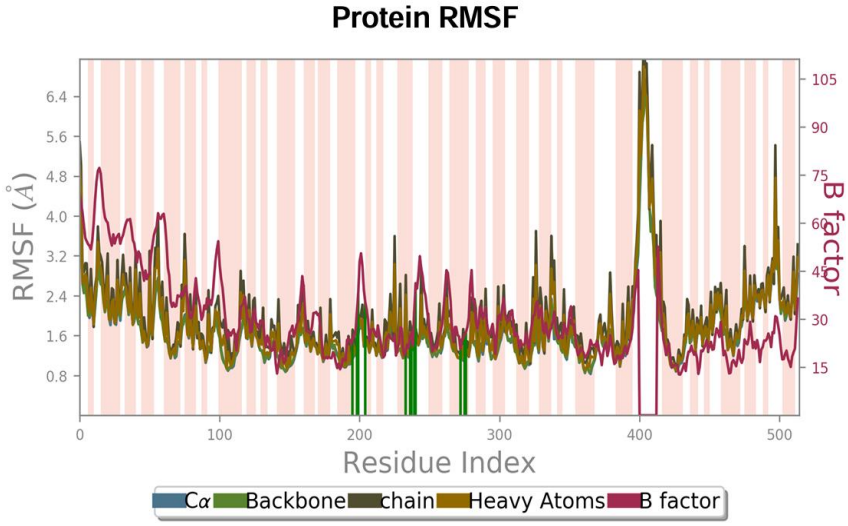

Figure 5.5.1B Protein-ligand RMSF plot

During the simulation, protein-ligand interactions might be seen. Figure **5.5.1C** reveals that Protein-ligand contacts (or 'contacts') may be classified into four different classes, as displayed in the plot: hydrogen bonds, hydrophobic, ionic, and water bridges, and each kind of interaction is further composed of more specific types, which could be evaluated in the 'Simulation Interactions Diagram' panel.

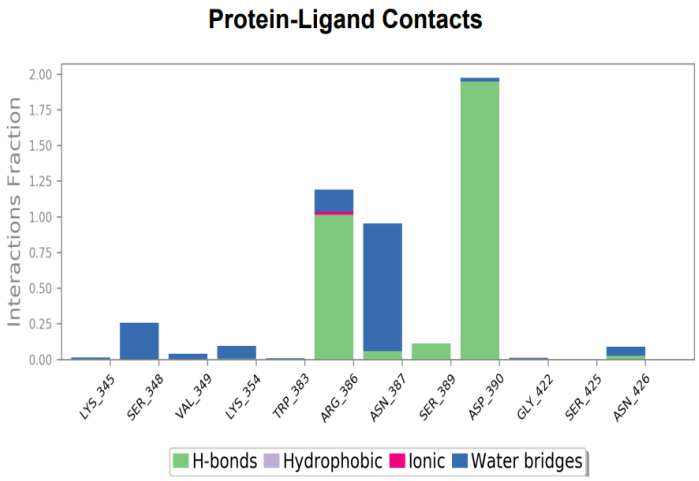

Figure 5.5.1C Protein-ligand interactions.

Figure 5.5.1D illustrates A complete diagram illustrating ligand atom interactions with protein residues. Interactions occurring greater than 30.0% of the time in the chosen trajectory (0.00 through 100 ns) are presented.

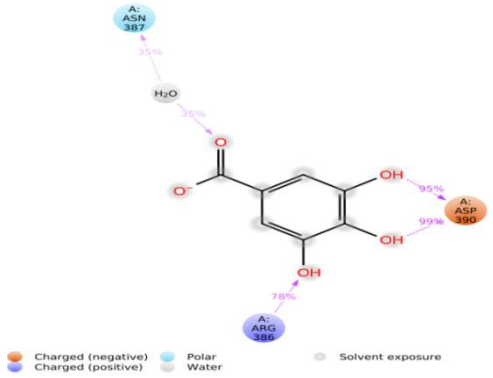

Figure 5.5.1D Protein-ligand interactions

5.6 (MM-GBSA) Analysis. Molecular Mechanics Generalized Born Surface area.

Table 5.6.1 Binding free energies (KCalmol-1) of β-catenin gallic acid along with individual energy components (KCalmol1) contribution

Name of target	ΔG Bind value KCalmol^{-1}	ΔG Coulomb KCalmol^{-1}	ΔG Covalent KCalmol^{-1}	ΔG H bond KCalmol^{-1}	ΔG Lipo KCalmol^{-1}	ΔG Solv GB KCalmol^{-1}	ΔG vdW KCalmol^{-1}
β catenin gallic acid	-15.07	-22.52	4.037	-1.132	-8.574	30.20	-19.53

Table 5.6.1 indicates that in a simulation study, the free binding energies for the best-docked protein-ligand complexes were estimated using the MM-GBSA analysis in the Prime module of the Schrodinger software. The values regarding ΔG Bind, the binding free energy for β-catenin, and gallic acid complex interactions were determined. Contributing energies in DG Bind calculation are Coulomb/Electrostatic energy (ΔG Coulomb), Covalent bond energy (ΔG Covalent), Hydrogen bond energy (ΔG H bond), Nonpolar salvation energy (ΔG Lipo), Polar solvation energy (ΔG Solv ΔB) and van der Waals energy (ΔG vdW). All values of energies calculated from MM-GBSA analysis are stated.

5.7 *In-silico* Result Discussion

Pulmonary artery hypertension (PAH) is a rare, progressive, and devastating disease characterized by increased pulmonary pressure and right heart failure. Key features in PAH are the progressive loss of small vessels and the proliferation of smooth muscle in the medial layer, resulting in luminal obliteration and an increase in pulmonary vascular resistance (Bachheti et al., 2022). Since none of the existing treatments for PAH have been demonstrated to accelerate angiogenesis or reduce already-present medial thickening, the condition progresses and eventually results in treatment failure. The discovery of disease-modifying agents to treat PAH may be aided by modulating Wnt signaling because of its recognized function in controlling angiogenesis and cell proliferation (Tarapore et al., 2012). *Mucuna pruriens* is a legume native to southeast Asia, particularly India. Mucuna pruriens has been widely used in India for over three thousand years. It has many actions, including antiparkinsonian, neuroprotective, aphrodisiac, and antiepileptic, apart from its use in cardiovascular diseases. (Parvatikar et al., 2023).

It has been reported that mutation of Wnt/ β-catenin pathway signaling genes like FZD and LRP5 result in defective vasculogenic, and the present in silico study also indicated that gallic acid, beta-sitosterol and L-dopa, which are bioactive compounds of *Mucuna pruriens* were found to be well docked with all six proteins of Wnt/β-catenin signaling pathways that include FZD, LRP5, etc (Su et al., 2013).

To screen potential bioactive molecules of Mucuna pruriens that can target Wnt5a, Frizzled, LRP 5/6, β-catenin, Disheveled, and cyclinD1 targeting the Wnt/β-catenin pathway, the present study used an in-silico analysis based on the molecular interaction studies. Different pharmacological properties of the biomolecule of *Mucuna pruriens* were investigated to analyze in silico ADME/T properties. Docking

analyses were further performed to evaluate the interaction of biomolecules with target proteins of the Wnt/ β -catenin pathway (Wnt5a, Frizzled, LRP 5/6, β -catenin, Disheveled, CyclinD1.

This study showed that different pharmacological properties of biomolecules of *Mucuna pruriens* are in order according to their ADME/T properties. The Lipinski filter was typically used to analyze the ADMET ligands derived from the seeds of the Mucuna pruriens plant. For molecular docking analysis, interaction energy score was used to select the best-docked complex among biomolecules of *Mucunna pruriens* with Wnt5a, Frizzeled1, LRP5/6, β -catenin, Disheveled and CyclinD1 proteins involved in Wnt /β -catenin pathway (Tarapore et al., 2012). The Gallic acid, β-sitosterol, and L-dopa showed the best interaction energy score compared to the other ligands. Molecular docking analysis further revealed that gallic acid, β -sitosterol, and L-dopa are also the best-docked bioactive compounds of *Mucuna pruriens*.

MD simulation on gallic acid was performed for 100ns to determine stability and conformational changes in the target protein when interacting with biomolecules. The RMSD and RMSF plot results indicated that gallic acid's binding to the protein stabilized it without causing structural changes. Although there were initially many random fluctuations, no conformational flipping was seen throughout the simulation. It eventually became entirely satisfactory and stable within 100 ns MD simulation.

The overall analysis of the present study by molecular docking and MD simulation hypothesized that gallic acid, β -sitosterol, and L-Dopa of *Mucuna pruriens* have good binding potential and may be considered therapeutic inhibitors against pulmonary vascular diseases (Khaparkhuntikar et al., 2023).

5.8 Phytochemical Extraction Result

5.8.1 Collection of seeds

Mucuna pruriens seeds are authenticated by Dr. Vidyalaxmi Pujari, Associate professor and authentification officer department of Dravyaguna BLDE Association of AVS Ayurveda Maha Vidyalaya Vijayapura Karnataka. The plant specimen reference no (Mucuna pruriens DC 10/25) and voucher Number is 2257.

5.9 Mucuna Pruriens Seed Extract Yield

A 20 gm sample of Mucuna pruriens seed powder yielded 1350 mg (1.35gm) of a reddish-brown extract upon extraction. This extract was subsequently dried and stored for further analysis. Phytochemical screening revealed the presence of various compounds, including phenolics, flavonoids, tannins, carbohydrates, starch, proteins, and micronutrients.

5.10 Isolation and Identification of Bioactive Molecules

5.10.1 Quantification of Gallic acid by HPLC

High-performance liquid chromatography (HPLC) was employed to quantitatively determine gallic acid in *Mucuna pruriens* seed extract.

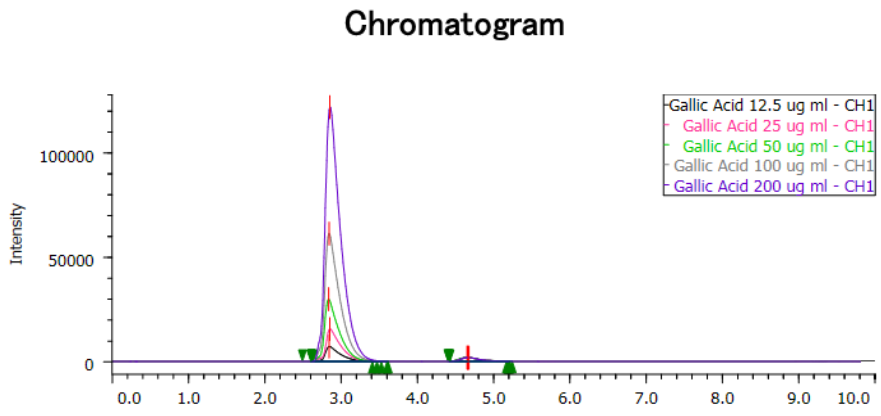

Figure 5.10.1A Chromatogram of Standard Gallic acid at different concentrations.

Figure 5.10.1A shows the chromatogram of the standard gallic acid at different concentrations. I got confirmation from the other concentrations of standard gallic acid processed in the HPLC instrument by setting 280nm wavelength, processed under the HPLC quantification by setting standard gallic acid and extracted sample with around 370nm mobile phase methanol and water using stationary phase Silica powder filled in C18 carbon I have confirmed with by running different concentration of standard and plant extraction with covered intensity of area uVsec.

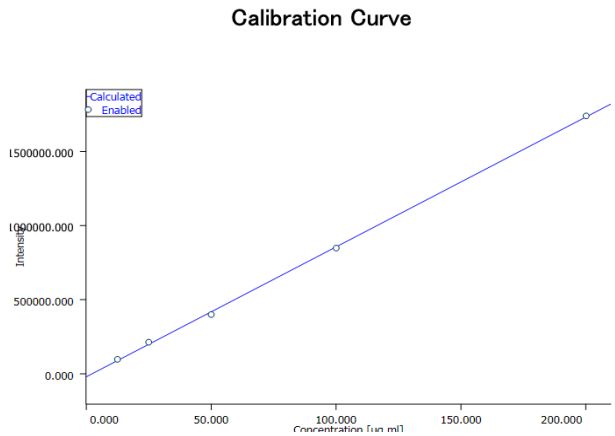

S.No	Concentration µg/ml	Intensity Area (µV.sec)
01	12.5	97579
02	25	213356
03	50	399788
04	100	847534
05	200	1739056

Figure 5.10.1 B Calibration Curve of Gallic acid

Figure 5.10.1B shows that A calibration curve was constructed by plotting the integrated peak areas against the corresponding concentrations of the gallic acid standard. The calibration curve exhibited excellent linearity, as evidenced by an R^2 value of 0.998, indicating a strong correlation between the standard and sample mean

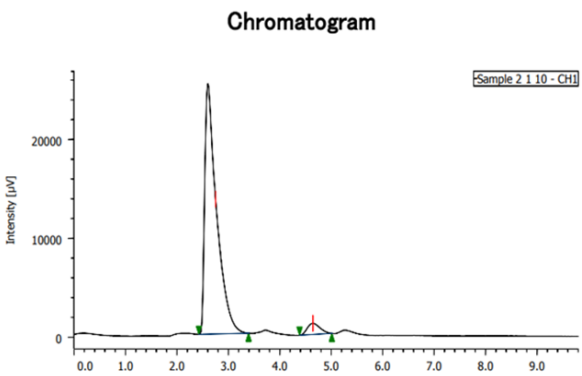

Figure 5.10.1 C Chromatogram of Gallic acid present plant extract

Figure 5.10.1C shows the presence of gallic acid in Mucuna pruriens plant seed extract, and the gallic acid concentration in the Mucuna pruriens seed extract was determined by comparing its peak area to the established calibration curve. The extract contained 54.625 µg/mL gallic acid at a retention time of 2.75, and the intensity of the area is covered by 45918 µV.sec, which was given in table 5.8.1

Sl. No	Retention Time (RT)	Intensity Area(µV.sec)	Quantity (µg/ml)
1	2.75	459158	54.625

5.10.2 Flash Chromatography of Gallic Acid

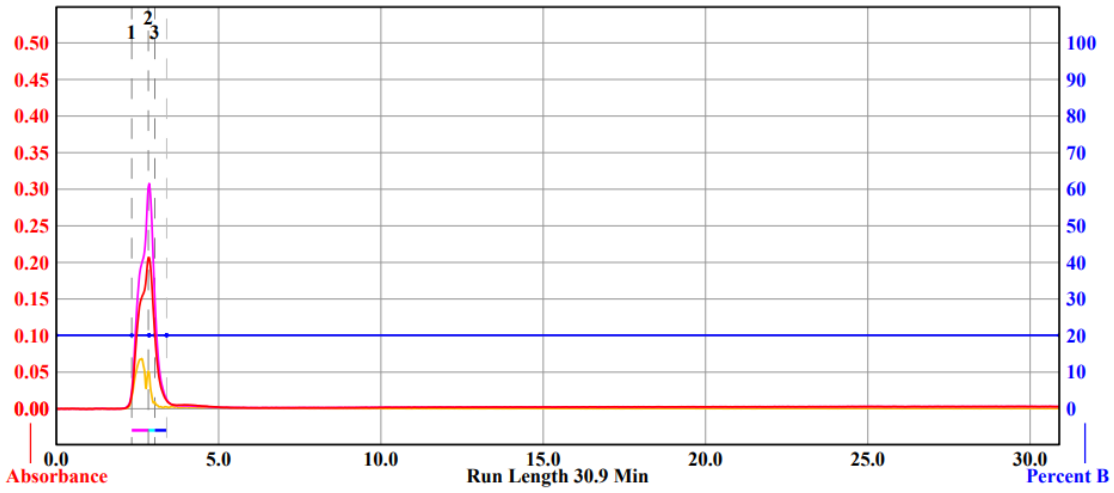

Figure 5.10.2 A CombiFlash Rf200i flash chromatography

The CombiFlash Rf 200i flash chromatography system separates gallic acid in Figure 5.10.2 A. The x-axis is presented as run length (in minutes). The y-axis has two components: absorbance in arbitrary units (AU) and the percentage of solvents used during gradient elution. The gradient elution loading type is solid, and the solvents used are Methanol and Water. The flow rate is 18ml/min, and the overall run length is 30.9 minutes. Gallic acid is collected in different fractions, and the concentration of gallic acid is 12µg/100gm was collected.

5.10.3 Quantification of β –sitosterol by HPLC

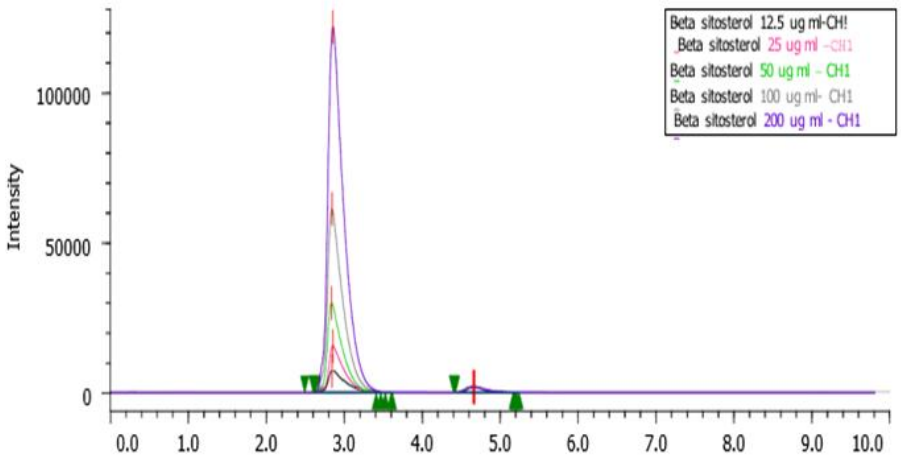

Figure 5.10.3A standard β –sitosterol chromatogram

Figure 5.10.3A shows the standard β –sitosterol chromatogram at different concentrations. I got confirmation from the different concentrations of standard β –sitosterol processed in the HPLC instrument by setting 280 nm wavelength, processed under the HPLC quantification by setting standard β –sitosterol and extracted sample with around 370nm mobile phase methanol and water using stationary phase silica Powder filled in C18 carbon I have confirmed with by running different concentration of standard and plant extraction with covered intensity of area uVsec.

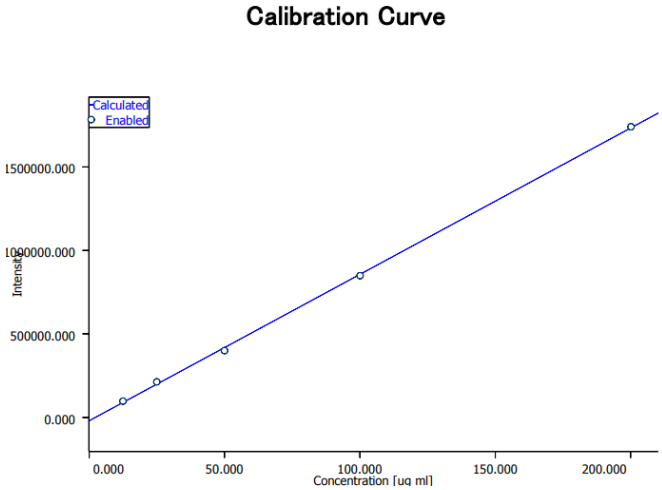

S. No	Concentration µg/ml	Intensity Area (µV.sec)
1	12.5	97579
2	25	823356
3	50	289788
4	100	937534
5	200	1939056

Figure 5.10.3 B Calibration Curve of β –sitosterol

Figure 5.10.3 B shows that A calibration curve was constructed by plotting the integrated peak areas against the corresponding concentrations of the β –sitosterol standard. The calibration curve exhibited excellent linearity, as evidenced by an R^2 value of 0.998, indicating a strong correlation between the standard and sample mean

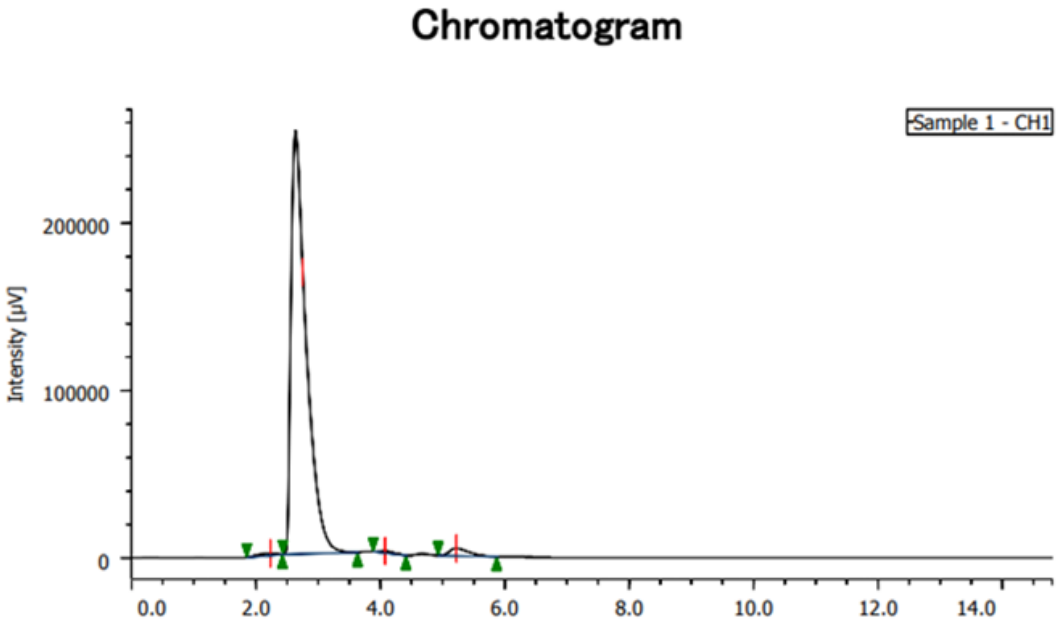

Figure 5.10.3 C Chromatogram of β –sitosterol present plant extract

Figure 5.10.3 C shows the presence of gallic acid in the *Mucuna pruriens* plant seed extract, and the β –sitosterol concentration in the *Mucuna pruriens* seed extract was determined by comparing its peak area to the established calibration curve. The extract contained 48.415 µg/mL.

Sl. No	Retention Time (RT)	Intensity Area(µV.sec)	Quantity (µg/ml)
1	2.75	459158	48.415

5.10.4 Flash Chromatography of β –sitosterol

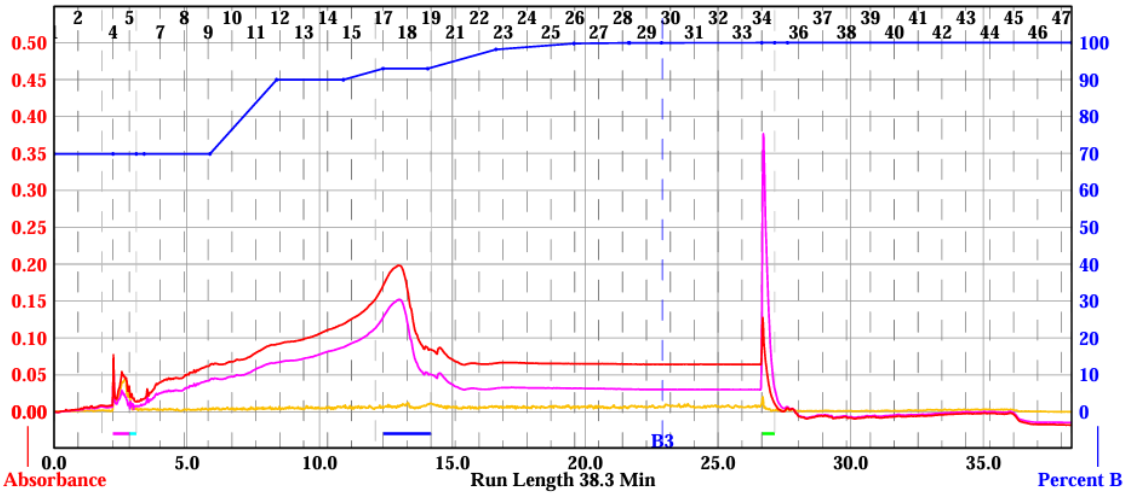

Figure 5.10.4 A CombiFlash Rf200i flash chromatography

The CombiFlash Rf200i flash chromatography system separates gallic acid in Figure 5.10.4A. The x-axis is presented as run length (in minutes). The y-axis has two components: absorbance in arbitrary units (AU) and the percentage of solvents used during gradient elution. The gradient elution loading type is solid, and the solvents used are Methanol and Water. The flow rate is 20ml/min, and the overall run length is 38.3 minutes. β-sitosterol is collected in different fractions, and the concentration of β-sitosterol is 10μg/100 gm.

5.11 Phytochemical Extraction Discussion

Cerebrovascular disorders have traditionally been treated with medicinal plants for decades. Such practices are prevalent in traditional medical systems, notably the centuries-old Indian medical system Ayurveda. According to (Tangsrisakda et al., 2022), phytochemicals have been credited with combating these disorders. Such biomolecules were shown to regulate different pathways, such as inflammation and oxidative stress, that operate in the pathophysiology of the pulmonary arteries. Therefore, phytochemicals are natural, cheap, safer, and better alternatives than synthetic drugs.

The plant *Mucuna pruriens* is widely used in Ayurvedic medicine and is known as the velvet bean (Pathania et al., 2020). Growing in tropical and subtropical regions of the world, it is extensively cultivated in the eastern states of India, owing to its status as a leguminous (Kamkaen et al., 2022). There have been numerous studies establishing its therapeutic effects such as anti-Parkinsonism, antidiabetic, antioxidant, antibacterial, antiepileptic, antineoplastic, improving male fertility, and aphrodisiac (Rane et al., 2019) (Theansungnoen et al., 2022). Since the Vedic period, *Mucuna pruriens* has been used in Ayurveda for its treatment of various disorders of the nervous system (Rane et al., 2019; Kamkaen et al., 2022).

In our research, the qualitative analysis of the phytochemicals from *Mucuna pruriens* seed extract revealed the presence of several biomolecules like Alkaloids, Flavonoids, Terpenoids, Steroids, Tannins, Saponins and Glycosides.

Molecular docking studies revealed L-DOPA, gallic acid, and β-sitosterol to have the best binding affinities with the target proteins. These results suggest that these compounds might bind to these important biomolecular targets, providing

reliance on their pharmacological importance. HPLC was used to identify and quantify these biomolecules isolated and purified from Mucuna pruriens seed extract. These were separated and purified by Flash chromatography. Amount of gallic acid was 12μg/100gm, and β-sitosterol was 10μg/100 gm.

Findings by Parvatikar et al., 2023 state that predominant constituents of *Mucuna pruriens* seed extract include L-DOPA and β-sitosterol, which are isolated and purified by HPLC and Flash chromatography.

INVITRO RESULT

5.12 Result from Seeding of the cells or Culture of cells:

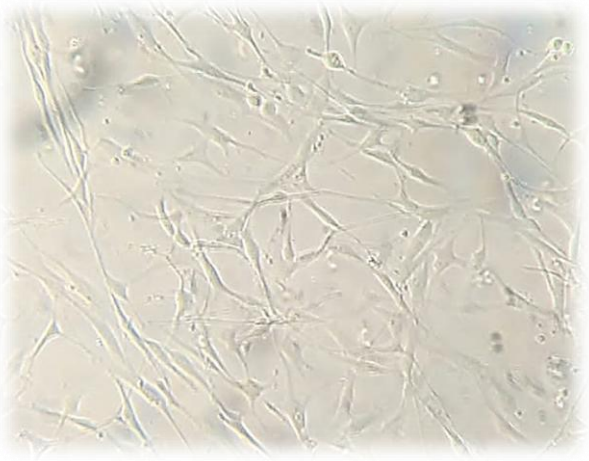

Fig 5.12.1 Normoxia cells observed under Microscope

Fig 5.12.1 Shows that Pulmonary artery smooth muscle cells, when cultured in Normoxia condition, exhibited a characteristic spindle-shaped morphology, often described as elongated with a centrally located Nucleus.

5.13 MTT Assay Result

The MTT (3-(4,5-dimethylthiazol-2-yl)-2,5-diphenyltetrazolium bromide) assay is a widely utilized colorimetric method for evaluating cellular viability, proliferation, and cytotoxicity across a variety of in vitro cell line models. This technique is predicated on converting the yellow tetrazolium compound, MTT, into a purple formazan product, a process catalyzed by the mitochondrial enzymes in metabolically active cells.

The IC50 value represents the concentration required to inhibit 50% of cell viability, a critical parameter for assessing the cytotoxic potential of chemical compounds or extracts. In this study, the cytotoxicity of three substances, β-sitosterol, plant crude extract, and gallic acid—was evaluated on the HPASM (Human Pulmonary Artery Smooth Muscle) cell line using the MTT assay.

The HPASMC are treated with biomolecules from higher concentration to lower concentration. β-Sitosterol showed the highest cytotoxicity among the tested substances, with an IC50 value of 33.7. ± 14.33 μg/mL, indicating the lowest concentration required to achieve 50% cell death. The moderate cytotoxicity of the plant crude extract was characterized by an IC50 value of 65.96. ± 0.72 μg/mL; the cytotoxicity of gallic acid was just slightly higher than that of the plant crude extract, having an IC50 value of 58.54. ± 0.84 μg/mL. This indicates that β-sitosterol is the most potent cytotoxic agent among the three substances tested and is followed by gallic acid and plant crude. The significantly lower IC50 value exhibited by β-sitosterol may highlight its more substantial inhibition of the HPASM cell line and possibly make it a lead compound worth investigating further for anticancer or cytotoxic studies.

MTT ASSAY RESULTS

β-sitosterol

Concentration ug/ml	Cell viability %	SD
200	33.25	1.38
100	38.22	2.44
50	49.14	4.14
25	59.37	0.31
12.5	70.32	3.96
6.25	77.12	2.3

IC50 value	SD
33.71	4.33

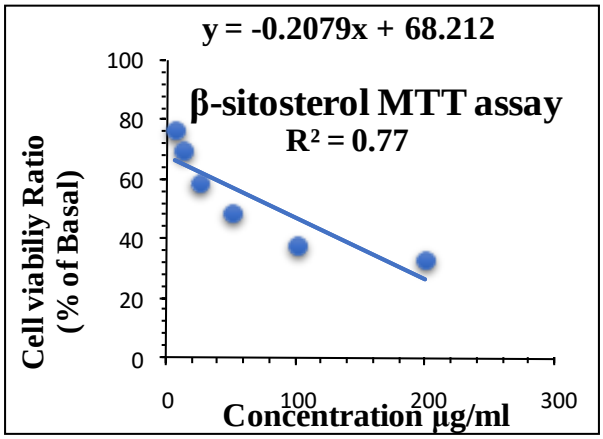

Plant crude extract

Concentration ug/ml	Cell viability %	SD
200	46.16	1.2
100	52.7	0.17
50	74.93	1.63
25	80.22	0.03
12.5	86.74	0.74
6.25	92.08	0.63

IC50 value	SD
65.96	0.721673

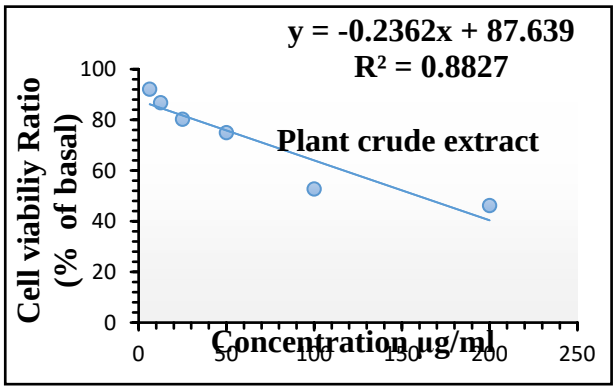

Gallic acid

Concentration ug/ml	Cell viability %	SD
200	44.16	0.35
100	49.27	3.4
50	65.23	0.38
25	73.13	1.91
12.5	77.61	3.36
6.25	83.709	2.48

IC50 value	SD
58.54	0.841457

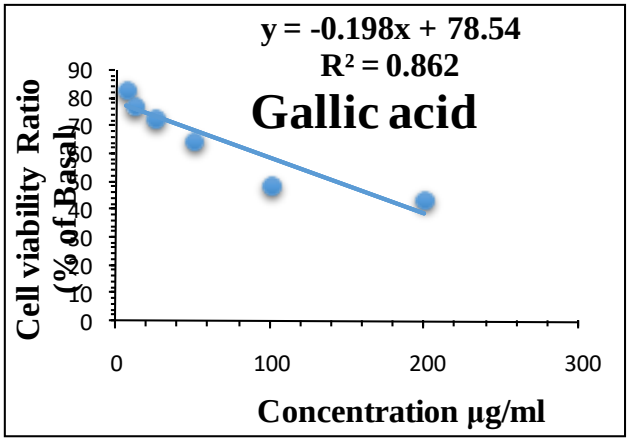

5.13.1A MTT ASSAY RESULTS OF COMPOUND β-SITOSTEROL

β-sitosterol 200 µg/ml

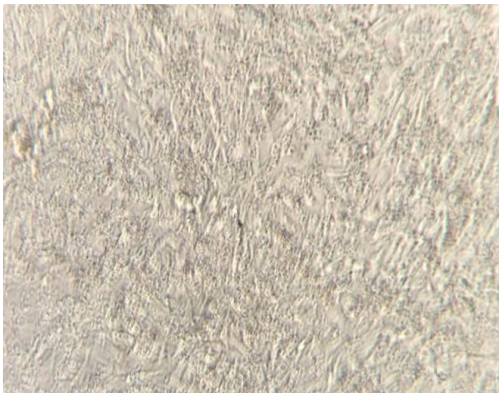

β-sitosterol 25 µg/ml

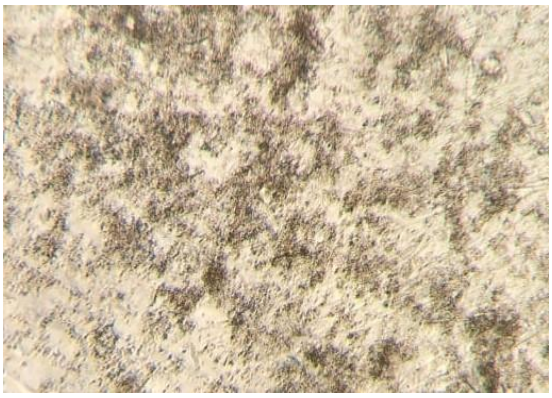

β-sitosterol 100 µg/ml

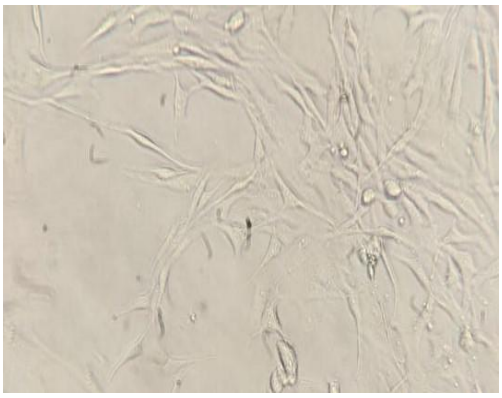

β-sitosterol 12.5 µg/ml

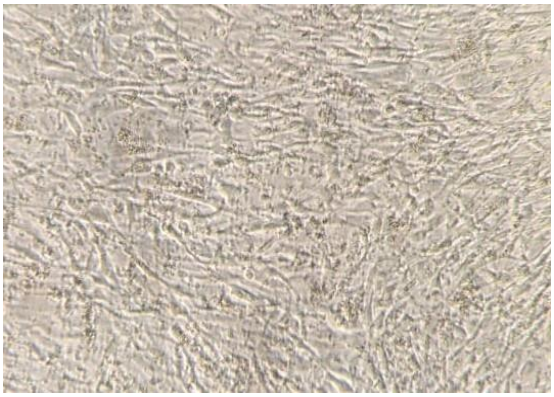

β-sitosterol 50 µg/ml

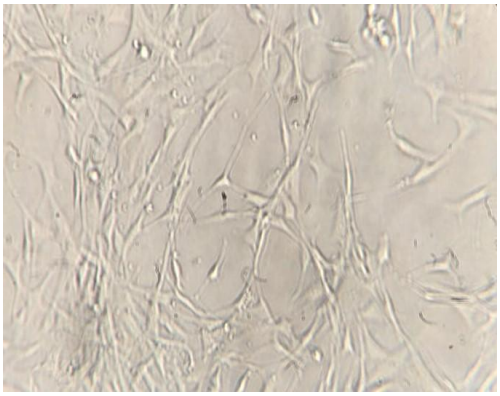

β-sitosterol 6.5 µg/ml

5.13.1B MTT ASSAY RESULTS OF COMPOUND PLANT CRUDE EXTRACT

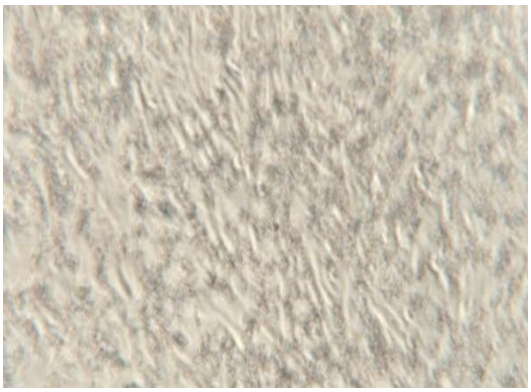

Plant Crude Extract 200 µg/ml

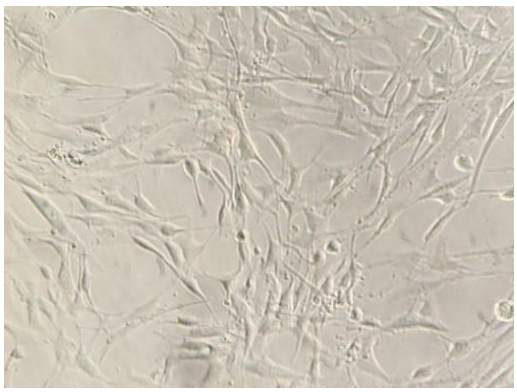

Plant Crude Extract 25 µg/ml

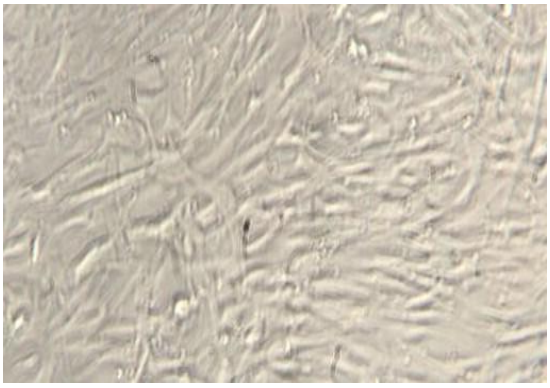

Plant Crude Extract 100 µg/ml

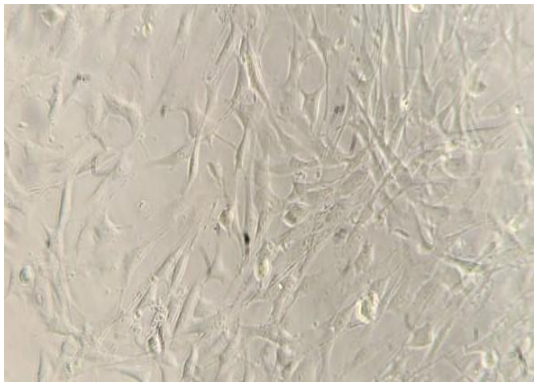

Plant Crude Extract 12.5 µg/ml

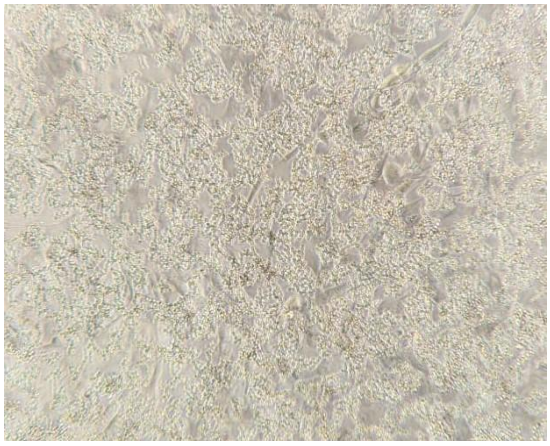

Plant Crude Extract 50 µg/ml

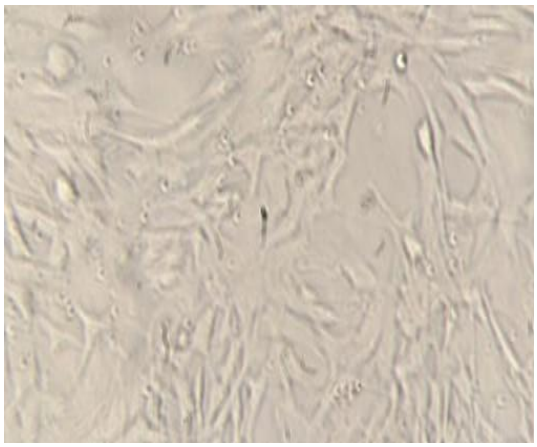

Plant Crude Extract 6.5 µg/ml

5.13.1C MTT ASSAY RESULTS OF COMPOUND GALLIC ACID

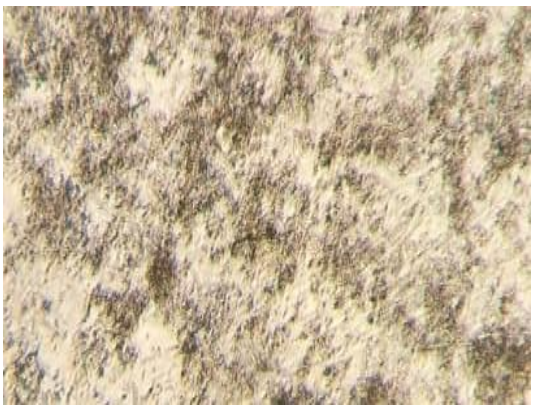

Gallic Acid 200 µg/ml

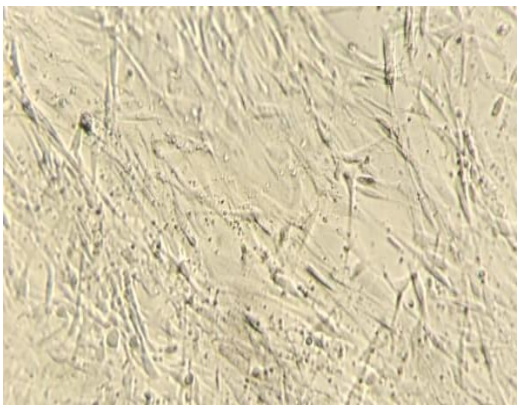

Gallic Acid 25 µg/ml

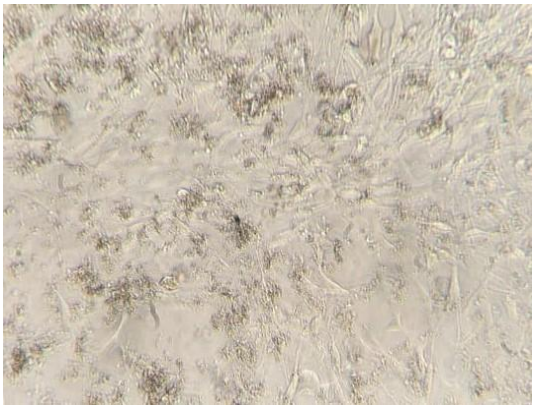

Gallic Acid 100 µg/ml

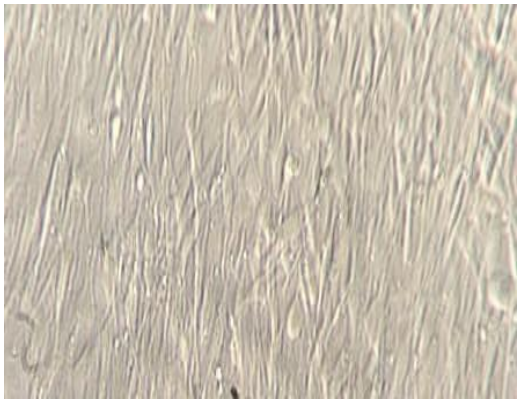

Gallic Acid 12.5 µg/ml

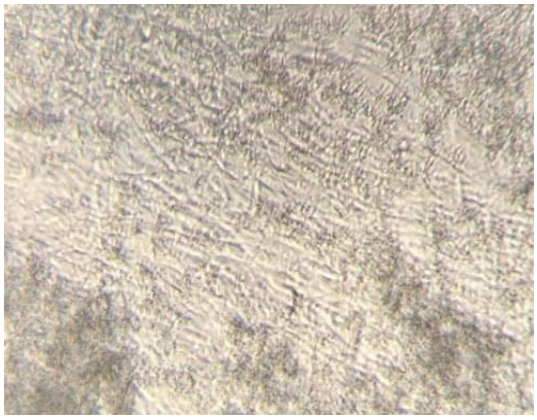

Gallic Acid 50 µg/ml

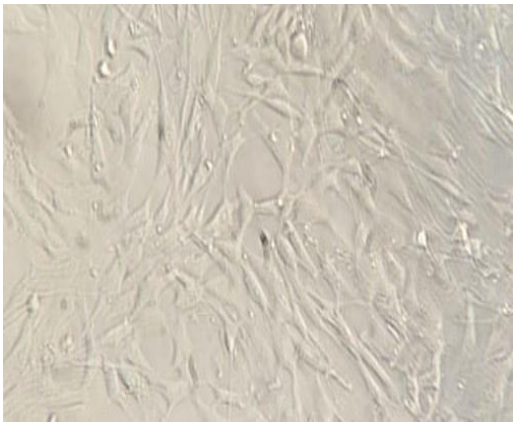

Gallic Acid 6.5 µg/ml

5.14 Microscopic Changes of the Human Pulmonary Artery Smooth Muscle Cell Line Exposed to hypoxia (5% Oxygen)

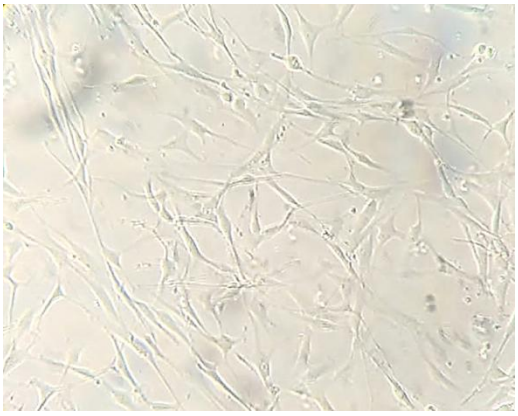

Fig 5.14.1A Cell cultured in Normoxia

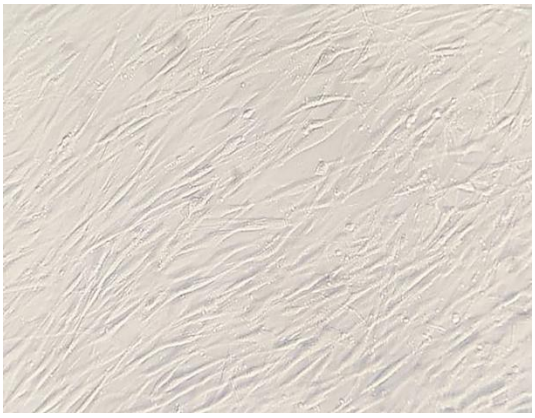

Fig 5.14.1B Cells exposed to Hypoxia

Fig 5.14.1A shows that when human pulmonary artery smooth muscle cells (HPASMCs) were cultured under normoxic conditions (21% oxygen, 74% nitrogen, and 5% carbon dioxide), they displayed a characteristic spindle-shaped morphology. The cells were elongated, with a centrally located nucleus, reflecting their typical phenotype under physiological oxygen levels. This morphology is commonly associated with a quiescent state and the functional integrity of smooth muscle cells within the pulmonary artery.

Fig 5.14.1B shows that significant microscopic alterations were observed in these cells upon exposure to hypoxic conditions (5% oxygen, 90% nitrogen, and 5% carbon dioxide) for 48 hours. An increase in cell size characterizes hypoxia-induced pronounced cellular hypertrophy. This hypertrophy was accompanied by structural reorganization, most notably the formation of prominent stress fibers within the cytoplasm. The cells displayed significant alterations in their shape, becoming less spindle-like and adopting a more irregular and massive approach. Such structural changes indicated a hypoxia-induced phenotypic transition of the cells to adjust to the changed microenvironment. The formation of stress fibers implies that, under

hypoxia, there was cytoskeletal remodeling, an essential aspect of cellular responses. Such remodeling is vital for the integrative role of these cells in vascular remodeling, focusing on the pathophysiology of hypoxia-induced pulmonary hypertension in particular. In addition, these modifications may have further activated the contractile capacities of the HPASMCs, allowing for more effective contributions to smooth muscle contraction and, ultimately, vascular tone under hypoxic circumstances.

5.15 Result of Gene Expression Studies

5.16 Effect of Hypoxia on the expression Wnt/β-catenin signaling pathway molecules (Wnt5a/β-catenin/cyclin D1)

In this research, we examined the expression of the key pathway components Wnt5a/β-catenin/cyclin D1 under normoxia and after exposure to hypoxia to explore the role of the Wnt/β-catenin signaling pathway in the hypoxia-induced proliferation of human pulmonary artery smooth muscle cells (PASMCs).

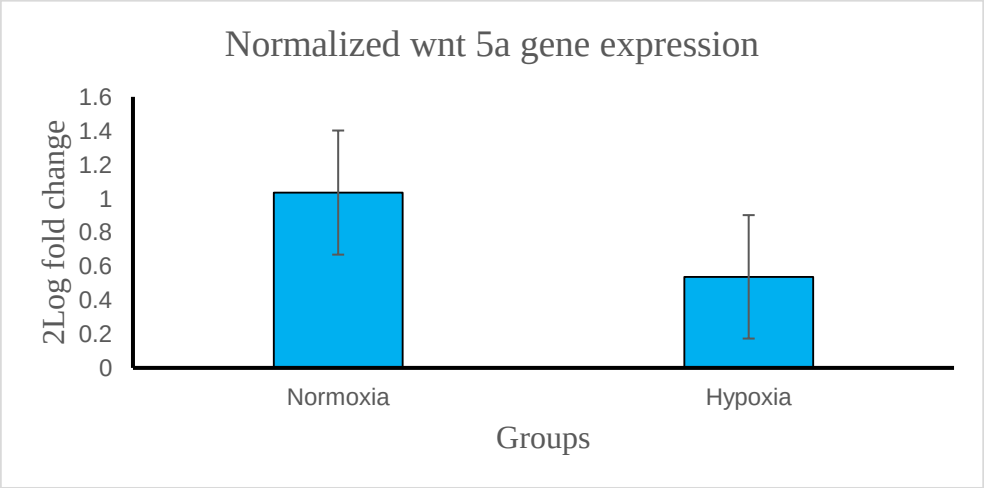

Fig 5.16.1A. An Expression of Wnt5a in human PASMCs was analyzed under normoxia and hypoxia by real-time RT-PCR (b) (n = 4). Values are means ± SE, and P > 0.157 are insignificant.

Fig. 5.16.1A Wnt5a pathway molecules. To determine if Wnt5a signaling is required for hypoxia-induced proliferation of human PASMCs, the expression of Wnt5a pathway molecules was analyzed after hypoxia treatment. As indicated in Fig. 5.13.1A, hypoxia (5% O 2, 48 h) reduced Wnt5a mRNA expression levels. These findings suggest that hypoxia inhibits Wnt5a expression.

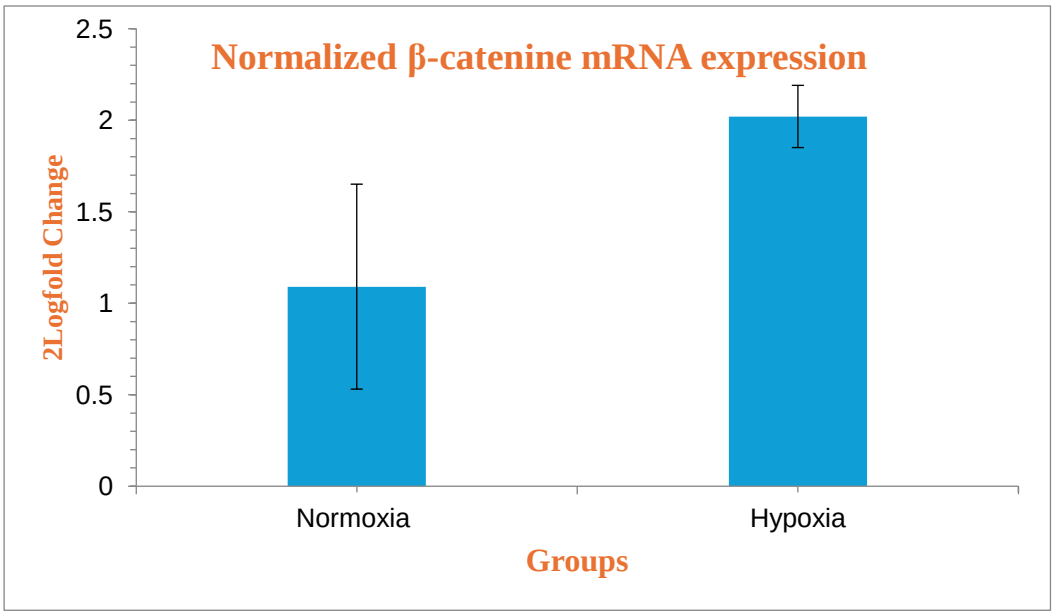

Fig 5.16.1B: Expression of β-catenin in human PASMCs was analyzed under normoxia and hypoxia by real-time RT-PCR (b) (n = 4). Values are means ± SE, * P < 0.05 are significant.

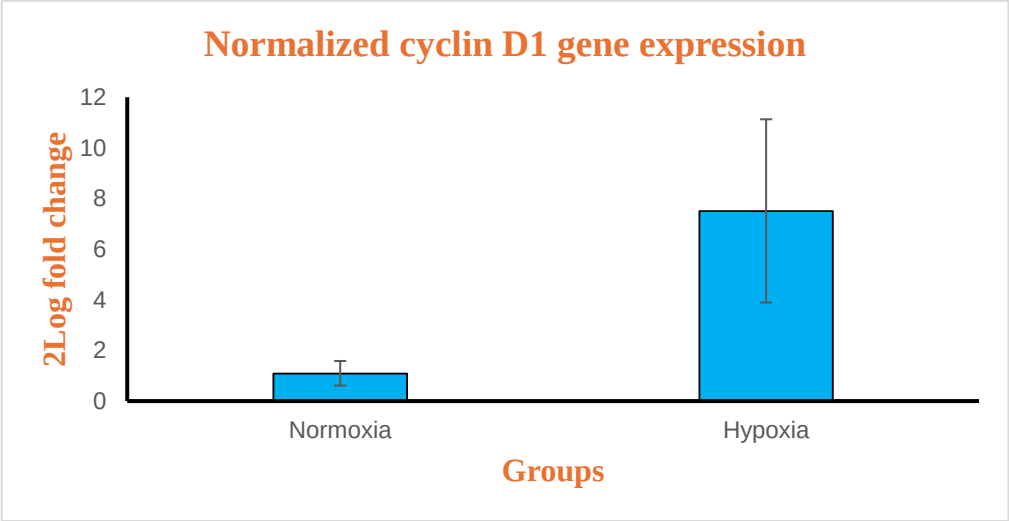

Fig 5.16.1C: Expression of CyclinD1 in human PASMCs was analyzed under normoxia and hypoxia by real-time RT-PCR (b) (n = 4). Values are means ± SE, * P < 0.05 are significant.

As shown in Fig. 5.10B, C hypoxia (5% O 2, 48 h) increased β-catenin and CyclinD1 mRNA expression levels. The inhibitory effect of hypoxia on Wnt5a expression suggested that Wnt5a may play an inhibitory role in hypoxia-induced PASMC proliferation, potentially mediated through its interaction with β-catenin.

5.17 Result of Wnt5a gene expression in hypoxia-exposed cells treated with bioactive molecules of *Mucuna pruriens* seed

Group 1 Hypoxia (H)	Group 2 H+βS 50ug/ml	Group3 H+βS 25ug/ml	Group4 H+CE 100ug/ml	Group 5 H+CE 50ug/ml	Group6 H+GA 100ug/ml	Group7 H+GA 50ug/ml	Significant value
1.24±0.84	6.26±0.22a	7.61±0.80a	4.81±0.19	4.11±3.00	2.30±0.81	1.89±0.001c	**P=0.05***
BS (β-sitosterol), CE(Crude extract),GA (Gallic acid) Superscripts a, and c indicate a significant difference between groups. 'a' depicts a comparison with Group 1, 'and 'c' depicts a comparison with Group 3. *p=0.05							

Table 5.17.1 Wnt5a gene expression in hypoxia-exposed cells treated with bioactive molecules of *Mucuna pruriens* seed

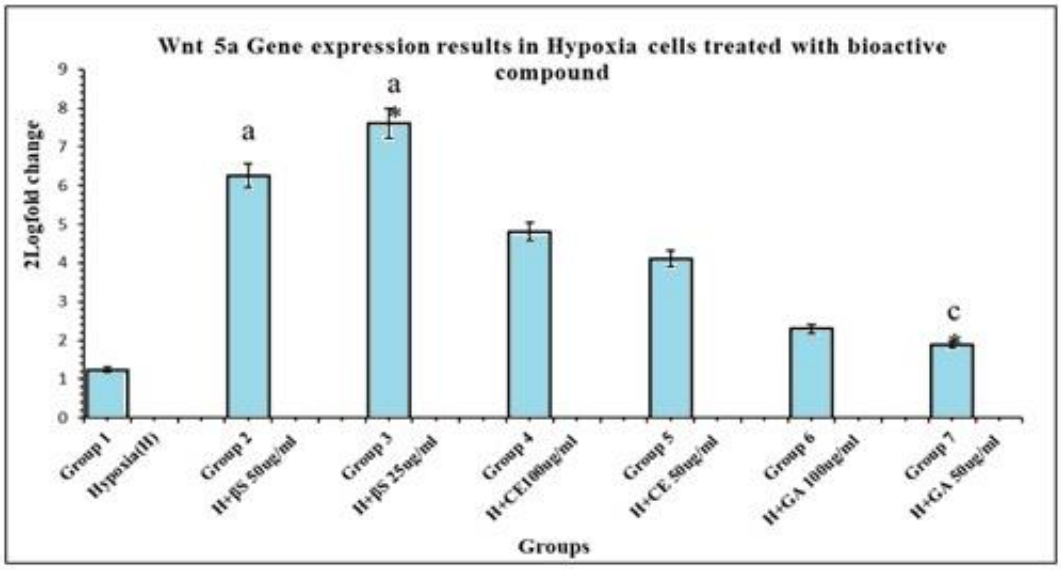

Figure 5.17.1 BS (β-sitosterol), CE (Crude extract), and GA (Gallic acid) Superscripts a and c indicate a significant difference between groups. 'a' depicts a comparison with Group 1, 'and 'c' depicts a comparison with Group 3. *P=0.05 is significant.

Table 5.17.1 and figure 5.17.1 illustrate the effects of biomolecules derived from *Mucuna pruriens* seed extract (β-sitosterol, gallic acid, and plant crude extract) on Wnt5a mRNA expression in human pulmonary artery smooth muscle cells under hypoxic conditions. The data demonstrate that exposure to hypoxia led to a reduction in Wnt5a mRNA expression. However, treatment with β-sitosterol at lower concentrations (25µg/ml) significantly upregulated Wnt5a mRNA levels, counteracting the hypoxia-induced suppression. Similarly, treatment with the crude Mucuna pruriens seed extract at higher concentrations(50µg/ml) also significantly increased Wnt5a mRNA expression. These findings suggest a concentration-dependent modulation of Wnt5a mRNA expression by the bioactive components of Mucuna pruriens seed extract in HPASMCs under hypoxic conditions. The observed upregulation of Wnt5a by β-sitosterol and the crude extract may indicate a potential protective or compensatory mechanism against the effects of hypoxia on Wnt signaling in these cells.

5.18 Result of β catenin expression in hypoxia-exposed cells treated with bioactive molecules of *Mucuna pruriens* seed

Group 1 Hypoxia (H)	Group 2 H+βS 50ug/ml	Group3 H+βS 25ug/ml	Group4 H+CE 100ug/ml	Group 5 H+CE 50ug/ml	Group6 H+GA 100ug/ml	Group7 H+GA 50ug/ml	Significant value
1.00±0.08	0.93±0.014 a	0.114±0.0045a	0.64±0.00 ab	0.07±0.01ab	0.13±0.01	0.34±0.44 a	**P=0.05***
BS (β-sitosterol), CE(Crude extract),GA (Gallic acid) Superscripts a and c indicate a significant difference between groups. 'a' depicts a comparison with Groups 1,2 and 7, 'and 'b' depicts a comparison with Groups 4 and 5. *p=0.05							

Table 5.18.1 β catenin expression in hypoxia-exposed cells treated with bioactive molecules of *Mucuna pruriens* seed

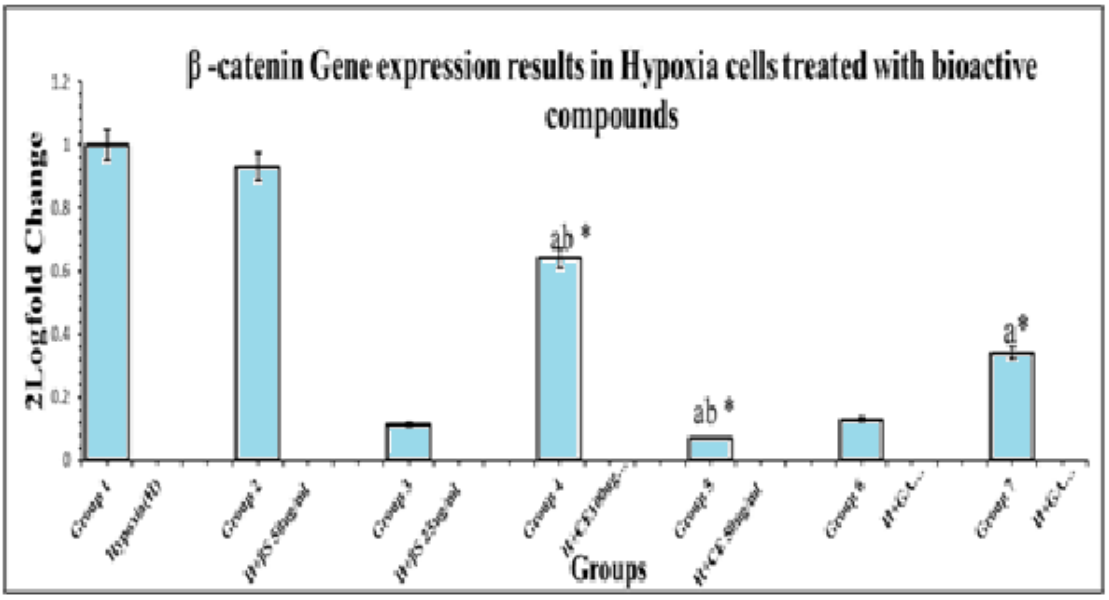

Figure 5.18.1 BS (β-sitosterol), CE (Crude extract), GA (Gallic acid) Superscripts a and c indicate a significant difference between groups. 'a' depicts a comparison with Groups 1,2 and 7, 'and 'b' depicts a comparison with Groups 4 and 5. *P=0.05 are significant

Table 5.18.1 and Figure 5.18.1 illustrate the effects of bioactive molecules derived from *Mucuna pruriens* seed extract (β-sitosterol, gallic acid, and plant crude extract) on β catenin mRNA expression in human pulmonary artery smooth muscle cells under hypoxic conditions. The data demonstrate that exposure to hypoxia led to an increase in β catenin mRNA expression. However, treatment with β-sitosterol at lower concentrations (25µg/ml) significantly downregulated β catenin mRNA levels; similarly, treatment with the crude *Mucuna pruriens* seed extract at higher concentrations(50µg/ml) also considerably decreased β catenin mRNA expression. These findings suggest a concentration-dependent modulation of β catenin mRNA expression by the bioactive components of *Mucuna pruriens* seed extract in HPASMCs under hypoxic conditions.

5.19 Result from Cyclin D1 gene expression in hypoxia-exposed cells treated with bioactive molecules of *Mucuna pruriens* seed

Group 1 Hypoxia (H)	Group 2 H+βS 50ug/ml	Group3 H+βS 25ug/ml	Group4 H+CE 100ug/ml	Group 5 H+CE 50ug/ml	Group6 H+GA 100ug/ml	Group7 H+GA 50ug/ml	Significant value
1.10±0.53	0.43±0.03	0.75±0.52	0.05±0.08	0.13±0.00	0.42±0.40	0.16±0.00	**P=0.78**
BS (β-sitosterol), CE(Crude extract),GA (Gallic acid)							

Table 5.19.1 Cyclin D1 gene expression in hypoxia-exposed cells treated with bioactive molecules of *Mucuna pruriens* seed

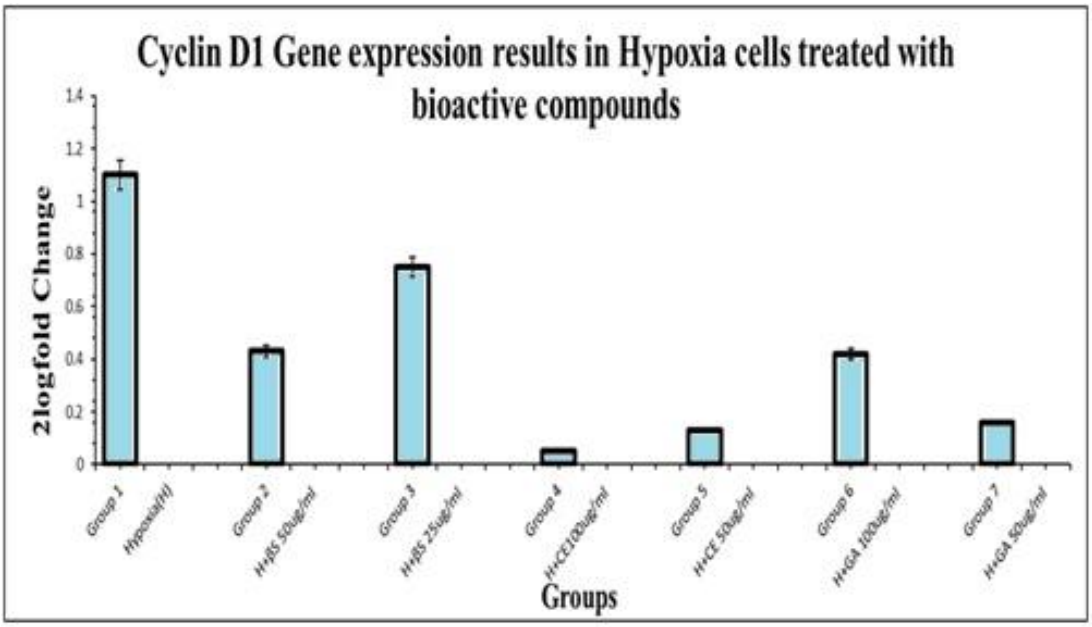

Figure 5.19.1 BS (β-sitosterol), CE (Crude extract), GA (Gallic acid) P=0.78 are insignificant

Table 5.19.1 and Figure 5.19.1 illustrate the effects of bioactive molecules derived from *Mucuna pruriens* seed extract (β-sitosterol, gallic acid, and plant crude extract) on CyclinD1 mRNA expression in human pulmonary artery smooth muscle cells under hypoxic conditions. The data demonstrate that exposure to hypoxia led to an increase in CyclinD1 mRNA expression.

However, treatment with β-sitosterol at lower concentrations (25µg/ml) significantly downregulated CyclinD1 mRNA levels; similarly, treatment with the

crude *Mucuna pruriens* seed extract at higher concentrations (100µg/ml) also considerably decreased CyclinD1mRNA expression. These findings suggest a concentration-dependent modulation of CyclinD1 mRNA expression by the bioactive components of *Mucuna pruriens* seed extract in HPASMCs under hypoxic conditions.

5.20 Invitro Discussion

The present study used human pulmonary artery smooth muscle cells (HPASMC) cultured under normoxic conditions (21% oxygen). Subsequently, the cells were treated with hypoxia conditions (5% oxygen) to study the expression of Wnt 5a, β-catenin, and cyclin D1 in both normoxia and hypoxia because these are key components of the signaling pathway of Wnt/β catenin. β-catenin is acting as one of the major regulators in this pathway.

Our study shows that during hypoxia, there is downregulation of Wnt 5a gene expression and upregulation of both beta-catenin and cyclin D1 gene expression in HPASMC. Through the beta-catenin pathway, Wnt5a prevents human PASMCs from proliferating in response to hypoxia. Similar findings were recorded in a study by Yu et al. (2012) in which hypoxia-induced proliferation of human PASMC was observed along with upregulation of cyclin D1, beta-catenin, and downregulation of wnt5a.

Another research by Jin et al. (2015) also suggested that hypoxic pulmonary hypertension goes along with the upregulation of beta-catenin/cyclin D1. In vivo, RmWnt5a administration improves pulmonary hemodynamic, pulmonary vascular remodeling, and RVH by inhibiting the β-catenin/cyclin D1 pathway.

(Meng H. et al. 2024) Research showed that β-catenin stimulates glycolysis, and the inflammatory response in macrophages favors the development of pulmonary hypertension. Inhibition of β-catenin may be able to slow the growth of pulmonary hypertension.

In this research, the cytotoxicity of the bioactive compound obtained from Mucuna pruriens seed extract was studied with an MTT assay on HPASMCs. The dosages of the drug were given based on the assay results to determine the concentration for hypoxia-induced cells. The subsequent application of the biomolecule on the hypoxia-induced HPASMCs was studied at various concentrations concerning its effects. Our findings indicate that the bioactive components of *Mucuna pruriens* seed extract have a concentration-dependent regulatory impact on the mRNA expression levels of Wnt5a, β catenin, and CyclinD1 mRNA expression in HPASMCs under hypoxic conditions.

A study by Patel S. et al., 2023 indicates altered cardiovascular physiology in L-NAME-treated hypertensive rats. Their analysis showed that simultaneous supplementation of bioactive Phyto-compound β-sitosterol was cardio-protective against L-NAME-induced hypertension.

Another study by Parvatikar et al.,2023 findings showed that pretreatment with Mucuna pruriens seed extract and its particular bioactive molecule β-sitosterol improved the neurological deficit score, reduced ischemic brain damage and decreased the expression of tau protein and NMDAR genes in experimental animals that had cerebral ischemia brought on by LCCAO.

A study by Li, J., Meng, Z et al., 2024 demonstrated that β-sitosterol may be an attractive agent for PH vascular remodeling by inhibiting proliferation and modulating the phenotypic switch in PASMCs via the DNA damage/cGAS/STING signaling pathway.

Our study demonstrated that treatment of hypoxia-exposed cells with β-sitosterol extracted from Mucuna pruriens seed extract modulated the expression of key Wnt signaling pathway gene in a concentration-dependent manner, specifically Wnt 5a expression was upregulated at lower concentrations(25µg/ml). In contrast, β-catenin mRNA expression was downregulated at the same concentration (25µg/ml). Additionally, cyclin D1 mRNA expression exhibited significant downregulation at higher concentrations (50µg/ml). These findings suggest that β-sitosterol may influence Wnt signaling dynamics and cell cycle regulation under hypoxic conditions.

The research findings by Tumbas et al. in 2020 suggest that the aqueous leaf extract of *Mucuna pruriens* has antioxidant activity. In another similar study, it has also been observed that the extract has cytotoxic effects on the human carcinoma cell line, HeLa cells.

A study by Chinnasamy, A. et al. 202 investigated the anticancer effect of ethanolic seed extract from *Mucuna pruriens* against human gastric cancer. Their findings suggest that *Mucuna pruriens* could be a valuable source of natural bioactive compounds with potential therapeutic applications.

Our study found that the extract's influence on the Wnt signaling pathway genes was concentration-dependent when hypoxia-exposed cells were treated with a plant crude extract. Notably, Wnt 5a expression was upregulated at a lower concentration (50 µg/ml), suggesting a possible role in noncanonical Wnt signaling. Conversely, at the same concentration, β-catenin mRNA expression was downregulated, possibly suppressing canonical Wnt signaling. In addition, there was also a significant reduction of cyclin D1 mRNA expression at a higher concentration (100 µg/ml), suggesting an effect on cell cycle regulation. These findings underscore

specific modulatory effects of the plant extract on Wnt signaling and potential pharmaceutical applications.

Research by (Yan X et al., 2020) proved that giving gallic acid to mice substantially lowered the onset of hypertension and vascular remodeling from Ang II. This means that gallic acid is a novel immunoproteasome inhibitor with great potential to treat diseases like hypertension and vascular remodeling.

A study found that Gallic acid therapy reduced ventricular dysfunction and fibrosis in a mouse model of pressure overload heart failure (Jin L. et al., 2018). Another study reported that gallic acid lowers systolic blood pressure and LVH in hypertensive rats by blocking Nox2 expression and oxidative stress via GATA4 suppression (Yan, X., Zhang et al., 2020).

As per the recent study by Kim, H. B., Hong, Et al., 2024, gallic acid can inhibit the proliferation and migration of vascular smooth muscle cells, reducing inflammation and neointimal hyperplasia in the pig-in-stent restenosis model. An adjunct treatment that may mitigate ISR after IC stenting is gallic acid.

Our study showed the regulatory effect of gallic acid extracted *from Mucuna pruriens* seed extract on Wnt signaling pathway components in hypoxia-exposed cells. The result revealed a concentration-dependent modulation of gene expression. Treatment with gallic acid at a lower concentration (50µg/ml) resulted in a significant upregulation of Wnt 5a mRNA expression while concurrently downregulating β catenin mRNA expression at the same concentration (50µg/ml). Furthermore, a higher concentration of gallic acid (100µg/ml) led to a downregulation of cycling D1. These findings indicate that gallic acid exerts regulatory influence on the Wnt signaling pathway.

Chapter-VI

Summary & Conclusion

6.1 Summary and Conclusion

Pulmonary hypertension is caused by changing patterns in smooth muscle cells. A significant remodeling of the pulmonary vasculature and a progressive increase in the pulmonary vascular load, which result in right ventricle hypertrophy and remodeling, are the hallmarks of pulmonary hypertension. Hypoxia is one of the triggers for pulmonary hypertension.

These pulmonary artery smooth muscle cell patterns cause pulmonary hypertension due to pulmonary ventricular resistance influenced by various under-expressed genes. The gene regulation of pulmonary artery smooth muscle cells is due to signal transduction. Wnt/β-catenin is one of the pathways that modulate PASMC architecture.

The present study aims to study the role of Wnt/ β-catenin signaling in the hypoxia-exposed human pulmonary artery smooth muscle cells and the effect of isolated biomolecules of *Mucuna pruriens* seeds with the following objectives.

1. Assessment of interaction between bioactive molecules of *Mucuna Pruriens* seeds with Wnt/β-catenin signaling by in-silico studies.

2. Phytochemical extraction, identification, and isolation of bioactive compound(s) from *Mucuna pruriens* seeds.

3. To study the Wnt/β-catenin mRNA expression in the human pulmonary artery smooth muscle cells exposed to hypoxia and to investigate the effect of isolated bioactive molecule(s) of *Mucuna pruriens* on Wnt/ β-catenin mRNA expression in them.

We proceed with our first objective with an in-silico screening of biomolecules of *Mucuna pruriens* seed extract (Nine bioactive molecules are selected from the literature review) and six proteins (Wnt5a, Frizzled 1, LRP5/6, β-catenin, Dishevelled, and CyclineD1) from Wnt/β-catenin signaling pathway proteins. We did ADMET analysis for biomolecules of Mucuna pruriens seed extract, and after this, we performed molecular docking analysis and MD simulation. Further, it has been observed that out of 09 screened ligands, only 03 ligands have effective binding with all six protein molecules.

We also fulfill objective 2. We collected Mucuna pruriens seed and proceeded for extraction by the Soxhlet method. We also identified bioactive molecules present in the extract by HPLC, and these bioactive molecules were isolated qualitatively and quantitatively by flash chromatography.

Further, we proceed to our third objective. This study is based on in-silico and phytochemical extraction results. We procured HPASMC lines from ATCC. Cells are cultured in normoxia conditions after the subculture cells are exposed to hypoxia, and cell cytotoxicity is performed by MTT assay to know the dosage concentration to treat hypoxia-exposed cells with biomolecules of Mucuna pruriens seed extract.

A gene expression study was done to know the Wnt5a, β-catenin and cyclin D1 gene levels both in normoxia and hypoxia conditions. Wnt 5a level decreased, and β-catenin and cyclin D1 gene levels were increased in hypoxia-exposed cells. Hypoxia-exposed cells were treated with different concentrations with a biomolecule of Mucuna pruriens extract, and mRNA was isolated from the cells by the triazole method. A gene expression study was done. The Wnt5a gene is downregulated, and β catenin and cyclin D1 genes are upregulated in hypoxia-exposed PASMC.

- The Invitro study revealed that when HPASMC is exposed to hypoxia, there is downregulation of the Wnt 5a gene and upregulation of β-catenin and Cyclin D1 genes.
- Wnt5a inhibits hypoxia-induced proliferation of human PASMCs through the β-catenin pathway.
- *Mucuna pruriens* seed extract, β-sitosterol, and gallic acid can be attributed to inhibiting the β-catenin pathway via the upregulation of Wnt 5a and the downregulation of β-catenin and Cyclin D1 gene expression. Interestingly, the crude extract of *Mucuna pruriens* seed was more effective than isolated bioactive molecules.

Hence, upregulating β-catenin and Cyclin D1 gene expression possibly prevents cyclin D1-induced remodeling of pulmonary artery smooth muscle cells and hypertension in hypoxic conditions. *Mucuna pruriens*, or its bioactive molecule gallic acid and β-sitosterol, may be a possible therapeutic agent against Pulmonary hypertension.

6.2 Conclusion

The present study focused on in-silico phytochemical analysis and in vitro investigations to evaluate the potential therapeutic role of isolated biomolecules from *Mucuna pruriens* seed extract β-sitosterol and gallic acid in hypoxia-exposed pulmonary artery smooth muscle cells (HPASMCs). These findings suggest that *Mucuna pruriens*, or its bioactive molecule gallic acid and β-sitosterol, may exert protective effects against hypoxia-induced vascular remodeling by targeting the Wnt/β-catenin signaling pathway.

Clinical Implication of the Study

This study shows that isolated biomolecules of *Mucuna pruriens* seed (β-sitosterol and gallic acid) and the crude extract may be beneficial in managing pulmonary hypertension, which requires further exploration and confirmation with in vivo studies.

Limitations of the study

This research is based on *in-silico* and in-vitro analysis. Validation of this study by an in vivo approach is needed.

Chapter-VII

References

- Abdul-Ghani, M., Dufort, D., Stiles, R., De Repentigny, Y., Kothary, R., & Megeney, L. A. (2011). Wnt11 promotes cardiomyocyte development by caspase-mediated suppression of canonical Wnt signals. Molecular and cellular biology, 31(1), 163-178.
- Bachheti, R. K., Worku, L. A., Gonfa, Y. H., Zebeaman, M., Deepti, Pandey, D. P., & Bachheti, A. (2022). Prevention and Treatment of Cardiovascular Diseases with Plant Phytochemicals: A Review. Evidence-Based Complementary and Alternative Medicine, 2022(1), 5741198.
- Bae, T., Hallis, S. P., & Kwak, M. K. (2024). Hypoxia, oxidative stress, and the interplay of HIFs and NRF2 signaling in cancer. Experimental & molecular medicine, 56(3), 501-514.
- Bhosle, S., Bagali, S., Parvatikar, P. P., & Das, K. K. (2024). Effect of bioactive compounds of Mucuna pruriens on proteins of Wnt/β catenin pathway in pulmonary hypertension by in silico approach. In Silico Pharmacology, 12(2), 110.
- Biovia, D. S. (2017). Materials studio. R2 (Dassault Systèmes BIOVIA, San Diego.
- Burley, S. K., Berman, H. M., Kleywegt, G. J., Markley, J. L., Nakamura, H., & Velankar, S. (2017). Protein Data Bank (PDB): the single global macromolecular structure archive. Protein crystallography: methods and protocols, 627-641.
- Cabral, C. E., & Klein, M. R. S. T. (2017). Phytosterols in the treatment of hypercholesterolemia and prevention of cardiovascular diseases. Arquivos brasileiros de cardiologia, 109, 475-482.
- Chinnasamy, A., Jayaprakash, V., Padmanaban, D., Sekar, N., Valayapathi, R., Azhagudurai, A., & Ethiraj, S. (2024). Effect of crude ethanolic seed extract from Mucuna pruriens on proliferation, apoptosis, and cell cycle arrest in gastric adenocarcinoma (AGS) cells. Future Journal of Pharmaceutical Sciences, 10(1), 141.
- Choubey, Sneha, Soniya Goyal, Lesley R. Varughese, Vinod Kumar, Anil K. Sharma, and Vikas Beniwal. "Probing gallic acid for its broad-spectrum applications." Mini-Reviews in Medicinal Chemistry 18, no. 15 (2018): 1283-1293.

- Christou, H., & Khalil, R. A. (2022). Mechanisms of pulmonary vascular dysfunction in pulmonary hypertension and implications for novel therapies. American Journal of Physiology-Heart and Circulatory Physiology.
- Dejana, E. (2010). The role of wnt signaling in physiological and pathological angiogenesis. Circulation research, 107(8), 943-952.
- Dwivedi, K., Sharkey, M., Condliffe, R., Uthoff, J. M., Alabed, S., Metherall, P., ... & Kiely, D. G. (2021). Pulmonary hypertension in association with lung disease: quantitative CT and artificial intelligence to the rescue? State-of-the-art review. Diagnostics, 11(4), 679.
- Fernandez, R. A., Sundivakkam, P., Smith, K. A., Zeifman, A. S., Drennan, A. R., & Yuan, J. X. J. (2012). Pathogenic Role of Store-Operated and Receptor-Operated Ca2+ Channels in Pulmonary Arterial Hypertension. Journal of signal transduction, 2012(1), 951497.
- Galiè, N., Hoeper, M. M., Humbert, M., Torbicki, A., Vachiery, J. L., Barbera, J. A., ... & Zamorano, J. L. (2009). Guidelines for the diagnosis and treatment of pulmonary hypertension: the Task Force for the Diagnosis and Treatment of Pulmonary Hypertension of the European Society of Cardiology (ESC) and the European Respiratory Society (ERS), endorsed by the International Society of Heart and Lung Transplantation (ISHLT). European heart journal, 30(20), 2493-2537.
- Hannan, M. A., Sohag, A. A. M., Dash, R., Haque, M. N., Mohibbullah, M., Oktaviani, D. F., & Moon, I. S. (2020). Phytosterols of marine algae: Insights into the potential health benefits and molecular pharmacology. Phytomedicine, 69, 153201.
- Harjacek, M., Diaz-Cano, S., Alman, B. A., Coburn, J., Ruthazer, R., Wolfe, H., & Steere, A. C. (2000). Europe PubMed Central. The Journal of Rheumatology, 27(2), 497-503.
- He, K., & Gan, W. J. (2023). Wnt/β-catenin signaling pathway in the development and progression of colorectal cancer. Cancer Management and Research, 435-448.
- Hema, M. K., Karthik, C. S., Pampa, K. J., Mallu, P., & Lokanath, N. K. (2020). Solvent induced mononuclear and dinuclear mixed ligand Cu (II)

complex: structural diversity, supramolecular packing polymorphism and molecular docking studies. New Journal of Chemistry, 44(41), 18048-18068.

- Hiremath, I. S., Goel, A., Warrier, S., Kumar, A. P., Sethi, G., & Garg, M. (2022). The multidimensional role of the Wnt/β-catenin signaling pathway in human malignancies. Journal of cellular physiology, 237(1), 199-238.
- Hoeper, M. M., Humbert, M., Souza, R., Idrees, M., Kawut, S. M., Sliwa-Hahnle, K., ... & Gibbs, J. S. R. (2016). A global view of pulmonary hypertension. The Lancet Respiratory Medicine, 4(4), 306-322.
- Huang, X., Akgün, E. E., Mehmood, K., Zhang, H., Tang, Z., & Li, Y. (2022). Mechanism of Hypoxia-Mediated Smooth Muscle Cell Proliferation Leading to Vascular Remodeling. BioMed research international, 2022(1), 3959845.
- Jin, L., Sun, S., Ryu, Y., Piao, Z. H., Liu, B., Choi, S. Y., et al., (2018). Gallic acid improves cardiac dysfunction and fibrosis in pressure overload-induced heart failure. Scientific reports, 8(1), 9302.
- Jin, Y., Wang, W., Chai, S., Liu, J., Yang, T., & Wang, J. (2015). Wnt5a attenuates hypoxia-induced pulmonary arteriolar remodeling and right ventricular hypertrophy in mice. Experimental biology and medicine, 240(12), 1742-1751.A
- Johnson, S., Sommer, N., Cox-Flaherty, K., Weissmann, N., Ventetuolo, C. E., et al., (2023). Pulmonary hypertension: a contemporary review. American journal of respiratory and critical care medicine, 208(5), 528-548.
- Jung, Y. S., & Park, J. I. (2020). Wnt signaling in cancer: therapeutic targeting of Wnt signaling beyond β-catenin and the destruction complex. Experimental & Molecular Medicine, 52(2), 183-191.

- Jung, Y. S., & Park, J. I. (2020). Wnt signaling in cancer: therapeutic targeting of Wnt signaling beyond β-catenin and the destruction complex. Experimental & Molecular Medicine, 52(2), 183-191.

- Kamkaen, N., Chittasupho, C., Vorarat, S., Tadtong, S., Phrompittayarat, W., Okonogi, S., & Kwankhao, P. (2022). Mucuna pruriens seed aqueous extract improved neuroprotective and acetylcholinesterase inhibitory effects compared with synthetic L-dopa. Molecules, 27(10), 3131.
- Karnati, S., Seimetz, M., Kleefeldt, F., Sonawane, A., Madhusudhan, T., Bachhuka, A., ... & Ergün, S. (2021). Chronic obstructive pulmonary disease

and the cardiovascular system: vascular repair and regeneration as a therapeutic target. Frontiers in Cardiovascular Medicine, 8, 649512.

- Khaparkhuntikar, K., Maji, I., Gupta, S. K., Mahajan, S., Aalhate, M., Sriram, A. et al., (2024). Acalabrutinib as a novel hope for the treatment of breast and lung cancer: an in-silico proof of concept. Journal of Biomolecular Structure and Dynamics, 42(3), 1469-1484.
- Kim, H. B., Hong, Y. J., Lee, S. H., Kee, H. J., Kim, M., Ahn, Y et al., (2024). Gallic acid inhibits the proliferation and migration of smooth muscle cells in a pig-in-stent restenosis model. Chonnam Medical Journal, 60(1), 32.
- Kim, S., Chen, J., Cheng, T., Gindulyte, A., He, J., He, S., et al., (2019). PubChem 2019 update: improved access to chemical data. Nucleic acids research, 47(D1), D1102-D1109.
- Kirubhanand, C., Selvaraj, J., Rekha, U. V., Vishnupriya, V., Nalini, D., Mohan, S. K., et al., (2020). Molecular docking data of piperine with Bax, Caspase 3, Cox 2 and Caspase 9. Bioinformation, 16(6), 458.
- Klein, M., Varga, I., Danišovič, Ľ., Gálfiová, P., Kleinová, M., Žiaran, S., Kuniaková, M. (2024). The role of histology in tissue engineering: Significance of complex morphological characterization of decellularized foreskin scaffolds. Tissue and Cell, 91, 102623.
- Kumar, S., Dubey, R., Mishra, R., Gupta, S., Dwivedi, V. D., Ray, S., ... & Dubey, N. K. (2024). Repurposing of SARS-CoV-2 compounds against Marburg Virus using MD simulation, mm/GBSA, PCA analysis, and free energy landscape. Journal of Biomolecular Structure and Dynamics, 1-20.
- Lampariello, L. R., Cortelazzo, A., Guerranti, R., Sticozzi, C., & Valacchi, G. (2012). The magic velvet bean of Mucuna pruriens. Journal of traditional and complementary medicine, 2(4), 331-339.
- Laskowski, R. A., Jabłońska, J., Pravda, L., Vařeková, R. S., & Thornton, J. M. (2018). PDBsum: Structural summaries of PDB entries. Protein science, 27(1), 129-134.
- Lee, J., Kim, S. K., Kang, H. G., Ha, I. S., Wang, K. C., Lee, J. Y., & Phi, J. H. (2019). High prevalence of systemic hypertension in pediatric patients with moyamoya disease years after surgical treatment. Journal of Neurosurgery: Pediatrics, 25(2), 131-137.

- Li, J., Meng, Z. Y., Wen, H., Lu, C. H., Qin, Y., Xie, Y. M., ... & Zeng, Z. Y. (2024). β-sitosterol alleviates pulmonary arterial hypertension by altering smooth muscle cell phenotype and DNA damage/cGAS/STING signaling. Phytomedicine, 135, 156030.
- Liu, J., Xiao, Q., Xiao, J., Niu, C., Li, Y., Zhang, X., et al., (2022). Wnt/β-catenin signaling: function, biological mechanisms, and therapeutic opportunities. Signal transduction and targeted therapy, 7(1), 3.
- Liu, J., Xiao, Q., Xiao, J., Niu, C., Li, Y., Zhang, X., Yin, G. (2022). Wnt/β-catenin signalling: function, biological mechanisms, and therapeutic opportunities. Signal transduction and targeted therapy, 7(1), 3.
- Luo, H., Mattes, W., Mendrick, D. L., & Hong, H. (2016). Molecular docking for identification of potential targets for drug repurposing. Current topics in medicinal chemistry, 16(30), 3636-3645.
- MacDonald, B. T., Tamai, K., & He, X. (2009). Wnt/β-catenin signaling: components, mechanisms, and diseases. Developmental cell, 17(1), 9-26.
- Madagi, S. B., Parvatikar, P. P. (2018). Docking studies on phytochemical derivatives as tissue transglutaminase-2 (TG2) inhibitors aganist lung Cancer. In Proceedings of the World Congress on Engineering and Computer Science (Vol. 1, pp. 23-25).
- McGarvey, P. B., Nightingale, A., Luo, J., Huang, H., Martin, M. J., Wu, C., et al., (2019). UniProt genomic mapping for deciphering functional effects of missense variants. Human mutation, 40(6), 694-705.
- Meng, H., Deng, Y., Liao, J., Wu, D. D., Li, L. X., Chen, X., & Lan, W. F. (2024). β-catenin mediates monocrotaline-induced pulmonary hypertension via glycolysis in rats. BMC Cardiovascular Disorders, 24(1), 381
- Michiels, C. (2004). Physiological and pathological responses to hypoxia. The American journal of pathology, 164(6), 1875-1882.
- Mocumbi, A., Humbert, M., Saxena, A., Jing, Z. C., Sliwa, K., Thienemann, F., et al., (2024). Pulmonary hypertension. Nature reviews Disease primers, 10(1), 1.
- Moghadamtousi, S. Z., Fadaeinasab, M., Nikzad, S., Mohan, G., Ali, H. M., et al., (2015). Annona muricata (Annonaceae): a review of its traditional uses,

isolated acetogenins and biological activities. International journal of molecular sciences, 16(7), 15625-15658.

- Moreno-Calvo, E., Temelli, F., Cordoba, A., Masciocchi, N., Veciana, J., et al., (2014). A new microcrystalline phytosterol polymorph generated using CO2-expanded solvents. Crystal Growth & Design, 14(1), 58-68.
- Morris, G. M., Huey, R., Lindstrom, W., Sanner, M. F., Belew, R. K., Goodsell, D. S., & Olson, A. J. (2009). AutoDock4 and AutoDockTools4: Automated docking with selective receptor flexibility. Journal of computational chemistry, 30(16), 2785-2791.
- Naranjo, M., Hassoun, P. M. (2021). Systemic sclerosis-associated pulmonary hypertension: spectrum and impact. Diagnostics, 11(5), 911.
- Parvatikar, P. P., Patil, S. M., Patil, B. S., Reddy, R. C., Bagoji, I., Kotennavar, M. S., et al., (2023). Effect of Mucuna pruriens on brain NMDA receptor and tau protein gene expression in cerebral ischemic rats. Frontiers in Physiology, 14, 1092032.

- Parvatikar, P. P., Patil, S. M., Patil, B. S., Reddy, R. C., Bagoji, I., Kotennavar, M. S., et al., (2023). Effect of Mucuna pruriens on brain NMDA receptor and tau protein gene expression in cerebral ischemic rats. Frontiers in Physiology, 14, 1092032.

- Parvatikar, P., Saha, B., Das, S. K., Reddy, R. C., Bagali, S., Kulkarni, R. V, et al., (2022). Molecular docking identifies novel phytochemical inhibitors against sars-cov-2 for COVID-19 therapy. Research Journal of Pharmacy and Technology, 15(2), 555-558.
- Pathania, R., Chawla, P., Khan, H., Kaushik, R., Khan, M. A. (2020). An assessment of potential nutritive and medicinal properties of Mucuna pruriens: a natural food legume. 3 Biotech, 10(6), 261.
- Peacock, A. J., Murphy, N. F., McMurray, J. J. V., Caballero, L., et al., (2007). An epidemiological study of pulmonary arterial hypertension. European Respiratory Journal, 30(1), 104-109.
- Prabhakar, N. R., Kumar, G. K., Nanduri, J., Semenza, G. L. (2007). ROS signaling in systemic and cellular responses to chronic intermittent hypoxia. Antioxidants & redox signaling, 9(9), 1397-1404.

- Primary Pulmonary Artery Smooth Muscle Cells; Normal, Human (PASMC) (ATCC PCS-100-023)
- Pulgar-Sepúlveda, R., Varas, R., Iturriaga, R., Del Rio, R., & Ortiz, F. C. (2018). Carotid body type-I cells under chronic sustained hypoxia: focus on metabolism and membrane excitability. Frontiers in Physiology, 9, 1282.
- Rai, S. N., Singh, P., Varshney, R., Chaturvedi, V. K., Vamanu, E., Singh, M. P., et al., (2021). Promising drug targets and associated therapeutic interventions in Parkinson's disease. Neural regeneration research, 16(9), 1730-1739.
- Ramírez, I., Melendez, J., Chanamé, J. (2012). Oxygen abundances in low-and high-α field halo stars and the discovery of two field stars born in globular clusters. The Astrophysical Journal, 757(2), 164.
- Rane, M., Suryawanshi, S., Patil, R., Aware, C., Jadhav, R., Gaikwad, S., Jadhav, J. (2019). Exploring the proximate composition, antioxidant, anti-Parkinson's and anti-inflammatory potential of two neglected and underutilized Mucuna species from India. South African Journal of Botany, 124, 304-310.
- Saetta, M., Turato, G., Maestrelli, P., Mapp, C. E., & Fabbri, L. M. (2001). Cellular and structural bases of chronic obstructive pulmonary disease. American journal of respiratory and critical care medicine, 163(6), 1304-1309.
- Saini, A. S., Meredith, S., Esquinas, A. M., & Mina, B. A. (2022). High-flow nasal cannula and noninvasive ventilation: effects on alveolar recruitment and overdistension. ERJ open research, 8(2).
- Sandeep, C., Venugopala, K. N., Khedr, M. A., Padmashali, B., Kulkarni, R. S., Rashmi, V., Odhav, B. (2017). Design and synthesis of novel indolizine analogues as COX-2 inhibitors: Computational perspective and in vitro screening. Indian J. Pharm. Educ. Res, 51(3), 452-460.
- Sayers, E. W., Beck, J., Bolton, E. E., Bourexis, D., Brister, J. R., Canese, K., et al. (2021). Database resources of the national center for biotechnology information. Nucleic acids research, 49(D1), D10-D17.
- Senthilkumar, A., Karuvantevida, N., Rastrelli, L., Kurup, S. S., & Cheruth, A. J. (2018). Traditional uses, pharmacological efficacy, and phytochemistry of

Moringa peregrina (Forssk.) Fiori. a review. Frontiers in pharmacology, 9, 465.

- Shang, S., Hua, F., Hu, Z. W. (2017). The regulation of β-catenin activity and function in cancer: therapeutic opportunities. Oncotarget, 8(20), 33972.
- Shapovalov, M. V., Dunbrack, R. L. (2011). A smoothed backbone-dependent rotamer library for proteins derived from adaptive kernel density estimates and regressions. Structure, 19(6), 844-858.

- Shapovalov, M. V., Dunbrack, R. L. (2011). A smoothed backbone-dependent rotamer library for proteins derived from adaptive kernel density estimates and regressions. Structure, 19(6), 844-858.

- Sheikh, A., Niazi, A. K., Ahmed, M. Z., Iqbal, B., Anwer, S. M. S., & Khan, H. H. (2014). The role of Wnt signaling pathway in carcinogenesis and implications for anticancer therapeutics. Hereditary Cancer in Clinical Practice, 12, 1-4.
- Song, P., Gao, Z., Bao, Y., Chen, L., Huang, Y., Liu, Y., ... & Wei, X. (2024). Wnt/β-catenin signaling pathway in carcinogenesis and cancer therapy. Journal of Hematology & Oncology, 17(1), 46.
- Sun, Y., Liu, S., Chen, C., Yang, S., Pei, G., Lin, M., ... & Yang, Y. (2023). The mechanism of programmed death and endoplasmic reticulum stress in pulmonary hypertension. Cell Death Discovery, 9(1), 78.
- Tangsrisakda, N., Kamollerd, T., Taoto, C., Bunsueb, S., Chaimontri, C., Choowong-In, P., ... & Iamsaard, S. (2022). Seed extract of Thai Mucuna pruriens (L.) DC. var. pruriens enhances sexual performance and improves male reproductive damages in ethanol-induced rats. Journal of ethnopharmacology, 292, 115219.
- Tao, L., Gu, Y., Zheng, J., Yang, J., Zhu, Y. (2019). Weichang'an suppressed migration and invasion of HCT116 cells by inhibiting Wnt/β-catenin pathway while upregulating ARHGAP25. Biotechnology and Applied Biochemistry, 66(5), 787-793.
- Tarapore, R. S., Siddiqui, I. A., & Mukhtar, H. (2012). Modulation of Wnt/β-catenin signaling pathway by bioactive food components. Carcinogenesis, 33(3), 483-491.

- Theansungnoen, T., Nitthikan, N., Wilai, M., Chaiwut, P., Kiattisin, K., & Intharuksa, A. (2022). Phytochemical analysis and antioxidant, antimicrobial, and antiaging activities of ethanolic seed extracts of four Mucuna species. Cosmetics, 9(1), 14.
- Tucker, T., Tsukasaki, Y., Sakai, T., Mitsuhashi, S., Komatsu, S., Jeffers, A., ... & Ikebe, M. (2019). Myocardin Is Involved in Mesothelial–Mesenchymal Transition of Human Pleural Mesothelial Cells. American journal of respiratory cell and molecular biology, 61(1), 86-96.
- Tumbas-Saponjac, V., Akpoveso, O. O. P., Oyeniran, O. I., Desančić, J., & Četojević-Simin, D. (2020). Antioxidant activity and enhanced cytotoxicity of aqueous Mucuna pruriens L. leaf extract by doxorubicin on different human cancer cell lines. Pharmacognosy Magazine, 16(68).Patel, S., Aithala, M., Patil, S., & Das, K. K. (2023). β-sitosterol on heart rate variability in L-NAME induced hypertensive rats.
- Vickery, B., Klein, A. (2017). Chronic Pulmonary Hypertension. Case Studies in Adult Intensive Care Medicine, 131.
- Waterhouse, R. M., Seppey, M., Simão, F. A., Manni, M., Ioannidis, P., Klioutchnikov, G., et al., (2018). BUSCO applications from quality assessments to gene prediction and phylogenomics. Molecular biology and evolution, 35(3), 543-548.
- Wu, K., Zhang, Q., Wu, X., Lu, W., Tang, H., Liang, Z., Wang, J. (2017). Chloroquine is a potent pulmonary vasodilator that attenuates hypoxia-induced pulmonary hypertension. British journal of pharmacology, 174(22), 4155-4172.
- Yan, X., Zhang, Q. Y., Zhang, Y. L., Han, X., Guo, S. B., & Li, H. H. (2020). Gallic acid attenuates angiotensin II-induced hypertension and vascular dysfunction by inhibiting the degradation of endothelial nitric oxide synthase. Frontiers in Pharmacology, 11, 1121.

- Yan, X., Zhang, Q. Y., Zhang, Y. L., Han, X., Guo, S. B., & Li, H. H. (2020). Gallic acid attenuates angiotensin II-induced hypertension and vascular dysfunction by inhibiting the degradation of endothelial nitric oxide synthase. Frontiers in Pharmacology, 11, 1121.

- Yang, Y. (2012). Wnt signaling in development and disease. Cell & bioscience, 2, 1-9.
- Yu, F., Yu, C., Li, F., Zuo, Y., Wang, Y., Yao, L., ... & Ye, L. (2021). Wnt/β-catenin signaling in cancers and targeted therapies. Signal Transduction and Targeted Therapy, 6(1), 307.
- Yu, X. M., Wang, L., Li, J. F., Liu, J., Li, J., Wang, W., ... & Wang, C. (2013). Wnt5a inhibits hypoxia-induced pulmonary arterial smooth muscle cell proliferation by downregulating β-catenin—American Journal of Physiology-Lung Cellular and Molecular Physiology, 304(2), L103-L111.
- Yuan, S. M. (2017). Pulmonary artery hypertension: pertinent vasomotor cytokines. European Cytokine Network, 28, 1-7.
- Zhang, R., Dai, L. Z., Xie, W. P., Yu, Z. X., Wu, B. X., Pan, L., ... & Jing, Z. C. (2011). Survival of Chinese patients with pulmonary arterial hypertension in the modern treatment era. Chest, 140(2), 301-309.

Annexure

BLDE

(DEEMED TO BE UNIVERSITY)

Smt. Bangaramma Sajjan Campus, B. M. Patil Road (Sholapur Road), Vijayapura-586103. Karnataka, India

PLAGIARISM VERIFICATION CERTIFICATE

1. **Name of Student**: Ms. Supriya Bhosale (Reg No: 20PHD025)

2. **Title of the Thesis**: "Wnt/β-catenin signaling in hypoxia-induced pulmonary artery smooth muscle cell proliferation -Role of bioactive molecule of *Mucuna pruriens*."

3. **Department:** Laboratory of Vascular Physiology and Medicine Department of Physiology

4. **Name of Guide & Designation**: **Prof. Kusal K. Das,** Distinguished Chair Professor, Laboratory of Vascular Physiology and Medicine, BLDE (Deemed to be University). Shri B.M.Patil Medical College, Hospital & Research Centre, Vijayapur.

5. **Name of Co-Guide & Designation**: **Dr. Shrilaxmi Bagali**. Professor, Department of Physiology, BLDE (Deemed to be University) Shri B.M.Patil Medical College, Hospital & Research Centre, Vijayapur.

The above thesis was verified for similarity detection. The report is as follows:

Software used: iThenticate Date: 5-3-2025

Similarity Index (%): 7% Total word count: 14745

The report is attached for review by the Student and Guide. The plagiarism report of the above thesis has been reviewed by the undersigned. The similarity index is below accepted norms. The thesis may be considered for submission to the university. The software report is attached.

Signature of Guide	Signature of Co-Guide	S D. Bhosale Signature of Student
Name & Designation	Name & Designation Dr Shrilaxmi Bagali	

Verified by (Signature)

Name & Designation

Dr. Prasanna Kumara BM
Deemed to be University)
B.M.Patil Medical College
Vijayapura - 586103

Page 126

Paper Publications

1. Repurposing of potential bioactive compounds from various databases to study their effects on MMP-7 by virtual screening. Research Journal of Biotechnology Vol. 19 (2) February (2024).

2. Effect of bioactive compounds of Mucuna pruriens on proteins of Wnt/β catenin pathway in pulmonary hypertension by in silico approach. In-silico-Pharmacology (Springer) DOI: 10.1007/s40203-024-00263-8 Volume 12, article number 110, 2024

Presentations

1. Participated and presented oral presentation in the 9th International e-conference of Federation of Indian Physiological Societies (FIPS)-2022 organized by FIPS and NIPER Hyderabad from 25th to 27th March 2022 on "*In-silico* analysis of the interaction of bioactive molecules of *Mucuna Pruriens* with beta-catenin targeting Wnt / beta-catenin pathway.

2. Presented a poster at the First National Symposium on Integrating Traditional Knowledge in Evidence-Based Medicine on 21-22 September 2023 at TATA Memorial Canter ACTREC Navi Mumbai.

Awards

- Participated and presented an e-poster titled **"IN-SILICO ANALYSIS OF THE INTERACTION OF BIOACTIVE MOLECULES OF MUCUNA PRURIENS WITH CYCLIN D1 TARGETING THE WNT/B CATENIN PATHWAY"** in the 8th Biennial Conference of the South Asian Association of Physiologists, Colombo, Sri Lanka and got **FIRST PRIZE** for poster.

- Participated and presented a poster in PHYSICON 2023, organized by BLDE (DU) on **"in-silico analysis of the interaction of bioactive molecules of Mucuna pruriens with proteins targeting the Wnt/β catenin pathway"** got the **BEST PAPER** award.

Copyright

Copyright for the graphical abstract of the Interaction of bioactive molecules of *Mucuna Pruriens* with proteins of the Wnt/ß catenin pathway to identify potential candidates for pulmonary hypertension by *in-silico* analysis. Registration Number (L-150995/2024) dated 15/07/2024.

INTELLECTUAL PROPERTY INDIA
PATENTS | DESIGNS | TRADE MARKS
GEOGRAPHICAL INDICATIONS

सत्यमेव जयते

Extracts from the Register of Copyrights

प्रतिलिप्यधिकार कार्यालय, भारत सरकार | Copyright Office, Government Of India

दिनांक/Dated:15/07/2024

1.	पंजीकरण संख्या/Registration Number	:	**L-150995/2024**
2.	आवेदक का नाम, पता तथा राष्ट्रीयता Name, address and nationality of the applicant	:	BLDE-DEEMED TO BE UNIVERSITY , SMT. BANGARAMMA SAJJAN CAMPUS, B. M. PATIL ROAD, SOLAPUR ROAD, VIJAYAPURA, KARNATAKA, INDIA-586103 INDIAN
3.	कृति के प्रतिलिप्यधिकार में आवेदक के हित की प्रकृति Nature of the applicant's interest in the copyright of the work	:	OWNER
4.	कृति का वर्ग और वर्णन Class and description of the work	:	LITERARY/ DRAMATIC WORK
5.	कृति का शीर्षक Title of the work	:	INTERACTION OF BIOACTIVE MOLECULES OF MUCUNA PRURIENS WITH PROTEINS OF THE WNT/β CATENIN PATHWAY TO IDENTIFY POTENTIAL CANDIDATES FOR PULMONARY HYPERTENSION BY IN-SILICO ANALYSIS
6.	कृति की भाषा Language of the work	:	ENGLISH
7.	रचयिता का नाम, पता और राष्ट्रीयता तथा यदि रचयिता की मृत्यु हो गई है, तो मृत्यु की तिथि Name, address and nationality of the author and if the author is deceased, date of his decease	:	MS. SUPRIYA BHOSALE , DEPARMENT OF PHYSIOLOGY, SRI B M PATIL, MEDICAL COLLEGE, HOSPITAL AND RESEARCH CENTRE, BLDE-DU, SMT. BANGARAMMA SAJJAN CAMPUS, B M PATIL ROAD, SOLAPUR ROAD, VIJAYAPURA, KARNATAKA-586103 INDIAN DR. PRACHI PARVATIKAR , ALLIED HEALTH SCIENCE, SRI B M PATIL, MEDICAL COLLEGE, HOSPITAL AND RESEARCH CENTRE, BLDE-DU, SMT. BANGARAMMA SAJJAN CAMPUS, B M PATIL ROAD, SOLAPUR ROAD, VIJAYAPURA, KARNATAKA-586103 INDIAN DR SHRILAXMI BAGALI , DEPARMENT OF PHYSIOLOGY, SRI B M PATIL, MEDICAL COLLEGE, HOSPITAL AND RESEARCH CENTRE, BLDE-DU, SMT. BANGARAMMA SAJJAN CAMPUS, B M PATIL ROAD, SOLAPUR ROAD, VIJAYAPURA, KARNATAKA-586103 INDIAN DR KUSAL DAS , DEPARMENT OF PHYSIOLOGY, SRI B M PATIL, MEDICAL COLLEGE, HOSPITAL AND RESEARCH CENTRE, BLDE-DU, SMT. BANGARAMMA SAJJAN CAMPUS, B M PATIL ROAD, SOLAPUR ROAD, VIJAYAPURA, KARNATAKA-586103 INDIAN
8.	कृति प्रकाशित है या अप्रकाशित Whether the work is published or unpublished	:	UNPUBLISHED
9.	प्रथम प्रकाशन का वर्ष और देश तथा प्रकाशक का नाम, पता और राष्ट्रीयता Year and country of first publication and name, address and nationality of the publisher	:	N.A.
10.	बाद के प्रकाशनों के वर्ष और देश, यदि कोई हों, और प्रकाशकों के नाम, पते और राष्ट्रीयताएँ Years and countries of subsequent publications, if any, and names, addresses and nationalities of the publishers	:	N.A.
11.	कृति में प्रतिलिप्यधिकार सहित विभिन्न अधिकारों के स्वामियों के नाम, पते और राष्ट्रीयताएं और समनुदेशन और अनुज्ञप्तियों के विवरण के साथ प्रत्येक के अधिकार का विस्तार, यदि कोई हो। Names, addresses and nationalities of the owners of various rights comprising the copyright in the work and the extent of rights held by each, together with particulars of assignments and licences, if any	:	BLDE-DEEMED TO BE UNIVERSITY , SMT. BANGARAMMA SAJJAN CAMPUS, B. M. PATIL ROAD, SOLAPUR ROAD, VIJAYAPURA, KARNATAKA, INDIA-586103 INDIAN
12.	अन्य व्यक्तियों के नाम, पते और राष्ट्रीयताएं, यदि कोई हों, जो प्रतिलिप्यधिकार वाले अधिकारों को समनुदेशित करने या अनुज्ञप्ति देने के लिए अधिकृत हों Names, addresses and nationalities of other persons, if any, authorised to assign or licence of rights comprising the copyright	:	BLDE-DEEMED TO BE UNIVERSITY , SMT. BANGARAMMA SAJJAN CAMPUS, B. M. PATIL ROAD, SOLAPUR ROAD, VIJAYAPURA, KARNATAKA, INDIA-586103 INDIAN
13.	यदि कृति एक 'कलात्मक कृति' है, तो कृति पर अधिकार रखने वाले व्यक्ति का नाम, पता और राष्ट्रीयता सहित मूल कृति का स्थान। (एक वास्तुशिल्प कृति के मामले में कृति पूरी होने का वर्ष भी दिखाया जाना चाहिए) If the work is an 'Artistic work', the location of the original work, including name, address and nationality of the person in possession of the work. (In the case of an architectural work, the year of completion of the work should also be shown).	:	N.A.
14.	यदि कृति एक 'कलात्मक कृति' है जो किसी भी माल या सेवाओं के संबंध में उपयोग की जाती है या उपयोग किए जाने में सक्षम है, तो आवेदन में प्रतिलिप्यधिकार अधिनियम, 1957 की धारा 45 की उप–धारा (i) के प्रावधान के अनुसार व्यापार चिह्न रजिस्ट्रार से प्रमाणन शामिल होना चाहिए। If the work is an 'Artistic work' which is used or capable of being used in relation to any goods or services, the application should include a certification from the Registrar of Trade Marks in terms of the provision to Sub-Section (i) of Section 45 of the Copyright Act, 1957.	:	N.A.
15.	यदि कृति एक 'कलात्मक कृति' है, तो क्या यह डिजाइन अधिनियम 2000 के अंतर्गत पंजीकृत है? यदि हां, तो विवरण दें। If the work is an 'Artistic work', whether it is registered under the Designs Act 2000, if yes give details.	:	N.A.

इन्द्रजीत पी पांडेय
Registrar of Copyrights

16. यदि कृति एक 'कलात्मक कृति' है, जो डिजाइन अधिनियम 2000 के तहत एक डिजाइन के रूप में पंजीकृत होने में सक्षम है, तो क्या यह औद्योगिक प्रक्रिया के माध्यम से किसी वस्तु पर प्रयुक्त की गई है और यदि हाँ, तो इसे कितनी बार पुनरुत्पादित किया गया है? : N.A.
If the work is an 'Artistic work', capable of being registered as a design under the Designs Act 2000.whether it has been applied to an article though an industrial process and ,if yes ,the number of times it is reproduced.

17. टिप्पणी, यदि कोई हो/Remarks, if any :

डायरी संख्या/Diary Number: 18619/2024-CO/L

आवेदन की तिथि/Date of Application: 07/06/2024

प्राप्ति की तिथि/Date of Receipt: 07/06/2024

उन्नत पी पंडित
Registrar of Copyrights

In Silico Pharmacology (2024) 12:110
https://doi.org/10.1007/s40203-024-00263-8

ORIGINAL RESEARCH

Effect of bioactive compounds of *Mucuna pruriens* on proteins of Wnt/β catenin pathway in pulmonary hypertension by in silico approach

Supriya Bhosle[1] · Shrilaxmi Bagali[1] · Prachi P. Parvatikar[2] · Kusal K. Das[1]

Received: 16 January 2024 / Accepted: 10 September 2024
© The Author(s), under exclusive licence to Springer-Verlag GmbH Germany, part of Springer Nature 2024

Abstract
Modulation of the Wnt/β-catenin signaling pathway may aid in discovering new medications for the effective management of pulmonary artery hypertension (PAH). Given the therapeutic potential of Mucuna pruriens in several diseases, the present study aimed to analyze interactions of different bioactive compounds of Mucuna pruriens plant seeds with Wnt/β-catenin pathway targeting its various components like Wnt 3a, Frizzled 1, LRP 5/6, β-catenin, Disheveled, cyclin D1 by in silico analysis. The proposed work is based on computational analysis including ADME/T properties, by a Swiss ADME server. To understand the molecular interaction pattern Schrodinger, suit a stand-alone software was used to predict the interaction of bioactive molecules of *Mucuna Pruriens* with target proteins that are involved in Wnt/ β catenin pathway. Further, the simulation pattern of the top docked complex was subjected to MD simulation in Desmond for 100 ns. Bioactive molecules from Mucuna Pruriens have drug-like properties and minimal toxicity. Further, the docking study revealed that among the nine compounds, three compounds (Gallic acid, L-dopa, and β-sitosterol) showed good interaction with target proteins. As gallic acid showed good interaction with all target proteins, the docked complex was subjected to MD simulation which was stable throughout the simulation time in terms of RMSD and RMSF. These findings suggest that the bioactive molecules of *Mucuna pruriens* compounds have potential therapeutic value in the treatment of pulmonary vascular disease. Further, in vivo and in vitro studies are necessary to determine its efficacy and validate its pharmacological activity conclusively.

Keywords Pulmonary arterial hypertension (PAH) · Pulmonary artery smooth muscle cell (PASMC) · Wnt/β catenin pathway · *M. pruriens* · Schrodinger suit · MD simulation · Gallic acid · L-Dopa · β-sitosterol

Introduction

The Wnt signalling pathway regulates fundamental physiological processes such as cell proliferation, differentiation, organogenesis, tissue repair, and malignancies. It is an evolutionarily conserved mechanism. (Jung and Oark et al., 2020) Wnt signaling pathways include canonical and non-canonical pathways. The Wnt/β-catenin, pathway also referred to as the canonical pathway, is primarily responsible for regulating cell proliferation and is β-catenin-dependent. The Wnt/Ca^{2+} and Wnt/Planar Cell Polarity pathways, which primarily regulate cell polarity and migration, are examples of non-canonical, β-catenin-independent pathways (Liu et al. 2022).

Wnt belongs to a family of secreted glycoproteins. The 19 Wnt proteins function as ligands for the Wnt/β catenin pathway (Yin Pet et al. 2018), and it consists of four components the extracellular signal segment, the membrane segment, the cytoplasmic segment, and the nuclear segment. The cell membrane segment is constituted of Frizzled (FZD) (specific sevenfold transmembrane receptor Frizzled protein) and LRP5/6 (Lipoprotein-Related Receptor Protein) co-receptor (Schatoff et al. 2017). The cytoplasmic segment mainly includes β-catenin, DVL (Disheveled), glycogen synthase kinase-3β (GSK-3β), AXIN, adenomatous polyposis coli (APC), and casein kinase I (CK1). The nuclear segment mainly includes β-catenin, which translocate to the nucleus, TCF/LEF family

✉ Shrilaxmi Bagali
shrilaxmi.bagali@bldedu.ac.in

[1] Laboratory of Vascular Physiology and Medicine, Department of Physiology, Shri B.M.Patil Medical College, Hospital and Research Centre, BLDE (Deemed to be University), Vijayapur, Karnataka 586103, India

[2] Faculty of Allied Health Science, BLDE (Deemed to be University), Vijayapur, Karnataka 586103, India

Published online: 19 November 2024

members, and β-catenin downstream target genes, such as cyclin-D1, c-myc, and axin2, MMPs (Chatterjee et al. 2022). When the Wnt/β-catenin signaling pathway is in the off state, a β-catenin destruction complex (DC) is formed in the cytoplasm, comprising AXIN, the APC protein, GSK-3β, CK-1α, and β-catenin (Yu et al. 2021). The kinases in this complex phosphorylate β-catenin, thereby targeting it for degradation by the ubiquitin–proteasome system. In the "On" state, Wnt proteins bind to the receptor complex consisting of FZD and LRP5/6, recruiting DVL protein to the plasma membrane (Moon et al. 2005). Subsequently, several components of the β-catenin destruction complex are recruited to the membrane, preventing the phosphorylation of β-catenin. β-catenin accumulates in the cytoplasm and translocates to the nucleus to associate with transcription factors and stimulate the transcription of Wnt target genes such as cyclin-D1, c-myc, and axin2 (MacDonald et al. 2009).

Abnormalities in Wnt/ β-catenin signaling have been linked to several clinical diseases. There is evidence suggesting the involvement of Wnt/β-catenin signaling in the pathogenesis of pulmonary artery hypertension (PAH). PAH is a rare, progressive, and devastating disease. (de Jesus Perez et al. 2014). The current therapies in pulmonary hypertension primarily focus on decreasing the contractility of the pulmonary vascular smooth muscle cell. Hence, there is a need to explore novel approaches to the treatment of PAH. Given the role of Wnt/β-catenin signaling in pulmonary hypertension (PAH), therapies targeting it can serve as a potentially novel approach.

In the Indian system of medicine, *Mucuna pruriens (*M. *pruriens)* is on an acceptable medicinal plant used for various therapeutic purposes generally known as Mucuna or velvet bean grows in tropical and subtropical regions all over the world (Lampariello et al. 2012). In Ayurveda M. *pruriens*, was used to treat various diseases including Parkinson's. Some reports suggested that this plant also possesses a neuroprotective effect and treats cardiovascular diseases (Rane et al. 2019) (Parvatikar et al. 2023). The plant seeds are very rich in bioactive compounds, according to the literature review the seeds contain the following bioactive compounds L-Dopa, B-sitosterol, Glutathione, 6-methoxyharman, Gallic acid, Stearic acids, Lecthin, Oleic acid.

The present study aimed to analyze interactions of plant-based different bioactive compounds of Mucuna pruriens with pulmonary hypertension regulatory Wnt/β-catenin pathways targeting proteins like wnt 3a, frizzled 1, LRP 5/6, β-catenin, Disheveled, cyclin D1 by in silico analysis.

Methodology

Target protein preparation

The 3-D crystal structure of the target proteins Wnt 3a (PDB ID 7DRT), Frizzaled1 (PDB ID 4IU6), LRP 5/6 (PDB ID 3S8V), β-catenin (PDB ID 1LUJ), Disheveled (PDB ID 6ZC7), CyclinD1(PDB ID 5VZU) were obtained from the Protein Data Bank (Ponnulakshm et al. 2020). The protein structures were then imported into Accelrys Discovery Studio for further analysis. Non-receptor atoms were removed from the structures, including water molecules, ions, and various compounds. The resulting protein structures were then saved in PDB format (Table 1) (Studio D 2008).

Screening of bioactive molecules

Bioactive molecules from Mucuna purines plant seeds were chosen based on the literature review, the corresponding compound structures were obtained from the database of PubChem and Naturally Occurring Plant-based Anti-cancer Compound-Activity-Target database NPACT (Madagi et al. 2018). To prepare all ligands for molecular docking, hydrogen atoms were added, charged groups were neutralized, and the ligands' geometrical properties were optimized (Table 2).

Analysis of drug likeness properties

The SWISS ADMET tool was used to determine the ADMET (absorption, distribution, metabolism, elimination, and toxicity) properties of bioactive molecules from Mucuna purines plant seeds (Parvatikar et al. 2022). (DeLano et al. 2002). These properties are important to determine the drug's ability to determine brain/blood barrier permeability (BBB) and human oral availability. This tool uses computational methods to predict the physicochemical properties of a molecule based on its structure, BBB permeability is crucial because it determines whether the drug can cross the blood–brain barrier and reach its target in the brain. Human oral availability measures the drug's ability to be absorbed

Table 1 PDB format of the crystal structure of the protein

S.No	Protein name	PDB ID	Resolution	Molecular weight kDa
01	Wnt 3a	7DRT	2.20 A	104.89
02	Frizzled 1(FZD)	4IU6	1.90 A	43.81
03	LRP 5/6	3S8V	3.10 A	151.43
04	β–catenin	1LUJ	2.5 A	64.50
05	Disheveled	6ZC7	1.48 A	21.51
06	CyclinD1	5VZU	2.71 A	150.14

Table 2 Bioactive compounds from seeds of *M. purines*

S.No	Compound name	Family	PubChem ID	Molecular weight
01	L-Dopa	Amino acid	6047	197.19 g/mol
02	Glutathione	Amino acid	124,886	307.33
03	Lecithin	Fat	823	258.23
04	Gallic acid	Phenolic acid	370	170.12
05	B-sitosterol	Plant sterol	222,284	414.7
06	6-methoxyharman	Carbolines	135,053,166	263.29
07	Stearic acids	Saturated fatty acid	18,962,935	540.9
08	Oleic acids	Fatty acid	23,665,730	304.4
09	Linoleic acids	Organic compound	5,282,798	280.4

through the gastrointestinal tract and reach its mark in the body. The SWISS ADMET tool uses machine learning algorithms to predict these properties based on the molecule (Honutagi et al. 2023).

Molecular interaction study

A molecular interaction study was carried out using Schrodinger software. The interactions of all proteins (Wnt3a, Frizzled, LRP 5/6, β-catenin, Disheveled, CyclinD1) with ligands (bioactive substances) were calculated using a genetic algorithm. A grid box was generated, at the centroid of the binding sites, and docked in three stages using GLIDE v6.7 (Huey et al. 2012). For the top ten leads, a chosen substrate, and the exiting inhibitors, the available energy of binding for each target was calculated using Prime/MM-GBSA (Parvatikar et al. 2022).

Molecular dynamics simulations (MD simulations)

MD simulation is used to understand conformational changes in the docked complex during the interaction. In the present study, Desmond software was used to calculate the energy and force of the docked complex during simulation time. The advantage of this software is that it is integrated with a molecular modeling environment and tools for analysis as well as viewing (Chow et al. 2008). The minimized solvated system was then used to run the MD simulation for 100 ns at normal pressure (1.01 bar) and temperature (300 K). A simulation interaction diagram was generated after the simulation to analyze the MD results, such as the plot for the protein–ligand RMSD and protein–ligand interactions during the simulation (Kumar et al. 2023).

Molecular mechanics generalized born surface area (MM-GBSA) analysis

The binding affinity and binding free energies were found to change during the simulation study due to the ligand's positional and orientational changes. Predicting these energies enables us to better understand the ligand's movement. Molecular Mechanics Generalised Born Surface Area (MM-GBSA) Analysis is the most efficient and compatible method for calculating binding energies. The MM-GBSA calculations of the individual ligand–protein complexes were carried out using the Schrodinger software's Prime module. (Khaparkhuntikar et al. 2023).

Result

Strucsture of target protein

Table 1 shows the crystal structure of Wnt 3a (PDB ID 7DRT) consists of 893 amino acid residues with a molecular weight of 104.89 kDa, at 2.20A resolution, Frizzaled1 (PDB ID 4IU6) consists of 384 amino acid residues with a molecular weight of 43.81 kDa, at 1.90 A and LRP 5/6 (PDB ID 3S8V) consists of 1334 amino acid residues with a molecular weight of 151.43 kDa, at 3.10 A, resolution, β-catenin (PDB ID 1LUJ), consists of 589 amino acid residues with a molecular weight of 64.50 kDa, at 2.5 A resolution, Disheveled (PDB ID 6ZC7) consists of 190 amino acid residues with a molecular weight of 64.50 kDa, at 1.48 A resolution, and Cyclin D1(PDB ID 5VZU) consists of 1308 amino acid residues with a molecular weight of 150.14 kDa at 2.70A resolution were retrieved from the protein data bank. Using Discovery Studio, non-receptor molecules, including water, were removed from these protein structures, and the data was saved in PDB format and the crystallographic structure (Fig. 1).

Ligand database

Our study is based on a literature review, the structures of bioactive compounds from Mucuna purines plant seeds were obtained in SDF format from the PubChem database and converted to PDB format. (Table 2 and Fig. 2).

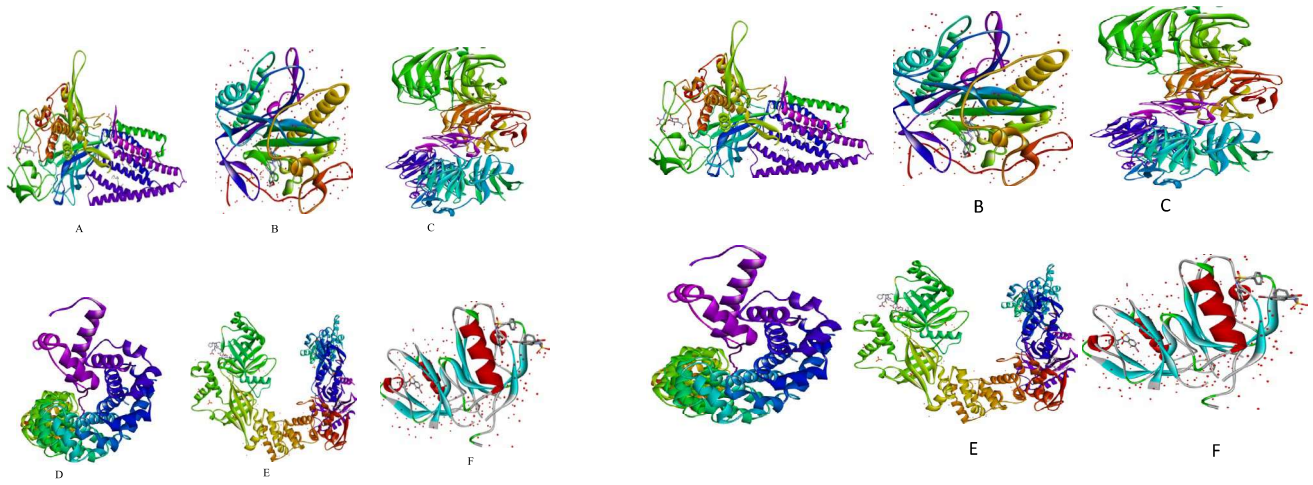

Fig. 1 3-D structure of selected target proteins from wnt signalling pathway **A** Wnt 3a, **B** Frizzled1, **C** LRP5/6, **D** β–catenin, **E** CyclinD1, **F** Disheveled

ADME/T properties of ligand

Table 3 shows the calculated ADMET properties of bioactive compounds of *M. purines* and standard drugs used in pulmonary hypertension treatment It was predicted that eight bioactive molecules obey Lipinski's rule. The selected active compounds' physicochemical properties included a molecular weight of < 500, an H-bond donor (HBD), an H-bond acceptor (HBA), a total number of rotatable bonds < 10 (TNRB), a total polar surface area of < 140 (TPSA), and an atomic molar refractivity of 42–130 (AMR). These properties are significant because they influence the drug's ability to interact with biological targets, as well as its solubility and ability to cross cell membranes. The SWISS ADMET tool was used to evaluate these properties. These molecules demonstrated no violation of the rules.

Molecular docking

Molecular docking predicts low binding energy confirmation. The inbuilt criteria of glide for docking analysis were used. (Table 4 and Fig. 3). Gallic acid, β-sitosterol, and L-dopa showed low binding energy with an efficient docking complex as compared to other bioactive molecules. Gallic acid interaction energy of − 16.557 kcal/mol inhibition energy of − 4.131 kcal/mol. The residues Thr89, Asn87, Arg295, Phe290, and Gly291 formed van der Wals interactions with Wnt3a. β–sitosterol has an interaction energy of − 35.076 kcal/mol inhibition energy of − 5.246 kcal/mol. The residue Asp294, Arg295, Thr292, Pro283, Gly291, Phe290, Asn87 formed van der Wals interactions with Wnt3a.

With Frizzeled1, Gallic acid has an interaction energy of − 29.214 kcal/mol inhibition energy of -7.041 kcal/mol. The residues Met309, Leu308, Tyr310, Phe311, Arg562, Asp471, Leu473, Phe603 formed van der Wals. β-sitosterol has an interaction energy of − 28.091 kcal/mol inhibition energy of − 4.728 kcal/mol. The residue Asp471, Arg562, Tyr607, Phe603, Pro538, Leu473, Phe311, Gly470, Val472, Arg562, formed van der Wals interactions with Frizzeled1.

In relation to LRP5/6 Gallic acid has an interaction energy of − 20.746 kcal/mol inhibition energy of − 5.101 kcal/mol and β-sitosterol has an interaction energy of − 31.582 kcal/mol inhibition energy of − 2.339 kcal/mol. The residue-Thr393, Asn426, Cys466, Ser425, His470, Asp390, Ser389, Asn387, Arg386, interacted.

With catenin, Gallic acid has an interaction energy of − 20.746 kcal/mol inhibition energy of − 5.101 kcal/mol. The residues Lys354, Asp390, Asn426, Arg386, Asn387 formed van der Wals interactions with β-sitosterol. β -sitosterol has an interaction energy of − 31.582 kcal/mol inhibition energy of − 2.339 kcal/mol. The residueThr393, Asn426, Cys466, Ser425, His470, Asp390, Ser389, Asn387, Arg 386, formed van der Wals interactions with β–catenin. with Disheveled, Gallic acid has an interaction energy of − 34.18 kcal/mol inhibition energy of − 8.559 kcal/mol. The residues Gly1070, Asp1068, His1065, Lys1121, Pro1086, Asp1063 formed van der Wals interactions with Disheveled. β–Sitosterol has an interaction energy of − 50.81 kcal/mol inhibition energy of − 6.111 kcal/mol. The residue Thr248, Gly253, Leu284, Tyr159, His236, Lys199, Arg87 formed van der Wals interactions with Disheveled.

With Cyclin D1, Gallic acid has an interaction energy of − 46.299 kcal/mol inhibition energy of − 7.387 kcal/mol. The residues Gly1079, Asp1068, His1065, Pro1086, Lys1121 formed van der Wals interactions with CylineD1. β–Sitosterol has an interaction energy of − 69.119 kcal/mol inhibition energy of − 8.711 kcal/mol. The residue

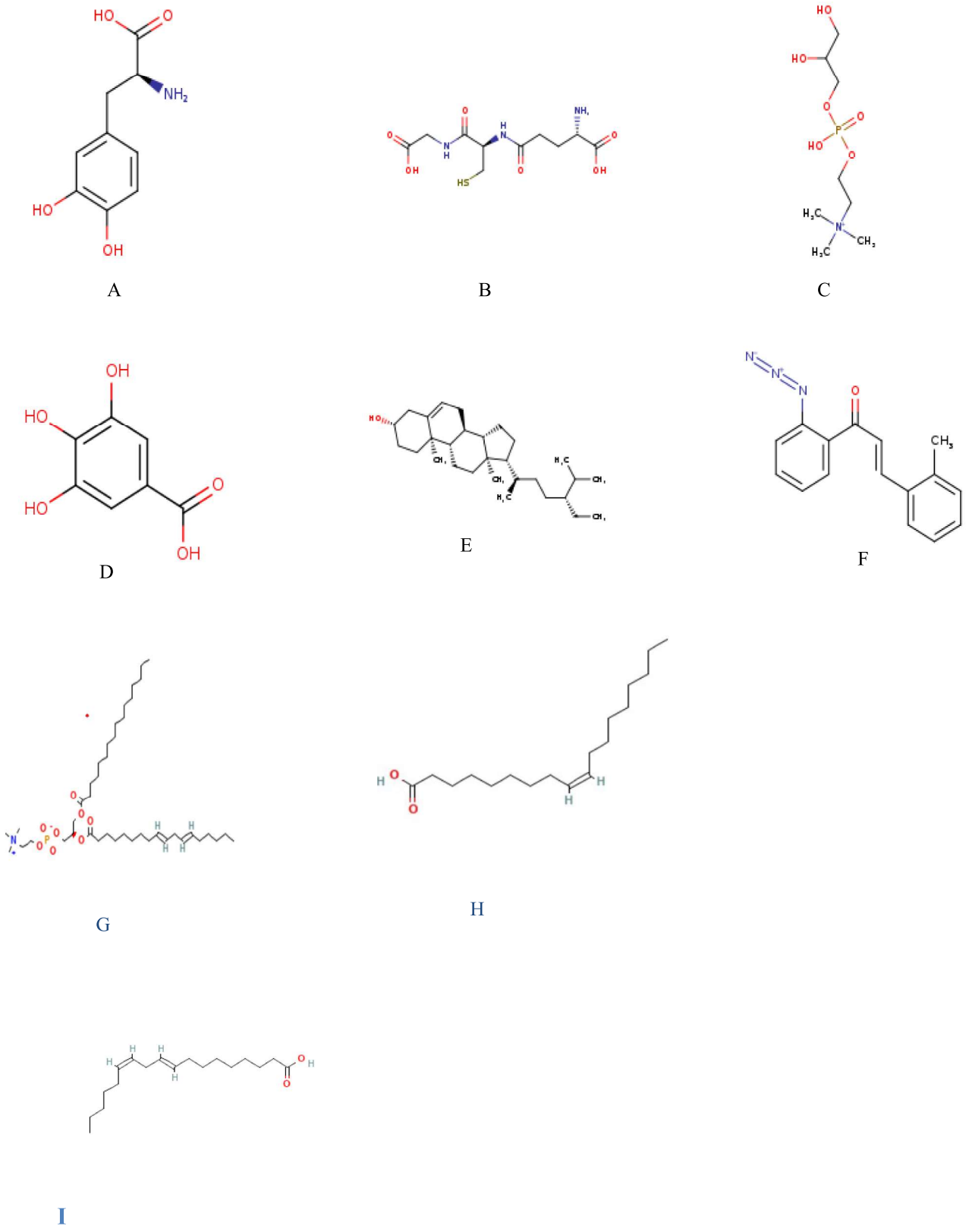

Fig. 2 3-D structure of selected bioactive compound from *M. purines* **A** L-Dopa, **B** B-sitosterol, **C** Glutathione, **D** 6-methoxyharman, **E** Gallic acid, **F** Stearic acids, **G** Lecithin, **H** Oleic acid, **I** Linoleic acid

Table 3 ADME/T of selected bioactive compounds from *M. purines*

S.No	Compound name	Molecular weight(g/mol)	Rotatable bonds	Hydrogen bond acceptor	Hydrogen bond donor	Lipinski rule	Violation
01	L-Dopa	197.19(g/mol)	3	5	4	yes	0
02	Glutathione	307.33	11	7	5	yes	0
03	Lecithin	258.23	8	6	3	Yes	0
04	Gallic acid	170.12	1	5	4	Yes	0
05	B-sitosterol	414.7	6	1	1	yes	1
06	6-methoxyharman	263.29	4	4	0	yes	0
07	Stearic acids	540.9	30	4	2	No	2
08	Oleic acids	304.4	15	2	0	yes	1
09	Linoleic acids	280.4	14	2	1	yes	1
10	Tadalafil	389.40	1	4	1	Yes	0
11	Amlodipine	408.88	10	6	2	Yes	0

Glu253, Thr248, Leu284, Tyr159, His236, Lys199, Arg87 formed van der Wals interactions with CyclinD1 (Table 4 and Fig. 4).

Docking results

MD simulation

Desmond package of Schrodinger was used for MD simulations of the best-docked target proteins. In this study, after molecular docking, a docked complex of beta-catenin with gallic acid was used for MD simulation. Out of the top three bioactive compounds (Gallic acid, L-dopa, and beta-sitosterol) gallic acid was used and beta-catenin is a key regulator for the pathway. The major goal of the MD simulation study was to evaluate the positional and structural changes of the inhibitor molecule near the protein binding site, which provides insight into the stability of the ligand–protein complex. The Root Mean Square Deviation (RMSD) is used to calculate the average change in displacement of a group of atoms for a given frame in relation to a reference frame. This method is carried out for each frame of the simulation trajectory.

The RMSD evolution of a protein is depicted in Fig. 4. In the simulation of the beta-catenin protein, the initiation of individual proteins in the trajectory was found to be from 3.5 Å RMSD, whereas the protein–ligand complex was found to be from 3 Å RMSD in simulation analysis. At 50 ns, the protein complex had 3.5 Å RMSD, but by 100 ns, it had stabilized to an RMSD value of around 4.5 Å.

Throughout the simulation, protein interactions with the ligand may be observed. Protein–ligand interactions (or 'contacts') can be divided into four distinct groups, as indicated in the plot: hydrogen bonds, hydrophobic, ionic, and water bridges. Each interaction type contains more specific subtypes which can be assessed using the 'Simulation Interactions Diagram' panel. A comprehensive diagram showing ligand atom interactions with protein residues. Interactions that occur more than 30.0% of the time in the selected trajectory (0.00 through 100 nsec) are shown.

Molecular mechanics generalized born surface area (MM-GBSA) analysis

Using a simulation study, the free binding energies of the best-docked protein–ligand complexes were calculated using the MM-GBSA analysis in the Schrodinger software's Prime module. The values were obtained in terms of ΔG Bind, which represents the binding free energy for the interactions of the beta-catenin gallic acid complex. The contributing energies in DG Bind calculation include Coulomb/Electrostatic energy (ΔG Coulomb), Covalent bond energy (ΔG Covalent), Hydrogen bond energy (ΔG H bond), Nonpolar salvation energy (ΔG Lipo), Polar solvation energy (ΔG Solv ΔB) and van der Waals energy (ΔG vdW). All the values of energies obtained from MM-GBSA analysis are mentioned in Table 5.

Discussion

PAH is a rare, progressive, and devastating disease characterized by increased pulmonary pressure and right heart failure. Key features in PAH are the progressive loss of small vessels and the proliferation of smooth muscle in the medial layer, resulting in luminal obliteration and an increase in pulmonary vascular resistance (Bachheti et al. 2022). Since none of the existing treatments for PAH have been demonstrated to accelerate angiogenesis or reduce already-present medial thickening, the condition progresses and eventually results in treatment failure. The discovery

Table 4 Multiple docking interaction of selected target proteins from Wnt signalling pathway with bioactive molecules from *M. purines*

S.No	Compound Name	Docking score Kcal/mol unit						Glide energy Kcal/mol unit					
		Wnt3a	Frizzled 1Receptor	LRP 5/6Receptor	β–catenin	Disheveled	Cyclin D1	Wnt3a	Frizzled 1Receptor	LRP 5/6Receptor	β–catenin	Disheveled	Cyclin D1
01	Gallic acid	−5.101	−5.291	−7.041	−4.131	−8.559	−7.387	−20.746	−22.691	−29.214	−16.557	−34.18	−46.299
02	β sitosterol	−2.339	−3.183	−4.782	−5.246	−6.111	−8.711	−31.582	−29.969	−31.606	−35.076	−50.81	−69.119
03	L-Dopa	−4.015	−5.679	−6.056	−4.361	−6458	−6.860	−22.437	−26.231	−28.091	−22.97	−30.60	−53.964
04	Glutathione	−2.339	−3.183	NR	NR	−2.821	−4.674	−23.907	−29.536	NR	NR	−28.14	−44.202
05	Lecithin	0.72	−2.869	−0.72	−3.649	−6.823	−6.858	−30.625	−37.063	−26.136	−23.887	−42.12	−48.068
06	Linolic acids	−1.604	0.874	−1.22	−0.622	−3.585	−5.848	−26.401	−23.747	−30.087	−26.875	−33.73	−37.796
07	Steoric acid	0.72	−0.74	−0.148	−2.257	−3.460	−6.007	−23.642	−32.085	−29.187	−22.096	−38.93	−37.491
08	Oleic acid	0.927	1.06	0.141	−1.266	−2.962	−7.494	−25.804	−26.877	−27.735	−26.69	−32.72	−47.294

of disease-modifying agents to treat PAH may be aided by modulating Wnt signaling because of its recognized function in controlling angiogenesis and cell proliferation (Tarapore et al. 2012). Mucuna pruriens is a legume native to southeast Asia, particularly India. Mucuna pruriens has been widely used in India for more than three thousand years. It has many actions, including antiparkinsonian, neuroprotective, aphrodisiac, and antiepileptic, apart from its use in cardiovascular diseases. (Parvatikar et al. 2023).

It has been reported that mutation of Wnt/beta-catenin pathway signaling genes like FZD and LRP5 result in defective vasculogenesis and the present in silico study also indicated that gallic acid, beta-sitosterol and L-dopa which are bioactive compounds of *M.pruriens* were found to be well docked with all six proteins of Wnt/beta-catenin signalling pathways that include FZD, LRP5, etc. (Su et al. 2013).

To screen potential bioactive molecules of Mucuna pruriens that can target Wnt3a, Frizzled, LRP 5/6, β-catenin, Disheveled, and cyclinD1 targeting the wnt/β-catenin pathway, the present study used an in-silico analysis based on the molecular interaction studies. Different pharmacological properties of bioactive compounds of Mucuna pruriens were investigated in order to analyze in silico ADME/T properties. Docking analyses were further performed to evaluate the interaction of bioactive molecules with target proteins of the Wnt/ β -catenin pathway (Wnt3a, Frizzled, LRP 5/6, β -catenin, Disheveled, CyclinD1.

This study showed that different pharmacological properties of bioactive molecules of *Mucuna pruriens* are in order according to their ADME/T properties, The Lipinski filter, was normally used to analyze the ADMET ligands derived from the seeds of the Mucuna purines plant. For molecular docking analysis interaction energy score was used to select the best docked complex among bioactive molecules of Mucunna pruriens with Wnt3a, Frizzeled1, LRP5/6, β -catenin, Disheveled and CyclinD1 proteins involved in Wnt β -catenin pathway (Tarapore et al. 2012). The Gallic acid, β-sitosterol, and L-dopa showed the best interaction energy score when compared with the other ligands. Molecular docking analysis further showed that gallic acid, β -sitosterol, and L-dopa are also the best-docked bioactive compounds of M. pruriens.

MD simulation on gallic acid was performed for 100 ns to find out stability and conformational changes in the target protein when interacting with bioactive molecules. The RMSD, and RMSF, plot results indicated that gallic acid's binding to the protein stabilized it without causing any structural changes. Although there were initially a number of random fluctuations, no conformational flipping was seen over the whole simulation period. It eventually became quite satisfactory and stable within 100 ns MD simulation.

The overall analysis of the present study by molecular docking and MD simulation hypothesized, gallic acid, β

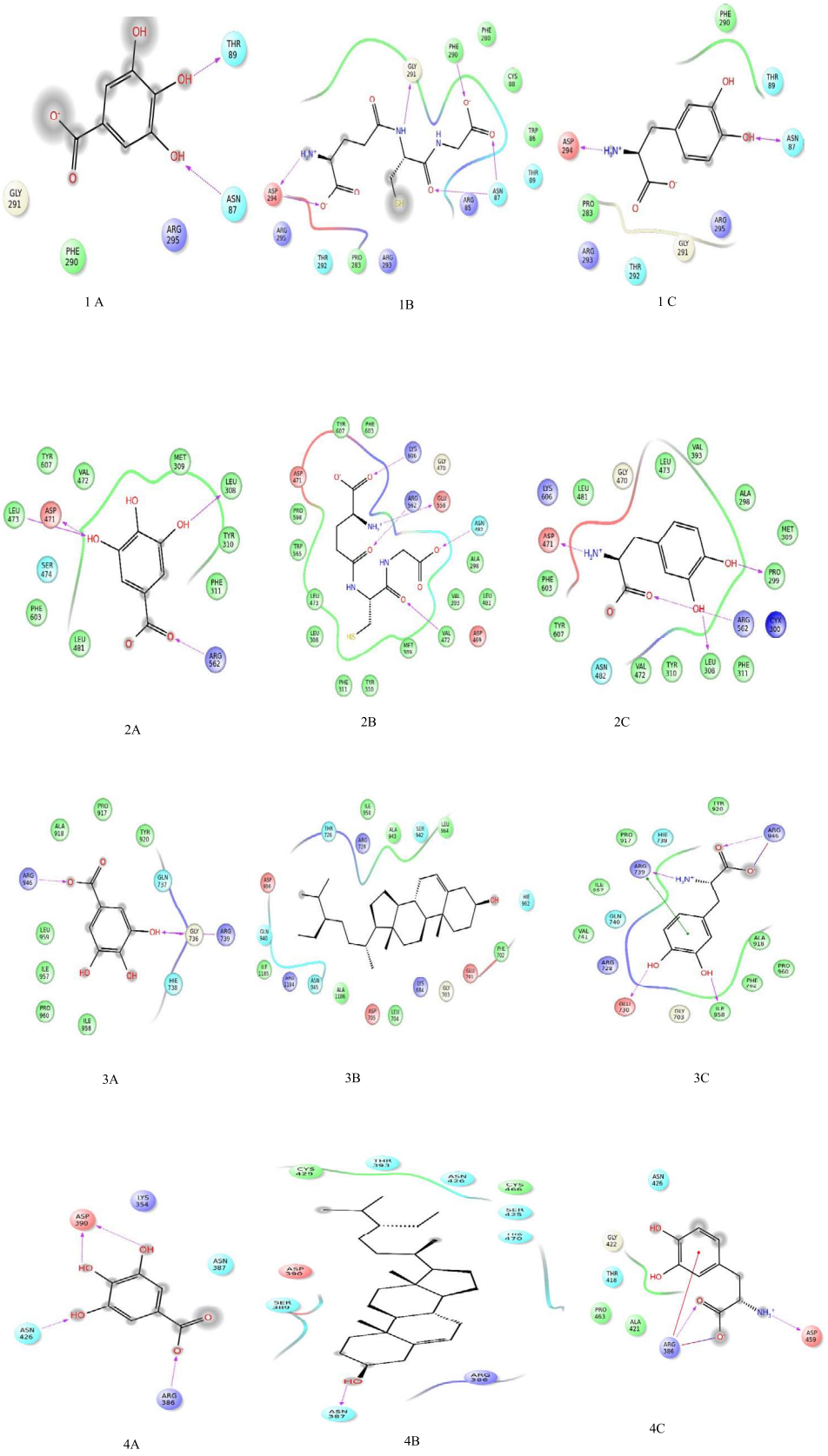

Fig. 3 Multiple docking interaction of selected target proteins from wnt signalling pathway with bioactive molecules from *M. purines*. 1A) Docking of Wnt3a with Gallic acid. 1B) Docking of Wnt3a with βsistosterol. 1C) Docking of Wnt3a with L-Dopa. 2A) Docking of Frizzled 1with Gallic acid. 2B) Docking of Frizzled 1 with βsistosterol. 2C) Docking Frizzled 1with L-Dopa. 3A) Docking of LRP 5/6with Gallic acid 3B) Docking of LRP 5/6with βsistosterol. 3C) Docking of LRP 5/6 with L-Dopa.4A) Docking of β–catenin with Gallic acid 4B) Docking of β–catenin with βsistosterol. 4C) Docking of β–catenin with L-Dopa. 5A) Docking of Disheveled with Gallic acid. 5B) Docking of Disheveled with βsistosterol 5C) Docking of Disheveled with L-Dopa. 6A) Docking of CyclinD1 with Gallic acid. 6B) Docking of CyclinD1 with βsistosterol. 6C) Docking of CyclinD1with L-Dopa

Fig. 3 (continued)

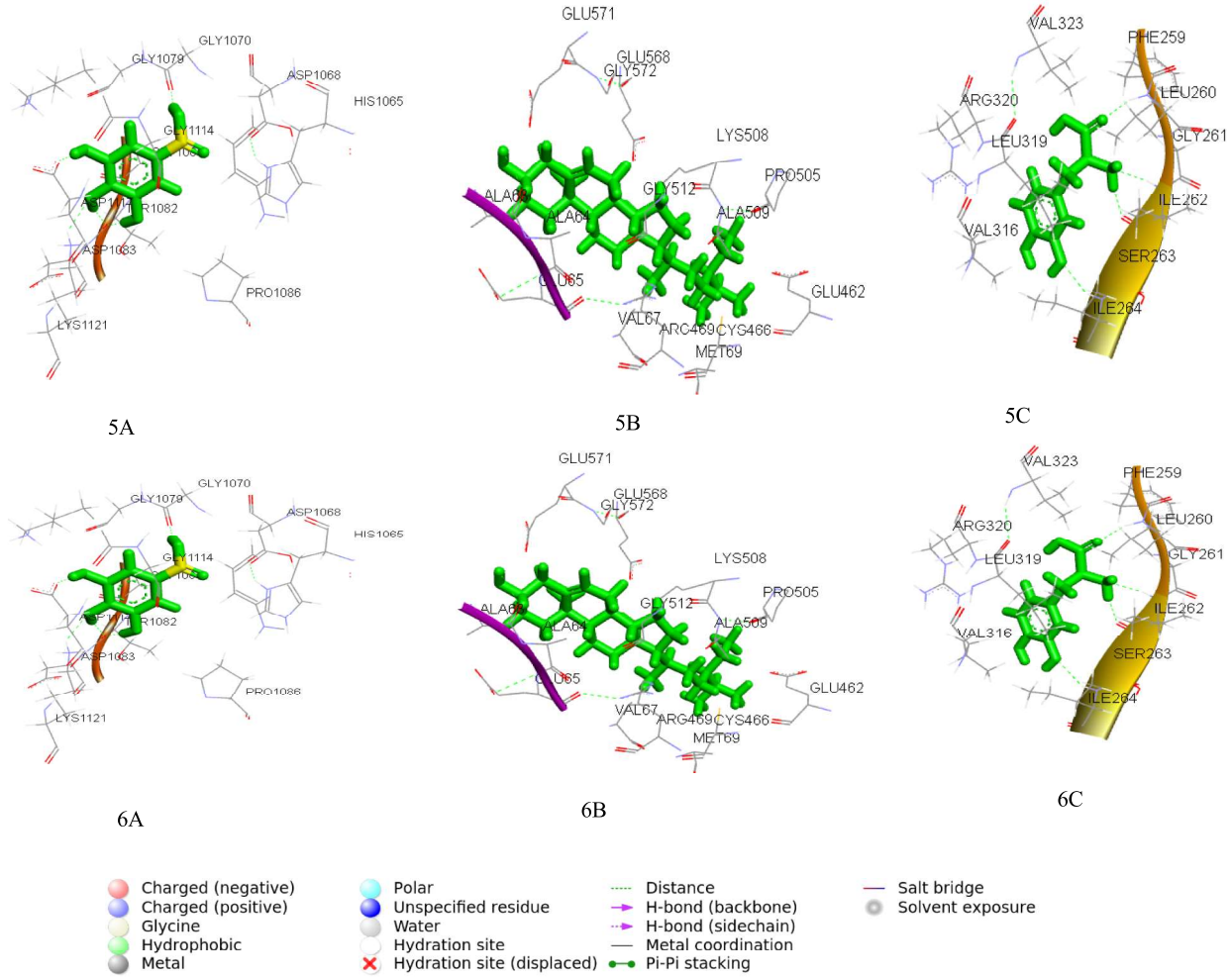

-sitosterol, and L-Dopa of *M. purines* has good binding potential and may be considered as therapeutic inhibitors against pulmonary vascular diseases. (Khaparkhuntikar et al. 2023).

Conclusion

The proposed study predicted three bioactive molecules of *M. purines* have good pharmacokinetic properties interacting with target molecules at low energy with stable binding potential which can be used in the treatment of pulmonary arterial hypertension but it needs to be validated with in vitro and in vivo experiments.

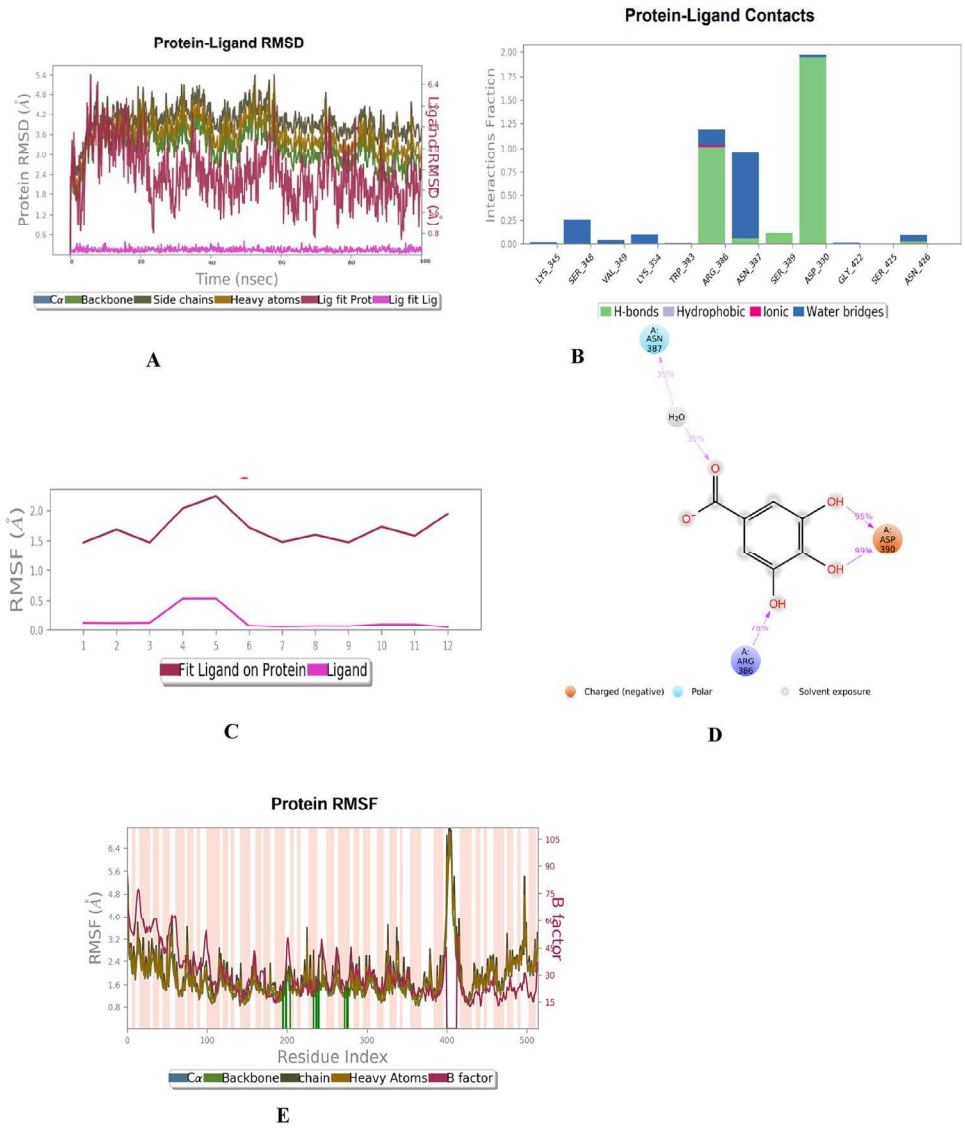

Fig. 4 **A** Protein RMSD Graph of β catenin with gallic, **B** Protein–ligand contacts, **C** Protein–ligand RMSF, **D** ligand atom interaction with the protein residue, **E** Protein RMSF

Table 5 Binding free energies (KCalmol^{-1}) of beta-catenin gallic acid along with individual energy components (KCalmol1) contribution showed in Table 4

Name of target	ΔG Bind value KCalmol^{-1}	ΔG Coulomb KCalmol^{-1}	ΔG Covalent KCalmol^{-1}	ΔG H bond KCalmol^{-1}	ΔG Lipo KCalmol^{-1}	ΔG Solv GB KCalmol^{-1}	ΔG vdW KCalmol^{-1}
beta-catenin gallic acid	– 15.07	– 22.52	4.037	– 1.132	– 8.574	30.20	– 19.53

Author contribution Kusal K Das manuscript proofreading Dr Shrilaxmi Bagali manuscript proofreading Dr Prachi P. Parvatikar Data analysis Supriya Bhosale manuscript writting.

Data availability No datasets were generated or analysed during the current study.

Declarations

Conflict of interest No potential conflict of interest was reported by the authors.

References

Bachheti RK, Worku LA, Gonfa YH, Zebeaman M, Pandey DP, Bachheti A (2022) Prevention and treatment of cardiovascular diseases with plant phytochemicals: A review. Evid-Based Complement Altern Med. https://doi.org/10.1155/2022/5741198

Chatterjee A, Paul S, Bisht B, Bhattacharya S, Sivasubramaniam S, Paul MK (2022) Advances in targeting the WNT/β-catenin signaling pathway in cancer. Drug Discov Today 27(1):82–101

Chow E, Rendleman CA, Bowers KJ, Dror RO, Hughes DH, Gullingsrud J, Sacerdoti FD, Shaw DE (2008) Desmond performance on a cluster of multicore processors. DE Shaw Res Tech Rep DESRES/TR 1:1–14

de Jesus Perez V, Yuan K, Alastalo TP, Spiekerkoetter E, Rabinovitch M (2014) Targeting the Wnt signaling pathways in pulmonary arterial hypertension. Drug Discov Today 19(8):1270–1276

DeLano WL (2002) Pymol: an open-source molecular graphics tool. CCP4 Newsl Protein Crystallogr 40(1):82–92

Honutagi RM, Sunil R, Patil SM, Bhosale S, Das SN, Parvatikar PP, Das KK (2023) Protein-protein interaction of LDH and CRP-1 with hematotoxin snake venom proteins of all species of snake: An *in silico* approach. Int J Health Sci 17(2):10–15

Huey R, Morris GM, Forli S (2012) Using AutoDock 4 and AutoDock vina with AutoDockTools: a tutorial. Scripps Res Inst Mol Graph Lab 10550(92037):1000

Jung YS, Park JI (2020) Wnt signaling in cancer: therapeutic targeting of Wnt signaling beyond β-catenin and the destruction complex. Exp Mol Med 52(2):183–191

Khaparkhuntikar K, Maji I, Gupta SK, Mahajan S, Aalhate M, Sriram A, Gupta U, Guru SK, Kulkarni P, Singh PK (2023) Acalabrutinib as a novel hope for the treatment of breast and lung cancer: an in-silico proof of concept. J Biomol Struct Dyn. https://doi.org/10.1080/07391102.2023.2217923

Kumar HB, Manandhar S, Rathi E, Kabekkodu SP, Mehta CH, Nayak UY, Pai KSR (2023) Identification of potential Akt activators: a ligand and structure-based computational approach. Mol Divers 28:1485–1503

Lampariello LR, Cortelazzo A, Guerranti R, Sticozzi C, Valacchi G (2012) The magic velvet bean of *Mucuna pruriens*. J Tradit Complement Med 2(4):331–339

Liu J, Xiao Q, Xiao J, Niu C, Li Y, Zhang X, Zhou Z, Shu G, Yin G (2022) Wnt/β-catenin signalling: function, biological mechanisms, and therapeutic opportunities. Signal Transduct Target Ther 7(1):3

MacDonald BT, Tamai K, He X (2009) Wnt/β-catenin signaling: components, mechanisms, and diseases. Dev Cell 17(1):9–26

Madagi SB, Parvatikar PP (2018) Docking studies on phytochemical derivatives as tissue transglutaminase-2 (TG2) inhibitors aganist lung Cancer. Proceed World Congress on Eng Comput Sci 1:23–25

Moon RT (2005) Wnt/β-catenin pathway. Sci STKE. https://doi.org/10.1126/stke.2712005cm1

Parvatikar PP, Patil S, Hoskeri J, Swargam S, Kulkarni RV, Das KK (2022) Screening and development of transglutaminase-2 inhibitors and their derivative as anti-lung cancer agent by in silico and in vitro approaches. Curr Comput Aided Drug Des 18(1):41–51

Parvatikar PP, Patil SM, Patil BS, Reddy RC, Bagoji I, Kotennavar MS, Patil S, Patil AV, Das KK, Das SN, Bagali S (2023) Effect of *Mucuna pruriens* on brain NMDA receptor and tau protein gene expression in cerebral ischemic rats. Front Physiol 14:1092032

Pinto-Junior VR, Osterne VJS, Santiago MQ, Lossio CF, Nagano CS, Rocha CRC, Nascimento JCF, Nascimento FLF, Silva IB, Oliveira AS, Correia JLA (2017) Molecular modeling, docking and dynamics simulations of the Dioclea lasiophylla Mart. Ex Benth seed lectin: an edematogenic and hypernociceptive protein. Biochimie 135:126–136

Ponnulakshmi R, Vishnupriya V, Mohan SK, Abilasha S, Ramajayam G, Vijayalakshmi P, Rajalakshmi M, Selvaraj J (2020) Molecular docking analysis of alkaloid compounds with beta-catenin towards the treatment of colon cancer. Bioinformation 16(3):283

Rane M, Suryawanshi S, Patil R, Aware C, Jadhav R, Gaikwad S, Singh P, Yadav S, Bapat V, Gurav R, Jadhav J (2019) Exploring the proximate composition, antioxidant, anti-Parkinson's and anti-inflammatory potential of two neglected and underutilized Mucuna species from India. S Afr J Bot 124:304–310

Schatoff EM, Leach BI, Dow LE (2017) Wnt signaling and colorectal cancer. Current Colorectal Cancer Reports 13(2):101–110

Studio D (2008) Discovery studio. Accelrys [2.1]

Su TR, Lin JJ, Tsai CC, Huang TK, Yang ZY, Wu MO, Zheng YQ, Su CC, Wu YJ (2013) Inhibition of melanogenesis by gallic acid: Possible involvement of the PI3K/Akt, MEK/ERK and Wnt/β-catenin signaling pathways in B16F10 cells. Int J Mol Sci 14(10):20443–20458

Tarapore RS, Siddiqui IA, Mukhtar H (2012) Modulation of Wnt/β-catenin signaling pathway by bioactive food components. Carcinogenesis 33(3):483–491

Yin P, Wang W, Zhang Z, Bai Y, Gao J, Zhao C (2018) Wnt signaling in human and mouse breast cancer: focusing on Wnt ligands, receptors and antagonists. Cancer Sci 109(11):3368–3375

Yu F, Yu C, Li F, Zuo Y, Wang Y, Yao L, Wu C, Wang C, Ye L (2021) Wnt/β-catenin signaling in cancers and targeted therapies. Signal Transduct Target Ther 6(1):307

Publisher's Note Springer Nature remains neutral with regard to jurisdictional claims in published maps and institutional affiliations.

Springer Nature or its licensor (e.g. a society or other partner) holds exclusive rights to this article under a publishing agreement with the author(s) or other rightsholder(s); author self-archiving of the accepted manuscript version of this article is solely governed by the terms of such publishing agreement and applicable law.

Repurposing of potential bioactive compounds from various database to study their effects on MMP-7 by virtual screening.

Patel Sanakousar K.[1], Parvatikar Prachi[2], Bhosale Supriya[1], Patil Sumangala[1] and Das Kusal K.[1]*
1. Laboratory of Vascular Physiology and Medicine, Department of Physiology, Shri B.M. Patil Medical College, Hospital and Research Centre, Vijayapur, Karnataka, INDIA
2. Faculty of Allied Health Science, BLDE (Deemed to be University), Vijayapur-586103, Karnataka, INDIA
*kusaldas@bldedu.ac.in

Abstract
Matrix metalloproteinase-7 (MMP7), a member of the matrix metalloproteinase (MMP) family, is involved in the mediation of both agonist-induced vascular tone and cardiac remodelling. We aimed to study the effect of a few bioactive molecules on (MMP-7) by in silico analysis. Data of bioactive molecules were collected from Pubchem and NPACT databases. PDB database was used for the generation of the 3D structure of protein MMP-7.

ADME/T properties showed 5 bioactive molecules obeying Lipkin's rule. Based on molecular docking, β-Sitosetrol and calyxin B are the top two compounds possessing higher ligand efficiency and interactive with higher number of amino acids while targeting MMP-7. The findings of this in silico study indicate 5 bioactive molecules obeying Lipkin's rule and out of these, two molecules may be considered as possible inhibitors of MMP-7.

Keywords: Bioactive molecules, MMP-7, ADME, Molecular Docking.

Introduction

Using bioactive compounds approved for one clinical use in another disease or syndrome is referred to as 'repurposing'. Most of the drive for repurposing is the high cost of developing a drug and the very long time it takes to determine the safety and specificity of a completely new drug[1].

Drug repositioning (DR) utilizes computational and experimental approaches to explore new clinical indications of existing drugs on a rational basis. Repurposing has investigated the clinical usefulness of many existing drugs as depicted above including some of the natural products such as ivermectin, colchicine etc. as prophylactic agents. FDA approved and clinical candidates, phytomedicine-derived bioactive compounds (or simply called phytochemicals such as curcumin, quercetin, epigallocatechin gallate EGCG and many others) have also been extensively investigated in search for potential lead molecules/drug candidates[2]. MMP-7 is a smallest protein member of MMP family. Matrix metalloproteinase (MMPs) are a family of proteolytic enzymes that regulate remodelling of the left ventricle (LV). MMP-7, also called matrilysin, is secreted as a 28 kDa proenzyme and is activated upon the removal of the pro-domain to generate a 19 kDa active enzyme[3]. Macrophages and cardiomyocytes are rich sources of MMP-7, 3, 4 and increased MMP-7 levels are detected in both the remote and infarct regions cardiovascular system. Naturally occurring bioactive compounds are ubiquitous in maximum nutritional better flora for human beings and livestock[4,5]. In systemic hypertension, the bioactive molecules may be explored for their function in modulating MMP-7, thereby regulating systemic hypertension[6, 7].

As *in sillico* screening of phytochemical database has gained tremendous interest in drug discovery research for the identification of new drugs, hence the present study was aimed to assess the effects of screened bioactive molecules on MMP-7 by *in silico* analysis.

Martial and Methods

Protein preparation: The crystal structure of human MMP-7 protein (PDB ID -2DDY) was obtained from the Protein Data Bank[8,9]. The protein structure was processed using Accelrys Discovery Studio by removing all non-receptor atoms including water, ion and various compounds. The refined and processed structure was saved as a "pdb" file format and viewed in Discovery studio[10]. The binding site for the inhibitor was searched based on a structural association of template with experimental evidence by using PDB-sum supported by a literature survey[11].

Ligand Preparation: A total of 130 biologically active plant-derived compounds (phytochemicals) with a wide range of structural diversity belonging to different phytochemical classes were selected based on their potential medicinal/biological interests as reported in traditional as well as modern phytomedicines. The 3D structures of compounds were downloaded from the PubChem database and saved in "sdf" files. Ligands were energetically minimized using the CHARMm-based minimizer on Biovia Discovery Studio (DS 2020)[12].

Pharmacokinetic Parameters: ADMET study is an essential step of drug screening for pharmacokinetic properties. The SWISS ADME tool analysed the properties including structural analogues; it predicts significant physical descriptors and pharmaceutically relevant properties. It consists of principle descriptors and physicochemical properties with a detailed analysis of the

logP (Octanol/Water), log S, molecular weight etc. It also calculates the analogues depending on Lipinski's rule of 5, an essential parameter for rational drug design[13].

Molecular Docking Studies: Maestro Schrödinger and molecular docking[14] 4.2 were used for selected 30 compounds (Table 1). Using genetic algorithm, extra precision docking was performed with the prepared protein and the ligands. Structures of ligands were kept flexible to generate different conformations. Receptor grid generation work flow was used to define a grid (box) around the ligand and to keep all the functional residues in the grid. Docking was performed on Intel® Core™ i3-7th gen laptop with 8 GB RAMS, Windows 10 system. All the results were visualized in Discovery studio.

Results

Structure of protein: The crystal structure of MMP-7 protein (PDB ID: 2ddy) was retrieved from PDB[15]. The MMP-7 protein is composed of 173 residues with molecular weight of 19 kDa and single motif. It is made of single A chain, contains 1 beta alpha beta unit, 1 beta hairpin, 1 psi loop, 7 strands, 3 helices, 22 beta turns and 2 gamma turns (Figure 1).

Binding site prediction: As per literature survey binding site information of target protein was predicted by performing PDBsum[16]. The ligand plot obtained from PDBsum showed binding site region of MMP-7 receptor containing 15 amino acid residues of chain A (Figure 2), viz. His 120, His 124, Glu 121, His 130, Leu 82, Ala 83, Ala 117, Thr 81, Pro 140, Tyr 116, Tyr 142, Thr 141, Ile 112 and MDW 178. These residues possess higher ligand efficiency and interaction with higher number of amino acids which are used for setting the grid of molecular docking.

Prediction of pharmacokinetic properties: *In silico* predictions of pharmacokinetic based on criteria via absorption, distribution metabolism and excretion (ADME)[17] properties have become important in drug selection and to determine their success for human therapeutic use.

Table 1
30 bioactive compounds selected for docking based on pharmacokinetics parameters

S.N.	Compound Name	Family	Molecular Weight
1	Calyxins B	Flavonoid	582.6
2	Artoindonesianin B	Flavonoid	468.5
3	Calyxins F	Flavonoid	582.6
4	Artoindonesianins V	Flavonoid	570.7
5	β- Sitosetrol	Flavonoid	414.7
6	Butein	Flavonoid	272.25
7	Calyxins A	Flavonoid	582.6
8	Calyxins C	Flavonoid	582.6
9	Calyxins D	Flavonoid	582.6
10	Calyxins E	Flavonoid	582.6
11	Calyxins G	Flavonoid	582.6
12	Calyxins H	Flavonoid	582.6
13	Calyxins J	Flavonoid	582.6
14	Artoindonesianin P	Flavonoid	368.3
15	Artoindonesianins A	Flavonoid	570.7
16	Artoindonesianins G	Flavonoid	570.7
17	Artoindonesianins H	Flavonoid	368.3
18	Artoindonesianins I	Flavonoid	368.3
19	Artoindonesianins U	Flavonoid	570.7
20	Baicalein	Flavonoid	270.24
21	Cajanol	Flavonoid	316.30
22	Biochanin A	Flavonoid	284.26
23	Blepharocalyxins A	Flavonoid	879.0
24	Blepharocalyxins B	Flavonoid	879.0
25	Blepharocalyxins C	Flavonoid	879.0
26	Blepharocalyxins D	Flavonoid	592.7
27	Blepharocalyxins E	Flavonoid	879.0
28	Burttinone	Flavonoid	438.5
29	Artoindonesianins V	Flavonoid	570.7
30	Apigenin	Flavonoid	270.24

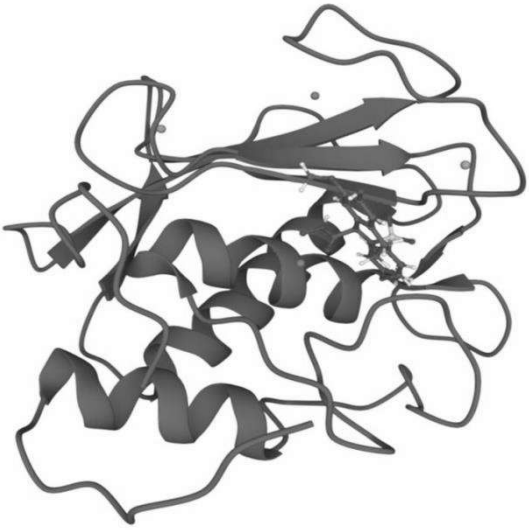

Figure 1: 2D structures of MMP-7

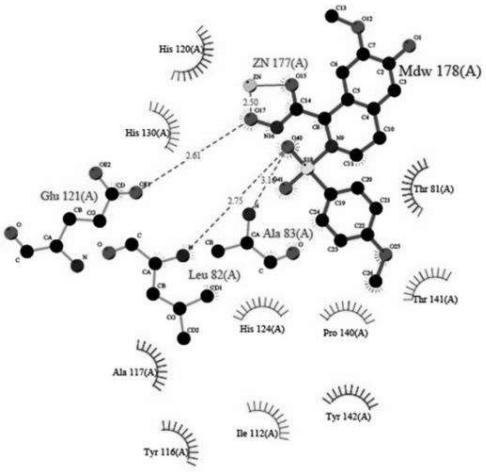

Figure 2: Amino acid residues lining higher ligand efficiency site of MMP-7.

Table 2
Top five compounds of ADME/T properties

S.N.	Compound Name	Molecular Weight (g / mole)	Rotatable Bonds	Hydrogen Bond Acceptor	Hydrogen Bond Donor	Lipinski Rule	Violation
01	Calyxins B	468.5	5	8	3	Yes	0
02	Artoindonesianin B	570.67	6	7	4	Yes	1
03	Calyxins F	582.64	12	8	6	No	2
04	Artoindonesianins V	582.64	9	8	5	Yes	1
05	β- Sitosetrol	414.7	6	1	1	Yes	1

So, these physiochemical properties were calculated to determine the ADME properties of the drugs. Bioactive molecules selected for present study were based on Lipinski's rule of five. All five ligands (Calyxins B, Artoindonesianin B, Calyxins F, Artoindonesianins V, β-Sitosetrol) have shown strong higher binding energy efficiency with target protein MMP-7 (-3.04 to -2.69 Kcal/ mol). The said compounds followed the Lipinski's rule in table 2 of five without any violation with respect to molecular weight (≤ 600KDa), number of H-bond acceptors (≤ 8) and number of H-bond donors (≤ 6). The Lipinski's screening is an essential filter that determines if a compound is suitable for drug designing and their chemical structures had shown (Figure 3).

Molecular Docking Study: The human MMP-7 showed higher ligand efficiency (-3.04, -5.17, -5.89, -3.7 and -2.69) and interaction with amino acids as shown in table 3 and

figure 4. Finally, comparing the higher ligand efficiency (-3.04 to -2.69) and interaction with amino acids scores of all five known inhibitors of human MMP-7. β-sitosterol and calyxins B were proposed in the study as possible inhibitors for the human MMP-7[18].

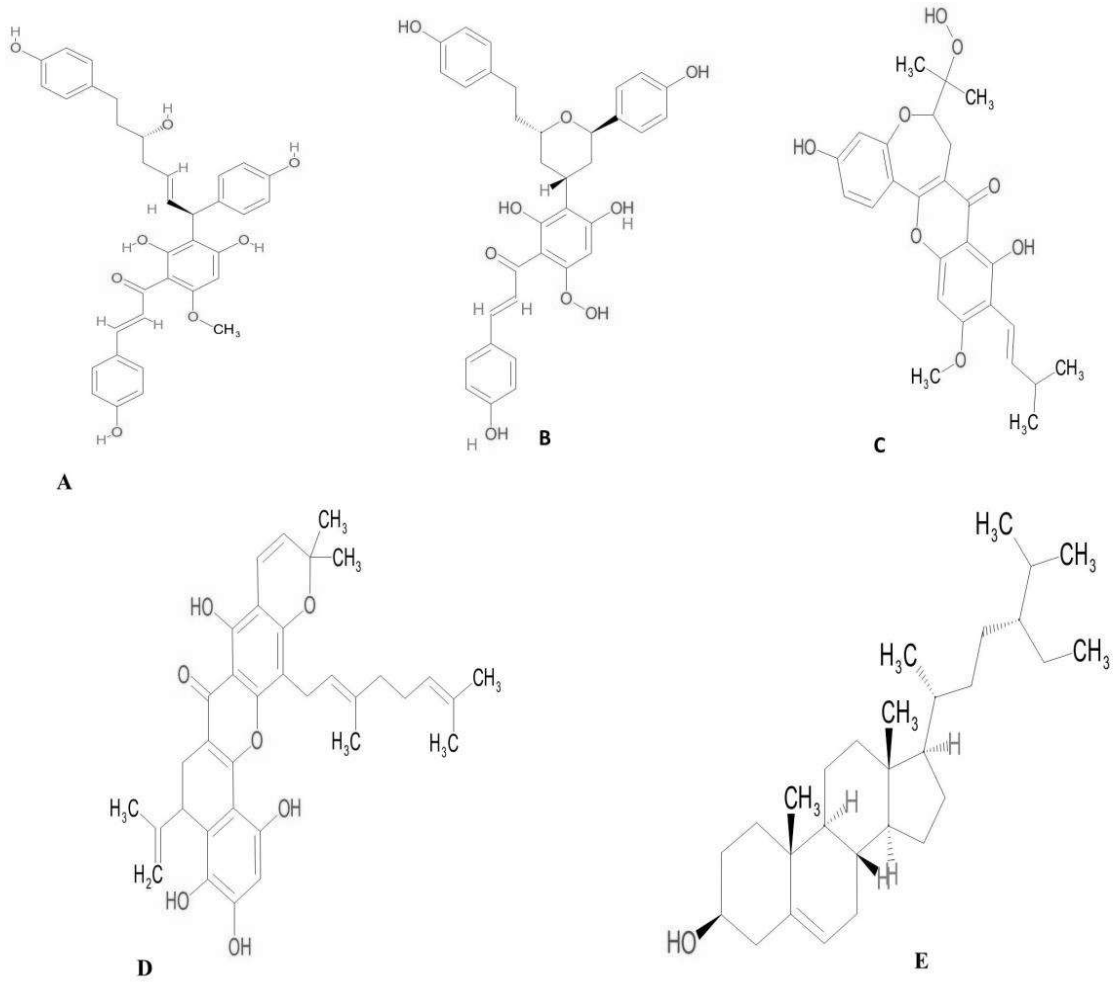

Figure 3: (A) Calyxins B (B) Calyxins F (C) Artoindonesianin B (D) Artoindonesianins V and (E) β- Sitosetrol

Table 3
Molecular Docking score

Molecules Name	Binding Energy (Kcal/mole)	Ligand Efficiency	Inhibition Constant	Interacting amino acid
Calyxins B	-3.04	-0.14	5.92	LYS 125, TYR 65,ALA 65, GLU 3, LYS 22, GLY 23,ASN 25
β- Sitosetrol	-2.69	-0.15	6.34	His 120, His 124, Glu 121, His130, Leu 82, Ala 83, Ala 117, Thr 81, Pro 140, Tyr 116, Tyr 142
Calyxins F	-5.89	-0.93	8.54	ARG103, VAL77, ALA105, ASN8, MET88, ALA86, PRO11, LYS113, ARG110, GLU118
Artoindonesianins V	-3.7	-0.18	1.94	ASN9, THR7, GLU63, ALA64, ALA63, ASN9, TYR67
Artoindonesianin B	-5.17	-0.25	10.29	ASN9, GLU8, GLU98, ASN70, LEU69,

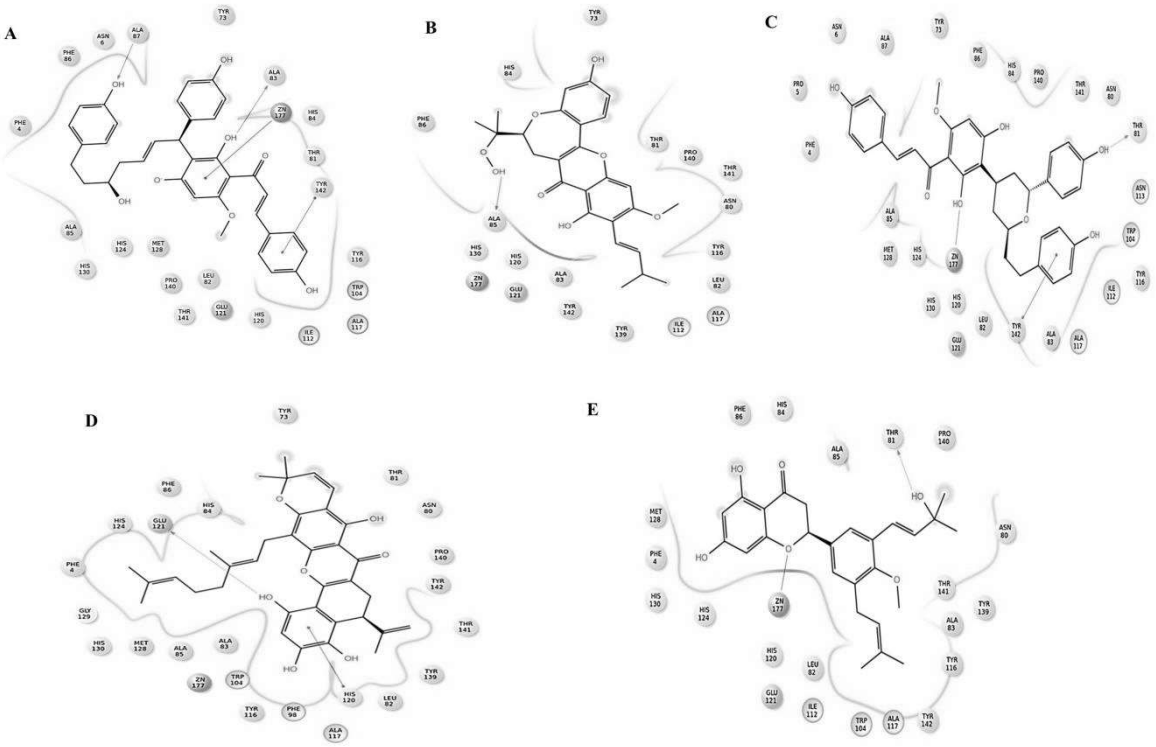

Figure 4: (A) Calyxins B (B) Calyxins F (C) Artoindonesianin B (D) Artoindonesianins V and (E) β- Sitosetrol

Discussion

Higher binding affinities were observed for docked compounds as compared to the co-crystal inhibitor. The more negative is the binding energy, the stronger will be the interaction. Affinity therefore depends on the energy of interaction. Thus negative binding energy depicts the strength of interactions as well as the affinity of a ligand molecule for its receptor molecule. Formation of stable complexes with well-defined interaction details predicts the significance of molecular docking and further molecular modelling studies[19].

From docking and drug-likeness/ADMET studies, five phytochemicals were found to exhibit remarkable inhibitory activities (best hit compounds), particularly against MMP-7. These phytochemicals are found in traditional Ayurvedic and Chinese medicines from plant sources such as neem, ashwagandha, ginseng soybean etc. All the identified compounds are basically tri-tetra-terpenoids, saponins or steroids with their wide natural abundance in traditional Ayurveda and Chinese medicines[19].

In the current work, ligands against the MMP-7 protein were selected from various phytochemical databases. Molecular docking was applied to explore the binding mechanism and correlate its docking score with the activity of the thirty (30) selected bioactive compounds. It has displayed good five (5) bioactive compounds with higher ligand efficiency and greater interaction with higher number of amino acids while targeting MMP-7. Molecular docking results further showed that calyxin B and β-sitosetrol are the best among the five (5) bioactive compounds with highest binding ligand efficiency and the maximum number of interactive amino acids. This present study can be useful for the design and development of novel compounds having better inhibitory activity against several diseases.

Conclusion

The results of the study indicate out of 30 selected bioactive compounds, 5 compounds were having higher ligand efficiency and interactivity with higher number of amino acids targeting MMP-7. Further out of 5 bioactive compounds, calyxin B and β-sitosetrol possesses the maximum ligand efficiency and interactivity with higher number of amino acids.

Acknowledgement

Authors thank to BLDE (DU) for providing research grant to author Ms. Sanakousar Patel (BLDE (DU)/REG/JRF-AO/2019-20/3647 (Dated: 18.02.2020).

References

1. Alazmi M. and Motwalli O., *In silico* virtual screening, characterization, docking and molecular dynamics studies of crucial SARS-CoV-2 proteins, *Journal of Bio Molecular Structure & Dynamics*, **39(17)**, 6761–6771 **(2021)**

2. Cabral-Pacheco G.A., Garza-Veloz I., Castruita-De la Rosa C., Ramirez-Acuna J.M., Perez-Romero B.A., Guerrero-Rodriguez J.F. and Martinez-Fierro M.L., The roles of matrix metalloproteinases and their inhibitors in human diseases, *International Journal of Molecular Sciences*, **21(24)**, 9739 **(2020)**

3. Chatterjee M., Le Roux J., Ahuja N. and Cherian A., Visual scene graphs for audio source separation, In Proceedings of the

IEEE/CVF International Conference on Computer Vision, 1204-1213 **(2021)**

4. Fu H., Zhou D., Zhu H., Liao J., Lin L., Hong X., Hou F.F. and Liu Y., Matrix metalloproteinase-7 protects against acute kidney injury by priming renal tubules for survival and regeneration, *Kidney International*, **95(5)**, 1167–1180 **(2019)**

5. Gandhi D., Bhandari S., Mishra S., Tiwari R.R. and Rajasekaran S., Non-malignant respiratory illness associated with exposure to arsenic compounds in the environment, *Environmental Toxicology and Pharmacology*, **94**, 103922, doi: 10.1016/j.etap.2022.103922103922 **(2022)**

6. Katari S.K., Pasala C., Nalamolu R.M., Bitla A.R. and Umamaheswari A., *In silico* trials to design potent inhibitors against matrilysin (MMP-7), *Journal of Biomolecular Structure and Dynamics*, **40(22)**, 11851-11862, doi: 10.1080/0739110 2.2021.1965032 **(2022)**

7. Lahiri D., Nag M., Dutta B., Mukherjee I., Ghosh S., Dey A. and Ray R.R., Catechin as the most efficient bioactive compound from Azadirachta indica with antibiofilm and anti-quorum sensing activities against dental biofilm: An *in vitro* and *in silico* study, *Applied Biochemistry and Biotechnology*, **193(6)**, 1617-1630 **(2021)**

8. Muhammad S.A. and Fatima N., *In silico* analysis and molecular docking studies of potential angiotensin-converting enzyme inhibitor using quercetin glycosides, *Pharmacognosy Magazine*, **11(42)**, 123 **(2015)**

9. Napoli S., Scuderi C., Gattuso G., Di Bella V., Candido S., Basile M.S. and Falzone L., Functional roles of matrix metalloproteinases and their inhibitors in melanoma, *Cells*, **9(5)**, 1151 **(2020)**

10. Parvatikar P., Bagali S., Hippargi S., Singh P.K., Singh S.B., Patil A.V. and Das K.K., Identification of Potent Bioactive Molecules Against NMDA Receptor and Tau Protein by Molecular Docking Approach, *Letters in Drug Design & Discovery*, **20(8)**, 1031-1039 **(2023)**

11. Rudrapal M., Gogoi N., Chetia D., Khan J., Banwas S., Alshehri B., Alaidarous M.A., Laddha U.D., Khairnar S.J. and Walode S.G., Repurposing of phytomedicine-derived bioactive compounds with promising anti-SARS-CoV-2 potential: Molecular docking, MD simulation and drug-likeness/ADMET studies, *Saudi Journal of Biological Sciences*, **29(4)**, 2432–2446 **(2022)**

12. Subbanna S., Basalingappa K.M., Maheshwari M.S., Gururaj H.B. and Gopenath T.S., *In silico* Analysis of Allium sativum Bioactive Compounds against Effector Protein from Pseudomonas syringae pv. pisi., *Journal of Pure and Applied Microbiology*, **16(1)**, 327-337 **(2022)**

13. Swargiary A., Ivermectin as a promising RNA-dependent RNA polymerase inhibitor and a therapeutic drug against SARS-CoV2: Evidence from *in silico* studies, *Research Square*, doi:10.21203/rs.3.rs-73308/v **(2020)**

14. Swargiary A., Mahmud S. and Saleh M.A., Screening of phytochemicals as potent inhibitor of 3-chymotrypsin and papain-like proteases of SARS-CoV2: an *in silico* approach to combat COVID-19, *Journal of Biomolecular Structure and Dynamics*, **40(5)**, 2067-2081 **(2022)**

15. Tahir R.A., Bashir A., Yousaf M.N., Ahmed A., Dali Y., Khan S. and Sehgal S.A., *In Silico* identification of angiotensin-converting enzyme inhibitory peptides from MRJP1, *PloS One*, **15(2)**, e0228265 **(2020)**

16. Teja P.H., *In Silico* Drug Designing and docking analysis for Hypertension using Nifedipine as lead molecule, *IJPRD*, **3**, 104-108 **(2011)**

17. Udosen B., Soremekun O., Ekenna C., Idowu Omotuyi O., Chikowore T., Nashiru O. and Fatumo S., *In-silico* analysis reveals druggable single nucleotide polymorphisms in angiotensin 1 converting enzyme involved in the onset of blood pressure, *BMC Research Notes*, **14(1)**, 1-6 **(2021)**

18. Udosen B., Soremekun O., Ekenna C., Idowu Omotuyi O., Chikowore T., Nashiru O. and Fatumo S., *In-silico* analysis reveals druggable single nucleotide polymorphisms in angiotensin 1 converting enzyme involved in the onset of blood pressure, *BMC Research Notes*, **14(1)**, 1-6 **(2021)**

19. Zalpoor H., Aziziyan F., Liaghat M., Bakhtiyari M., Akbari A., Nabi-Afjadi M., Forghaniesfidvajani R. and Rezaei N., The roles of metabolic profiles and intracellular signaling pathways of tumor microenvironment cells in angiogenesis of solid tumors, *Cell Communication and Signaling: CCS*, **20(1)**, 186 **(2022)**.

(Received 03rd February 2023, accepted 06th April 2023)

View publication stats